Mathematisches Forschungsinstitut Oberwolfach

Report No. 60/2012

DOI: 10.4171/OWR/2012/60

Dynamics of Patterns

Organised by
Wolf-Jürgen Beyn, Bielefeld
Bernold Fiedler, Berlin
Björn Sandstede, Providence

16 December – 22 December 2012

Abstract. Patterns and nonlinear waves arise in many applications. Mathematical descriptions and analyses draw from a variety of fields such as partial differential equations of various types, differential and difference equations on networks and lattices, multi-particle systems, time-delayed systems, and numerical analysis. This workshop brought together researchers from these diverse areas to bridge existing gaps and to facilitate interaction.

Mathematics Subject Classification (2000): 35B40, 35P05, 65M12.

Introduction by the Organisers

Nonlinear waves and patterns arise in partial differential equations and in systems posed on infinite lattices. While nonlinear waves and patterns are important in many biological and physical applications, many of their properties are still poorly understood from a mathematical viewpoint. Some outstanding problems in this area are the long-time behavior and nonlinear stability of localized and nonlocalized patterns on unbounded domains, the development of numerical algorithms to compute patterns and to assess their stability, analytical and geometric approaches for waves in lattice dynamical systems, and their control-theoretic aspects. Techniques range from dynamical systems, the analysis of nonlinear partial and functional differential equations including multiscale problems, to spectral analysis and numerical methods for patterns. It is the pattern aspect which unifies these widely separate technical aspects and provides substantial links between the proposed key topics. Over the past few decades, dynamical-systems techniques and bifurcation theory have helped tremendously in extending our understanding of the formation and dynamics of nonlinear waves on spatially extended domains. Most of these

efforts, however, are restricted to structures that respect an underlying periodic spatial lattice.

The goal of the workshop on "Dynamics of Patterns", which was organized by W.-J. Beyn (Bielefeld), B. Fiedler (FU Berlin), and B. Sandstede (Brown), was to bring together researchers from the aforementioned diverse areas to bridge existing gaps and to facilitate interaction. The formal scientific program consisted of 5 longer talks, 24 shorter talks, and 4 brief talks given by participating graduate students. No talks were scheduled in the afternoons on Tuesday, Thursday and Friday: instead, participants were encouraged to form small groups and discuss open problems in order to facilitate informal interaction. This worked very well, and several groups met to talk about a wide range of topics from new software tools to theoretical questions. Some specific topics were blow-up problems, lattice dynamical systems, front propagation, interaction of multi-dimensional patterns, delay equations, and functional-analytic tools in stability problems.

Despite much progress over the past decades, our understanding of when nonlinear waves exist and when they are stable under small perturbations is still limited. The talks by Ghazaryan, Hoffman, Hupkes, McCalla, Rademacher, and Veerman addressed a wide range of topics related to these questions. Some of these talks focused on studying models for combustion processes and chemical reactions that involve small parameters which affect the dynamical properties of fronts and pulses. Also discussed were existence and stability problems of planar fronts in lattice dynamical systems, which involved the development of new techniques suited to deal with the essential spectrum.

Since it is often difficult to prove the existence of waves rigorously in a given model, the development of efficient and accurate algorithms that can be used to find such structures numerically is important for applications. The talks by Hochbruck, Latushkin, Otten, and Rottmann-Matthes focused on recent developments in exponential integrators, which can be used for fast direct numerical simulations, and on techniques for analyzing methods that allow one to "freeze" a traveling wave to find its profile and determine its stability. Among the new results that were presented were approaches that deal with waves in hyperbolic PDEs.

Another area of considerable interest are generalized patterns and waves which arise when long-lived structures exhibit a complicated irregular spatial and/or temporal form. Among these structures are time-periodic breather solutions in wave equations, composite front solutions, generalized fronts that arise in systems with inhomogeneities or noise, turbulent patterns in pipe flow, and quasi-periodic as well as transient patterns in Faraday experiments. Recent progress in this area was presented in the talks by Barkley, Chirilus–Bruckner, Mallet–Paret, Matano, Nishiura, Pego, Rucklidge, and Tuckerman.

Multiscale problems provide a rich source of interesting patterns that are often difficult to analyze: examples are patterns that arise in ferromagnetic materials or in media with periodic imperfections that occur on small scales, and long-wave frequency and amplitude modulations of large-scale periodic structures. The talks by Matthies, Mielke, Otto, and G. Schneider addressed various challenges in this

area, including the use of homogenization methods, the analysis of domain wall structures, and the derivation and validity of reduced modulation equations for wave structures.

Another topic that was of significant interest to participants is the dynamics and control of structures involving delay equations and networks. The talks by Atay, Luecken, I. Schneider, Schöll, Walther, and Wolfrum focused on synchronization, chimera solutions, and control of structures in coupled oscillator systems with delay, and on the dynamics of delay differential equations with state-dependent delays.

For several classes of systems, it is possible to describe not just certain nonlinear wave structures but, in fact, all long-lived solutions on the attractor. The talks by Beck, Ben–Gal, Gurevich, Krisztin, and Rocha outlined recent progress on the dynamics of metastable patters in the 2D Navier–Stokes equations, the dynamics of reaction-diffusion systems with hysteresis, and the surprising analogies of global attractors in one-dimensional reaction-diffusion equations and in delay differential equations.

Workshop: Dynamics of Patterns

Table of Contents

Hiroshi Matano (joint with Thomas Giletti, Arnaud Ducrot)
Propagating terrace in one-dimensional semilinear diffusion equations . . 3557

Hermen Jan Hupkes (joint with E. S. Van Vleck)
Negative Diffusion in High Dimensional Lattice Systems - Travelling Waves 3559

Martina Chirilus-Bruckner (joint with C. E. Wayne)
On the existence of breathers in nonlinear wave equations: An approach via inverse spectral theory 3559

Jens Rottmann-Matthes
Freezing traveling waves with application to a hyperbolic Hodgkin-Huxley system 3562

Pavel Gurevich, Sergey Tikhomirov
Reaction-diffusion equations with hysteresis 3565

Scott Gregory McCalla (joint with Björn Sandstede)
Radially symmetric spot solutions for the Swift–Hohenberg equation 3568

Frits Veerman (joint with Arjen Doelman)
Pulses in singularly perturbed reaction-diffusion equations 3570

Denny Otten
Spatial decay of rotating waves in parabolic systems 3571

Leonhard Lücken (joint with Jan Philipp Pade, Kolja Knauer and Serhiy Yanchuk)
Reduction of delays in networks 3574

Isabelle Schneider
Stabilization of symmetrically coupled oscillators by time-delayed feedback control 3576

Nitsan Ben-Gal (joint with Kristen S. Moore, Juliette Hell)
Non-compact Global Attractors for Slowly Non-dissipative Reaction-Diffusion Equations 3577

Eckehard Schöll
Control of delay-coupled network dynamics 3578

Fatihcan M. Atay (joint with Özge Erdem)
Patterns of synchrony in networks of coupled oscillators 3581

Aaron Hoffman (joint with Hermen Jan Hupkes, Erik Van Vleck)
Multidimensional stability of traveling waves in lattice differential equations 3582

Yuri Latushkin (joint with W.-J. Beyn and J. Rottmann-Matthes)
Finding eigenvalues of holomorphic Fredholm operator pencils using boundary value problems and contour integrals 3584

Margaret Beck (joint with C. Eugene Wayne)
Rapid convergence to quasi-stationary states of the 2D Navier-Stokes equation 3585

Alexander Mielke
Multiscale gradient systems and their amplitude equations 3588

Guido Schneider (joint with Kourosh, Sanei Kashani)
About the validity of Whitham's equation 3591

Laurette S. Tuckerman (joint with Nicolas Périnet, Damir Juric)
Exotic behavior of hexagonal Faraday waves 3594

Alastair Rucklidge (joint with Gérard Iooss, Anne Skeldon, Mary Silber)
Three-Wave Interactions, Quasipatterns and Spatiotemporal Chaos 3597

Robert L. Pego (joint with G. Menon, B. Niethammer, G. Iyer, N. Leger)
Coagulation dynamics for random fronts and branching processes 3599

David A. Hipp, Marlis Hochbruck, Alexander Ostermann
Exponential integrators for parabolic problems with time dependent coefficients 3602

John Mallet-Paret (joint with Shui-Nee Chow, Kening Lu, and Wenxian Shen)
Waves in lattices with imperfections 3606

Hans-Otto Walther
Chaos via Variable Delay 3607

Tibor Krisztin (joint with Gabriella Vas, Hans-Otto Walther, Jianhong Wu)
Attractor Spindles for Delay Differential Equations 3609

Carlos Rocha (joint with Bernold Fiedler, Matthias Wolfrum)
Connection Graphs for Sturm Attractors of S^1-Equivariant Parabolic Equations 3611

Anna Ghazaryan (joint with Stephen Schecter, and Peter Simon)
Combustion fronts in a gasless combustion model with heat loss 3613

Jens D. M. Rademacher (joint with (in part) M. Chirilus-Bruckner, P. van Heijster, A. Doelman)
Singularities and intrinsic front dynamics of FitzHugh-Nagumo type systems 3614

Yasumasa Nishiura (joint with Masaki Yadome and Takashi Teramoto)
Heterogeneity-induced pulse generators 3617

Karsten Matthies (joint with Adam Boden)
Existence and Homogenisation of Travelling Waves Bifurcating from Resonances of Diffusion and Reaction in Periodic media 3619

Felix Otto
Domain and wall pattern in ferromagnets 3620

Matthias Wolfrum
Chimera states: patterns of coherence and incoherence in coupled oscillator systems 3622

Dwight Barkley
Death, life, and afterlife in shear turbulence 3625

Abstracts

Propagating terrace in one-dimensional semilinear diffusion equations

Hiroshi Matano
(joint work with Thomas Giletti, Arnaud Ducrot)

My talk is a summary of our recent work [1] and an ogoing work [3] concerning the front propagation in one-dimensional semilinear diffusion equations of the form

$$u_t = u_{xx} + f(x,u) \quad (x \in \mathbf{R}). \tag{1}$$

We consider a large class of spatially periodic nonlinearities f – including multi-stable ones – and study the asymptotic behavior of solutions with Heaviside type initial data. More precisely, f is a smooth function satisfying

$$f(x,0) = 0 \ \ ({}^\forall x \in \mathbb{R}), \qquad f(x+L,u) = f(x,u) \ \ ({}^\forall x \in \mathbb{R}, \ {}^\forall u \geq 0)$$

for some constant $L > 0$, and we assume that there exists a positive stationary solution $p(x)$:

$$p'' + f(x,p) = 0 \ \ (x \in \mathbf{R}), \qquad p(x+L) \equiv p(x) > 0.$$

We first discuss the existence of the propagating terrace, following the paper [1]. For this, we need a rather mild stability assumption on p; there exists a solution $0 \leq u(x,t) < p(x)$ such that its initial data $u_0(x) := u(x,0)$ is compactly supported and that $u(x,t)$ converges to $p(x)$ as $t \to \infty$. Such an assumption is satisfied by a large class of nonlinearities f and we do not need any further assumption.

Our analysis reveals some new dynamics where the profile of the propagation is not characterized by a single front, but by a layer of several fronts which we call a "propagating terrace". More precisely, a **propagating terrace** connecting 0 to p is a pair of finite sequences $(p_k)_{0\leq k\leq N}$ and $(U_k)_{1\leq k\leq N}$ such that:

- Each p_k is an L-periodic stationary solution of (1) satisfying
$$p = p_0 > p_1 > ... > p_N = 0.$$
- For each $1 \leq k \leq N$, U_k is a pulsating traveling wave solution of (1) connecting p_k to p_{k-1}.
- The speed c_k of each U_k satisfies $0 < c_1 \leq c_2 \leq \cdots \leq c_N$.

Furthermore, a propagating terrace $T = ((p_k)_{0\leq k\leq N}, (U_k)_{1\leq k\leq N})$ connecting 0 to p is said to be **minimal** if it also satisfies the following:

- For any propagating terrace $T' = ((q_k)_{0\leq k\leq N'}, (V_k)_{1\leq k\leq N'})$ connecting 0 to p, one has that $\{p_k \mid 0 \leq k \leq N\} \subset \{q_k \mid 0 \leq k \leq N'\}$.
- For each $1 \leq k \leq N$, the traveling wave U_k is steeper than any other traveling wave connecting p_k to p_{k-1}.

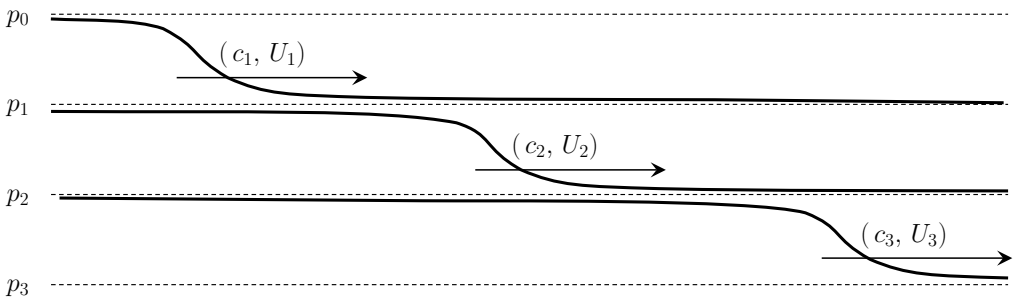

FIGURE 1. A three-step terrace

Roughly speaking, a propagating terrace can be pictured as a layer of several traveling fronts going at various speeds, the lower the faster (Figure 1). In the special case where $N = 1$, a propagating terrace is nothing but a traveling wave.

In [1], we have shown that, for any $a \in \mathbb{R}$, the solution of (1) with a Heaviside function type intial data $u_0(x) = p(x)$ $(x \le a)$, $= 0$ $(x > a)$ converges as $t \to \infty$ to a **minimal propagating terrace**. This convergence result automatically implies the existence of a propagating trerrace for equation (1).

Note that the meaning of *convergence* here is a bit nonstandard. Indeed, since the traveling waves $U_1, U_2, \dots, U_N$, which comprise the terrace, have different propagation speeds, we need multiple frames to define the convergence. Furthermore, the speeds $c_1, c_2, \dots, c_N$ are not *a priori* known, nor even the number N, therefore, one should use a rather flexible notion of generalized ω-limit points, as we did in [1]. The proof in [1] depends largely on the intersection number argument, without much relying on standard linear analysis. This allows us to deal with even highly degenerate type of nonlinearities.

Early analysis of such phenomena is found in Fife and McLeod [2], who studied propagating terraces (under different terminology) for a certain class of spatially homogeneous multistable nonlinearities f. However, it should be emphasized that we are not giving just another example of propagating terraces but are showing that convergence to a propagating terrace is a universal phenomenon for a very large class of nonlinearities, even with periodic heterogeneity.

Our second work [3] is concerned with the uniqueness of the propagating terrace. For this, we no longer need the stability assumption on p, but we instead need a mild nondegeneracy assumption on f.

REFERENCES

[1] A. Ducrot, T. Giletti and H. Matano, *Existence and convergence to a propagating terrace in one-dimensional reaction-diffusion equations*, to appear in Trans. Amer. Math. Soc.

[2] P.C. Fife, J. McLeod, *The approach of solutions of nonlinear diffusion equations to traveling front solutions*, Arch. Rational Mech. Anal. **65** (1977), 335–361.

[3] T. Giletti and H. Matano, *Uniqueness of propagating terraces*, in preparation.

Negative Diffusion in High Dimensional Lattice Systems - Travelling Waves

Hermen Jan Hupkes
(joint work with E. S. Van Vleck)

We consider bistable reaction diffusion systems posed on rectangular lattices in two or more spatial dimensions. The discrete diffusion term is allowed to have positive spatially periodic coefficients and the two spatially periodic equilibria are required to be well-ordered. We establish the existence of travelling wave solutions to such pure lattice systems that connect the two stable equilibria. In addition, we show that these waves can be approximated by travelling wave solutions to systems that incorporate both local and non-local diffusion. In certain special situations our results can also be applied to reaction diffusion systems that include (potentially large) negative coefficients. Indeed, upon splitting the lattice suitably and applying separate coordinate transformations to each sublattice, such systems can sometimes be transformed into a periodic diffusion problem that fits within our framework. In such cases, the resulting travelling structure for the original system has a separate wave profile for each sublattice and connects spatially periodic patterns that need not be well-ordered. There is no direct analogue of this procedure that can be applied to reaction diffusion systems with continuous spatial variables.

On the existence of breathers in nonlinear wave equations: An approach via inverse spectral theory

Martina Chirilus-Bruckner
(joint work with C. E. Wayne)

Consider the nonlinear wave equation

$$s(x)\partial_t^2 u(x,t) = \partial_x^2 u(x,t) + q(x)u(x,t) + \gamma u(x,t)^3, \tag{1}$$

where $x, t, u(x,t) \in \mathbb{R}$, s, q are real-valued, 1-periodic, even coefficients that are bounded from below by a positive constant and $\gamma \in \mathbb{R}$. We investigate the existence of solutions that are time-periodic and spatially localized, so-called breathers (see Figure 1). For constant coefficients this equation is not known to support such solutions, unless the nonlinearity is changed to turn it into the Sine-Gordon equation for which explicit formulas for breathers are known. In the setting of (1), a more common solution type related to breathers are generalized modulating pulses – as described in [4] for constant coefficients and [3] for periodic coefficients – featuring oscillating tales (see Figure 1). In this sense, breathers are a rare phenomenon.

We explore a new construction mechanism (already proposed in [1]) leading to a surprisingly large class of coefficients for which (1) supports breathers. In [1] a combination of spatial dynamics, center manifold reduction, bifurcation and averaging theory was used in order to construct small amplitude breathers. In contrast to breathers for the Sine-Gordon equation, whose existence seems to be

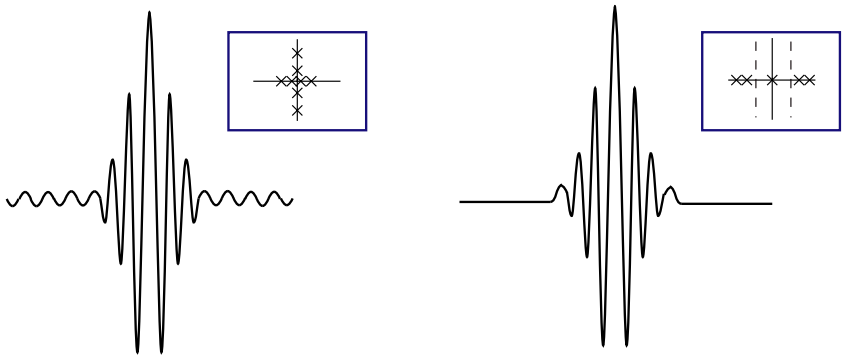

FIGURE 1. *Left panel*: Generalized modulating pulse and corresponding spectral picture with infinitely many eigenvalues on and off the imaginary axis. *Right panel*: Breather and corresponding spectral picture with all eigenvalues – except two creating a bifurcation – uniformly bounded away from the imaginary axis.

related to the special algebraic structure of the nonlinearity, the new mechanism for breather creation for (1) uses the degrees of freedom coming from the spatially periodic coefficients to tailor the linear part appropriately. The key idea is to tune s such that the band structure (whose evaluation at integer multiples of the breather frequency $\omega_* \in \mathbb{R}$ yields the spectral picture for the center manifold reduction) features uniformly open gaps at the locations $n^2\omega_*^2, n \in \mathbb{N}_{odd}$, for some $\omega_* \in \mathbb{R}$ and the band edges are uniformly bounded away from $n^2\omega_*^2, n \in \mathbb{N}_{odd}$, such that the spectral picture for the center manifold reduction yields only eigenvalues that are uniformly bounded away from the imaginary axis. The coefficient q is then used to create a bifurcation while leaving the asymptotic behavior of gaps untouched.

In general, it is not possible to derive explicit formulas for the band structure of the linear part of (1). However, in [1] this was achieved for the special choice of coefficients

$$s(x) = 1 + 15\chi_{[6/13,7/13)} \bmod(1), \quad q(x) = (q_0 - \varepsilon^2)s(x), \quad \omega_* = \frac{13}{16}\pi, \tag{2}$$

where q_0 is some explicitly defined number and $0 < \varepsilon \ll 1$ is a small bifurcation parameter that is used to construct the small amplitude breather. Note, however, that the direct tuning of coefficients and breather frequency in (2) is very sensitive, any arbitrary deviation will destroy the spectral picture and, hence, the breather construction. Moreover, other choices of coefficients lead to tedious computations involving special functions, hence, inhibiting a clean tuning as was possible for (2). Therefore, we pursue a different strategy for adjusting the band structure by formulating an inverse spectral problem for (the distance between) eigenvalues of specific boundary value problems. It is well-known (see for instance [2]) that the gap edges are given by a pair λ_n, λ_{n+1} of either periodic or anti-periodic eigenvalues for the second order ODE

$$y''(x) + [s(x)\lambda - q(x)]y(x) = 0, \quad x \in [0,1], \tag{3}$$

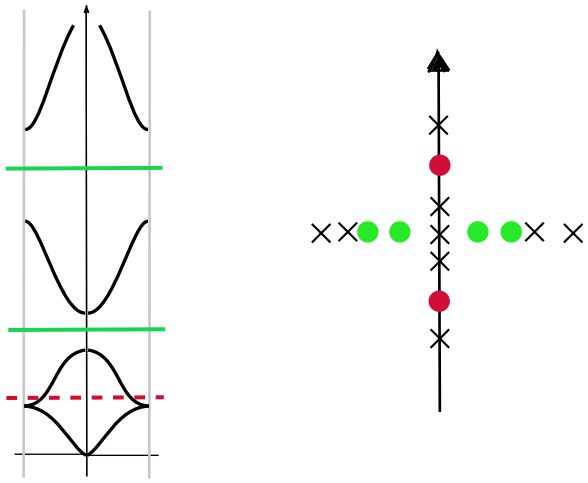

FIGURE 2. Band structure associated with the linear part of (1) and location of eigenvalues related to its evaluation at multiples of the breather frequency: Landing in gaps gives eigenvalues off the imaginary axis while hitting the band structure gives eigenvalues on the imaginary axis.

and that the corresponding Dirichlet and Neumann eigenvalues μ_n, ν_n are always situated in gaps, so $\lambda_n \leq \mu_n, \nu_n \leq \lambda_{n+1}, n \in \mathbb{N}$, which indicates that the distance of Dirichlet and Neumann eigenvalues gives a lower bound for the gap lengths. There is a vast amount of literature on inverse spectral theory for (3) (mostly for $s = 1$). We refrain from giving a complete list and simply highlight the most relevant references for the special setting we have in mind. The strategy for solving the inverse problem related to the special band structure set-up is inspired by the book [6] which deals with the inverse Dirichlet problem for (3) with $s = 1$ and $q \in L^2(0,1)$. Classic results in Sturm-Liouville theory show that the smoother the coefficients s, q the faster the asymptotic decay of gaps. More specifically, the possiblity for asymptotically open gaps is given if, for instance, s or s' feature jumps (cf. citeeastham), or, expressed in terms of function spaces, in case $s = 1$, we need $q \in H^m(0,1), m \in [-1, -1/2)$, which – in the spirit of the Liouville transformation – corresponds to $s \in H^r(0,1), r \in [1, 3/2)$ (although the transformation is not well-defined here). The Schrödinger case (*i.e.* (3) with $s = 1$) with singular potential q has been discuss in numerous recent articles, amoung the most relevant for our case being [5] and [7]. We follow estimation strategies from [5] in order to compute a refined eigenvalue estimate for Dirichlet and Neumann eigenvalues for the case $s \in H^r(0,1), r \in [1, 3/2), q = 0$, which is the backbone of the solution of the inverse problem. Our next step is to explore how q can be used to create the bifurcation and adapt the breather construction via center manifold theory as carried out in [1] to this new class of coefficients.

The problem of finding breathers for (1) is inspired by applications in photonics, the ultimate goal being the designing of a material (whose properties are encoded

by the coefficient s) that can be used as optical storage system based on standing light pulses, which – in the language of nonlinear wave equations – are breathers.

References

[1] C. Blank, M. Chirilus-Bruckner, V. Lescarret, G. Schneider. *Breathers in periodic media.* Journal **32** (2011), 100–120.

[2] M. S. P. Eastham. *Spectral theory for periodic differential equations.* Scottish Academic Press (1973)

[3] V. Lescarret, C. Blank, M. Chirilus-Bruckner, Ch. Chong, G. Schneider. *Standing generalized modulating pulse solutions for a nonlinear wave equation in periodic media.* Nonlinearity **22** (8) p. 1869-1898 (2009)

[4] M. D. Groves and G. Schneider. *Modulating pulse solutions for a class of nonlinear wave equations.* Comm. Math. Phys. **219**, 489–522 (2001).

[5] R.O. Hryniv and Y.V. Mykytyuk. *Eigenvalue asymptotics for Sturm-Liouville operators with singular potentials.* Journal of Functional Analysis **238** (2006) 27–57

[6] J. Pöschel, E. Trubowitz *Inverse spectral theory.* Academic Press, Inc. (1987)

[7] A.M. Savchuk, A.A. Shkalikov. *Sturm-Liouville operators with distributional potentials.* Mathematical Notes, Vol. **80**, No. 6, (2006), 814–832

Freezing traveling waves with application to a hyperbolic Hodgkin-Huxley system

Jens Rottmann-Matthes

In this talk we analyze the method of freezing for traveling waves [1]. Our main focus is on semilinear hyperbolic systems. The analysis for this class of systems is quite different from the analysis of the pure parabolic case done in [4] and which makes use of the strong results of analytic semigroup theory. Moreover, many of the technical difficulties that show up when analyzing the freezing method for coupled hyperbolic-parabolic problems already appear in the simpler hyperbolic case considered here.

The class of semilinear hyperbolic systems is of relevance not only from an academic point of view. As motivation consider the spatially extended Hodgkin-Huxley model. Recall that the change of the membrane potential $\frac{\partial}{\partial t}V(x,t)$ is made up of ionic currents I_{ionic}, given by ions passing through channels in the membrane, and a current q_x along the axon:

$$V_t + q_x = I_{\text{ionic}}.$$

Typically one assumes that the flux q is given by Fourier's law, i.e. $q = -kV_x$. This implies that the flux instantaneously depends on the gradient V_x and that the resulting system has infinite speed of information. We follow an approach of Cattaneo [2] to face these unphysical properties and replace Fourier's law by the Maxwell-Cattaneo law $\tau q_t + q = -kV_x$. Using this constitutive relation, the full

Hodgkin-Huxley system becomes

$$
\begin{aligned}
V_t + q_x &= -\overline{g_{\mathrm{K}}} n^4 (V - V_K) - \overline{g_{\mathrm{Na}}} m^3 h (V - V_{\mathrm{Na}}) - \overline{g_l}(V - V_l),\\
\tau q_t + q &= -k V_x,\\
n_t &= \alpha_n(V)(1-n) - \beta_n(V) n,\\
m_t &= \alpha_m(V)(1-m) - \beta_m(V) m,\\
h_t &= \alpha_n(V)(1-h) - \beta_h(V) h.
\end{aligned} \tag{1}
$$

The system develops a traveling wave solution. We then consider the Cauchy problem for abstract semilinear hyperbolic systems

$$
v_t = B v_x + f(v),\ v(x,0) = v_0, \qquad v(x,t) \in \mathbb{R}^m, x \in \mathbb{R}, t \geq 0. \tag{2}
$$

System (1) can be written in this form. Note that it is neither strictly hyperbolic (all eigenvalues of B are simple and distinct) nor is it a simple transport (B is a multiple of the identity. We impose on (2)

H1: B is real diagonalizable,
H2: $f \in \mathcal{C}^3(\mathbb{R}^m, \mathbb{R}^m)$,
H3: there exists a traveling wave solution $v(x,t) = \underline{v}(x - \underline{\lambda} t)$ of (2) with profile $\underline{v} \in \mathcal{C}^1_b$, $\underline{v}_x \in H^2$, $f(\underline{v}) \in L^2$, and velocity $\underline{\lambda}$.

In [3] it is shown that if the linear operator $\underline{B} v_x + \underline{C} v := (B + \underline{\lambda} I) v_x + f_v(\underline{v}) v$ satisfies the spectral assumptions

S1: $\underline{B}$ is invertible,
S2: let $\underline{C}_\pm := \lim_{x \to \pm\infty} C(x)$, there is $\delta > 0$ so that $s \in \sigma(i\xi \underline{B} + \underline{C}_\pm)$ for some $\xi \in \mathbb{R}$ implies $Re(s) < -\delta < 0$,
S3: zero is an algebraically simple eigenvalue of P and $\sigma_{\mathrm{pt}} \cap \{Re(s) \geq -\delta\} = \{0\}$,

nonlinear stability of the traveling wave with asymptotic stability follows. The proof is based on a nonlinear change of coordinates. Namely, one uses the ansatz

$$
v(\cdot, t) = \widetilde{v}(\cdot, t) + \underline{v}(\cdot - \Lambda(t)), \quad 0 = \Psi(\widetilde{v}), \tag{3}
$$

for the solution v of (2). This leads to a partial differential algebraic equation for Λ, $\lambda = \dot{\Lambda}$, and $\widetilde{v}$:

$$
\begin{aligned}
\widetilde{v}_t &= \underline{B} \widetilde{v}_x + f_v(\underline{v}) \widetilde{v} + \lambda \underline{v}_x + Q_{\mathrm{hen}}(\Lambda, \lambda, \widetilde{v}),\\
0 &= \Psi(\widetilde{v}).
\end{aligned} \tag{4}
$$

Here Q_{hen} is a quadratic function of its arguments. Stability is then proved by deriving linear stability using energy and resolvent estimates for the linear part. A bootstrap argument closes the argument for nonlinear stability.

In the special case of traveling waves for (2), the freezing method can be derived from the ansatz $v(x,t) = u(x - \Lambda(t), t)$, where u is a time dependent profile and Λ is a time dependent location of the profile. Similar to (3) one requires a constraint $\Psi(u - \widehat{u}) = 0$. The method then leads to a partial differential algebraic equation

for the unknowns u and $\lambda = \dot{\Lambda}$:

$$\begin{aligned} u_t &= Bu_x + \lambda u_x + f(u), \qquad u(0) = u_0, \\ 0 &= \Psi(u - \widehat{u}). \qquad \text{(phase condition)} \end{aligned} \tag{5}$$

On the phase condition we impose

Ph1: $\Psi \in \big(L^2(\mathbb{R}, \mathbb{R}^m)\big)'$,
Ph2: $\underline{v} - \widehat{v} \in H^1$ and $\Psi(\underline{v} - \widehat{v}) = 0$,
Ph3: $\Psi(\underline{v}_x) \neq 0$.

Under these conditions we can prove that stability with asymptotic phase for the original system (2) becomes stability in the sense of Lyapunov for the freezing system (5):

Theorem 1. *Impose* **H1**–**H3**, **S1**–**S3**, **Ph1**–**Ph3**. *Then for all* $0 < \delta_0 < \delta$ *there exists* $\rho_0 > 0$ *so that for all consistent initial data* (u_0, λ_0) *of the freezing equation* (5) *with* $\|u_0 - \underline{v}\|_{H^2} \leq \rho_0$ *hold exists a unique global solution* (u, λ) *of* (5) *and* $u - \underline{v} \in \mathcal{C}([0,T]; H^1) \cap H^1(0,T; L^2)$, $\lambda \in \mathcal{C}([0,T]; \mathbb{R}$ *for all* $T > 0$. *Moreover, there is* $C = C(\delta_0)$ *so that for all* $t \geq 0$ *holds*

$$\|u(t) - \underline{v}\|_{H^1}^2 + |\lambda(t) - \underline{\lambda}|^2 \leq C\|u_0 - \underline{v}\|_{H^2}^2 e^{-2\delta_0 t}. \tag{6}$$

The theorem is proved by using the result on asymptotic stability with asymptotic phase. To use the asymptotic stability with asymptotic phase for the proof limits the applicability to the all-line problem. But the freezing method is of particular interest on finite intervals and, therefore, a direct proof is sought.

In the talk we show that (5) leads to a system of the form

$$\begin{aligned} \widetilde{u}_t &= \underline{B}\widetilde{u}_x + f_v(\underline{v})\widetilde{u} + \lambda \underline{u}_x + Q_{\text{freeze}}(\lambda, \widetilde{u}, \widetilde{u}_x), \\ 0 &= \Psi(\widetilde{u}). \end{aligned} \tag{7}$$

The linear parts of (4) and (7) are precisely the same and the linear analysis for (4), outlined above, identically applies to (7). But because of a term $\lambda\widetilde{u}_x$ appearing in Q_{freeze} the linear estimates are not strong enough to close the argument and derive nonlinear stability. This term comes from the term λu_x in (5) which is a perturbation of the principal part and cannot be discussed as a small perturbation as in the parabolic case [4].

References

[1] W.-J. Beyn, V. Thümmler, *Freezing solutions of equivariant evolution equations*, SIAM J. Appl. Dyn. Syst. **3** (2004), 85–116.

[2] C. Cattaneo, *Sulla conduzione del calore.*, Atti Semin. Mat. Fis. Univ., Modena **3** (1948), 83–101.

[3] J. Rottmann-Matthes, *Stability and freezing of nonlinear waves in first order hyperbolic PDEs*, J. Dynam. Differential Equations **24** (2012), 341–367.

[4] V. Thümmler, *Numerical analysis of the method of freezing traveling waves*, PhD Thesis, Bielefeld (2004).

Reaction-diffusion equations with hysteresis

Pavel Gurevich, Sergey Tikhomirov

1. Hysteresis

Hysteresis operators arise in mathematical description of various physical, chemical and biological processes: thermocontrol, chemical reactors, ferro-magnetism, etc. (see the monographs [6, 7, 1]). It also appears as a formal limit in systems with different time scales.

We consider reaction-diffusion equations involving a hysteretic discontinuity defined at each spatial point. In particular, such problems describe chemical reactions and biological processes in which diffusive and nondiffusive substances interact according to hysteresis law. This leads to various spatial and spatio-temporal patterns. We concentrate on existence and uniqueness theory, connection with free boundary problems, and pattern formation. We treat both spatially continuous and spatially discrete systems.

Hysteresis $\mathcal{H}(g)(t)$ for a real-valued function $g(t)$ is defined as follows (cf. [6, 7] and Fig. 1). One fixes two thresholds $\alpha < \beta$ and two outputs $H_1 > H_{-1}$. If $g(t) \le \alpha$, then $\mathcal{H}(g)(t) = H_1$; if $g(t) \ge \beta$, then $\mathcal{H}(g)(t) = H_{-1}$; if $g(t)$ is between α and β, then $\mathcal{H}(g)(t)$ takes the same value as "just before."

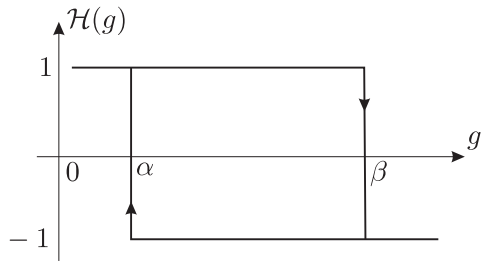

Figure 1. Hysteresis $\mathcal{H}$

2. Model problem

As a model problem, consider a growth of a colony of bacteria (Salmonella typhimurium) on a petri dish (see [2]). Let $Q \subset \mathbb{R}^n$ be a bounded domain, $B(x,t)$ denote the density of nondiffusing bacteria in Q, while $u(x,t)$ and $v(x,t)$ denote the concentrations of diffusing buffer (pH level) and histidine (nutrient) in Q, respectively. These three unknown functions satisfy the following equations in Q:

$$\begin{cases} B_t = aHB, \\ u_t = D_1 \Delta u - a_1 HB, \\ v_t = D_2 \Delta v - a_2 HB \end{cases}$$

supplemented by initial and no-flux (Neumann) boundary conditions. Here $D_1, D_2, a, a_1, a_2 > 0$ are given constants and the function $H = H(x,t)$ corresponds to the growth rate of bacteria and is defined by hysteresis law. In the simplest case, $H(x,t)$ takes value 1 if $u(x,t)$ and $v(x,t)$ are large enough, 0 if $u(x,t)$ and $v(x,t)$ are small enough, and remains constant in between (see Fig. 2, left image). Due to hysteresis (see [2]), concentric rings formed by $B(x,t)$ as $t \to \infty$ appear (see Fig. 2, right image).

3. Well-posedness

Due to discontinuity of hysteresis, well-posedness is not trivial. In [4, 3, 5], we found a broad class of initial data (transverse functions) for which a solution

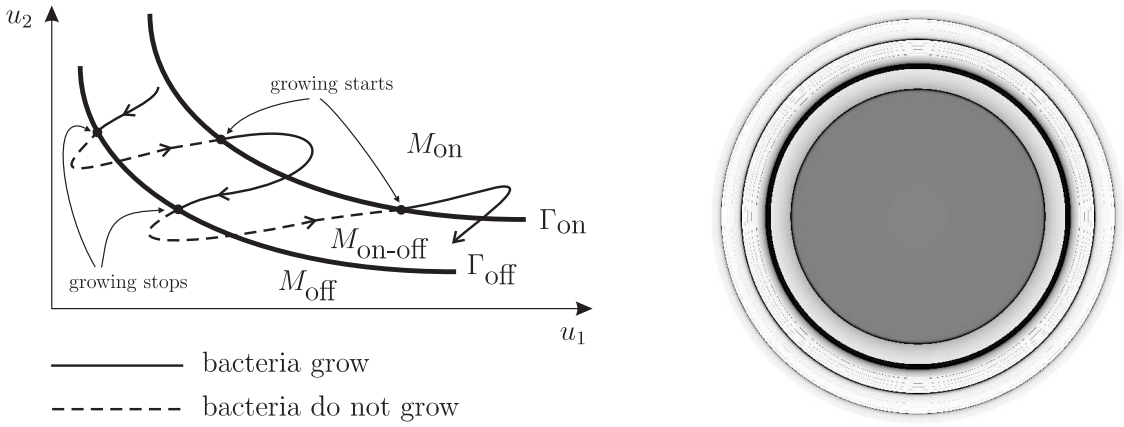

FIGURE 2. Left image: hysteresis depends on a region: $H = 1$ in M_{on}, $H = 0$ in M_{off}, H is constant in $M_{\text{on-off}}$. Right image: density of bacteria.

exists, is unique, and continuously depends on initial data. As far as we know, this is the first uniqueness result for such systems with hysteresis. The approach is based on tracking free boundaries which define the hysteresis topology. The main advantage of this approach is that one gets necessary information on the precise form of emerging spatio-temporal patterns.

4. Rattling

The transversality condition is typically satisfied at the initial moment, but it can fail as the solution evolves. To understand mechanisms of pattern formation, we need to consider nontransverse initial data as well. The simplest equation where complications arise is

$$u_t = u_{xx} + \mathcal{H}(u(x,\cdot))(t),$$

where $u(x,t) \in \mathbb{R}$, $x \in \mathbb{R}$, $t > 0$, and the initial condition is $u(x,0) = -cx^2$ with $c > 0$. Hysteresis $\mathcal{H}$ is defined as in Fig. 1 with $H_1 > 0$ and $H_{-1} < 0$. Its spatially discretized version reads

$$\dot{u}_n = \frac{u_{n-1} - 2u_n + u_{n+1}}{h^2} + \mathcal{H}(u_n), \quad n \in \mathbb{Z}, \tag{1}$$

with the initial condition $u_n(0) = -c(hn)^2$, where $u_n(t) = u(hn,t)$ and $h > 0$ is the grid size. Numerical simulation of (1) indicated that the hysteresis spatial profile is a step-like function continuous on intervals of length of order h (see Fig. 3). This phenomenon might have been a result of numerical errors, but we have proved that it is not. Further, analyzing results of numerical simulations, we conjecture that

$$\frac{\#\text{switched points}}{\#\text{not switched points}} \approx \left|\frac{H_1}{H_{-1}}\right|.$$

Situation becomes even more interesting in multidimensional domains. Spatial profile of hysteresis now depends on a type of lattice in the discretization scheme (see Fig. 4). This is a subject of future work.

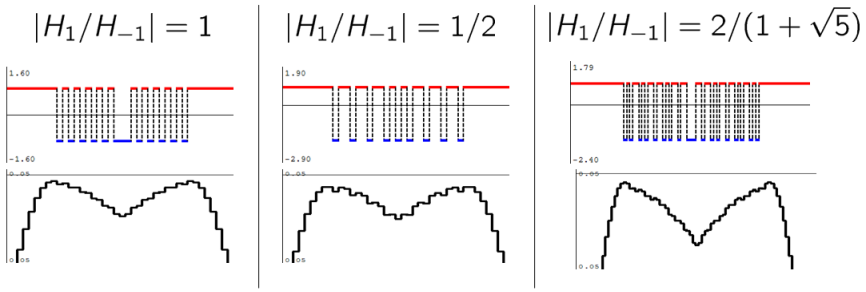

FIGURE 3. Spatial profile of $\mathcal{H}$ at a fixed time moment

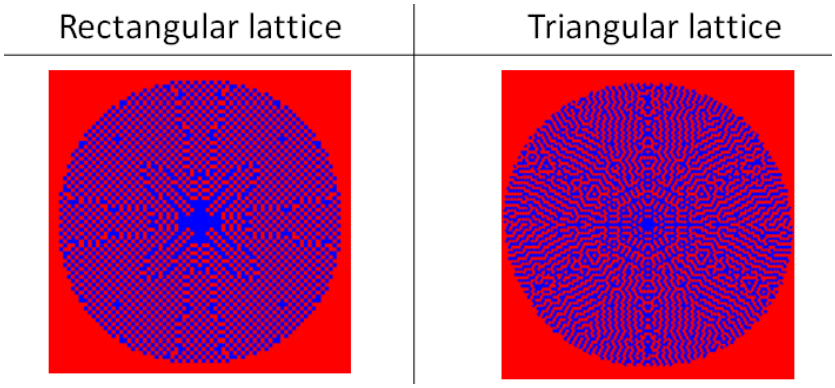

FIGURE 4. Hysteresis pattern depending on lattice for $|H_1/H_{-1}| = 1$.

REFERENCES

[1] M. Brokate, J. Sprekels, *Hysteresis and Phase Transitions*, Springer, Berlin, 1996.
[2] F. C. Hoppensteadt, W. Jäger, *Pattern formation by bacteria* Lecture Notes in Biomathematics **38**, 68–81 (1980).
[3] P. Gurevich, S. Tikhomirov *Uniqueness of transverse solutions for reaction-diffusion equations with spatially distributed hysteresis*, Nonlinear Analysis, **75**, 6610–6619 (2012).
[4] P. Gurevich, R. Shamin, S. Tikhomirov *Reaction-diffusion equations with spatially distributed hysteresis*, http://arxiv.org/abs/1205.3580
[5] P. Gurevich, S. Tikhomirov *Systems of reaction-diffusion equations with spatially distributed hysteresis*, http://arxiv.org/abs/1210.6252
[6] M. A. Krasnosel'skii, A. V. Pokrovskii, *Systems with Hysteresis*, Springer-Verlag, Berlin–Heidelberg–New York (1989).
[7] A. Visintin *Differential Models of Hysteresis*. Springer-Verlag. Berlin — Heidelberg (1994).

Radially symmetric spot solutions for the Swift–Hohenberg equation

Scott Gregory McCalla
(joint work with Björn Sandstede)

We are interested in the formation and parameter dependence of localized stationary radial solutions $u(x,t) = u(|x|)$ of the variational Swift–Hohenberg equation

$$u_t = -(1+\Delta)^2 u - \mu u + \nu u^2 - u^3, \qquad x \in \mathbb{R}^n, \tag{1}$$

that are bounded as $|x| \to 0$ and with $\lim_{|x|\to\infty} u(|x|) = 0$. These solutions satisfy

$$-\left(\partial_r^2 + \frac{n-1}{r}\partial_r + 1\right)^2 u - \mu u + \nu u^2 - u^3 = 0, \qquad r > 0 \tag{2}$$

with the boundary conditions $u_r(0) = u_{rrr}(0) = 0$ and $\lim_{r\to\infty} u(r) = 0$, where $r := |x|$. We treat the dimension n as a continuous parameter and discuss the bifurcation structure of these localized solutions for varying n, as well as rigorous existence results for localized spots at onset in two and three dimensions.

This equation was first derived by Swift and Hohenberg [6] to describe the effects of random thermal fluctuations on fluid convection just below onset. More generally, the Swift–Hohenberg equation serves as a paradigm for bistable pattern-forming systems. As shown in [5], the steady Swift–Hohenberg equation is also the normal-form equation for small-amplitude radial solutions at Turing bifurcations in reaction-diffusion systems. In [2], localized solutions of (2) were studied. For each fixed $\nu > 0$, it was shown there that (2) admits a spot (a localized solution whose amplitude is maximal at the core $r = 0$) for each $0 < \mu \ll 1$ and for each fixed $\nu > \nu_* := \sqrt{27/38}$ two ring solutions (localized solutions whose amplitude is maximal away from the core) for each positive μ close to zero. The amplitude of the spots and rings constructed in [2] scale like $\sqrt{\mu}$ as μ goes to zero. In the subsequent work [3], we numerically found a second family of spots that exists in (2) for $\nu > \nu_*$ and whose amplitude appears to scale like $\mu^{\frac{3}{8}}$ as μ goes to zero; in particular, their amplitude is larger than that expected from the asymptotic Ginzburg–Landau equation. We remark that this second family was also found numerically in [1, Figure 11(c)] but the amplitude scaling was not investigated there. To distinguish this family from the one found earlier in [2], we refer to the spots with amplitudes of order $\mathrm{O}(\mu^{\frac{1}{2}})$ as spot A and to those with amplitudes of order $\mathrm{O}(\mu^{\frac{3}{8}})$ as spot B.

In equation (2), we can consider n as a continuous parameter and examine the dependence of localized patterns on the continuous dimension parameter n. We are particularly interested in solution profiles $u(r)$ that exist for $\mu > 0$ and are composed of stable roll structures. In one space dimension, these radial profiles resemble stable rolls with a localized envelope superimposed on them, so that they can be thought of as localized rolls. In two dimensions, the radial profiles are localized target patterns.

As we follow spot A up on its bifurcation curve, the curve eventually turns around, and the L^2-norm of the spots begins to decrease again. At this point,

the profile of the underlying pattern transforms from a spot to a ring. Similarly, spot B broadens for a while, but eventually transforms into a different ring and follows the ring bifurcation curve downwards. In particular, spots and rings are pairwise connected in parameter space. Above these two connected curves lies a family of stacked isolas of localized structures, which also terminates for a large enough value of the L^2-norm. Above these stacked isolas, there is a connected U-shaped solution curve that seems to extend up to infinite L^2-norm and exhibits defect-mediated snaking. Both of the two branches of this curve snake and the associated profiles cycle through spot A and B solutions. These branches seem to continue indefinitely towards increasing L^2-norm, but the width of the snaking regions in the μ-direction decreases.

We also discuss the proofs of the following theorems from [4] on the existence of two and three dimensional spot solutions in the region $0 < \mu \ll 1$ and explain the origin of the anomalous amplitude scaling using geometric blow-up techniques. The geometric blow-up analysis produces the exponent $\frac{3}{8}$ that appears in the amplitude scaling in 2D. For the planar result, we need to make the following assumption.

Hypothesis 1. *The equation*

$$A_{ss} = -\frac{A_s}{s} + \frac{A}{4s^2} + A - A^3, \qquad A \in \mathbb{R} \tag{3}$$

has a bounded nontrivial solution $A(s) = q(s)$ on $[0, \infty)$. In addition, the linearization of (3) about $q(s)$ does not have a nontrivial solution that is bounded uniformly on $\mathbb{R}^+$.

Theorem 1. *Fix $\nu > \nu_* := \sqrt{27/38}$ and assume that Hypothesis 1 is met; then there is a $\mu_0 > 0$ such that equation (1) with $n = 2$ has a stationary localized radial solution $u(x,t) = u^{\mathrm{B}}(|x|)$ of amplitude $\mathrm{O}(\mu^{\frac{3}{8}})$ for each $\mu \in (0, \mu_0)$. More precisely, there is a constant $d > 0$ such that $u^{\mathrm{B}}(|x|)$ has the expansion*

$$u^{\mathrm{B}}(r) = -d\mu^{\frac{3}{8}} J_0(r) + \mathrm{O}(\sqrt{\mu})$$

uniformly on bounded intervals $[0, r_0]$ as $\mu \to 0$, where J_0 is the Bessel function of the first kind of order zero.

Theorem 2. *First, fix $\nu > 0$; then there is a $\mu_0 > 0$ such that equation (1) with $n = 3$ has a stationary localized radial solution $u(x,t) = u^{\mathrm{A}}(|x|)$ of amplitude $\mathrm{O}(\mu^{\frac{1}{2}})$ for each $\mu \in (0, \mu_0)$: there is a constant $d_{\mathrm{A}} > 0$ such that*

$$u^{\mathrm{A}}(r) = d_{\mathrm{A}}\mu^{\frac{1}{2}} \frac{\sin r}{r} + \mathrm{O}(\mu)$$

uniformly on bounded intervals $[0, r_0]$ as $\mu \to 0$. Second, fix $\nu > \nu_* = \sqrt{27/38}$; then there is a $\mu_0 > 0$ such that equation (1) with $n = 3$ has a stationary localized radial solution $u(x,t) = u^{\mathrm{B}}(|x|)$ of amplitude $\mathrm{O}(\mu^{\frac{1}{4}})$ for each $\mu \in (0, \mu_0)$: there is a constant $d_{\mathrm{B}} > 0$ such that

$$u^{\mathrm{B}}(r) = -d_{\mathrm{B}}\mu^{\frac{1}{4}} \frac{\sin r}{r} + \mathrm{O}(\sqrt{\mu})$$

uniformly on bounded intervals $[0, r_0]$ *as* $\mu \to 0$.

References

[1] N. E. Kulagin, L. M. Lerman, and T. G. Shmakova, *On radial solutions of the Swift-Hohenberg equation*, Tr. Mat. Inst. Steklova **261** (2008), no. Differ. Uravn. i Din. Sist., 188–209. MR 2489705 (2010b:35221)

[2] D. J. B. Lloyd and B. Sandstede, *Localized radial solutions of the Swift–Hohenberg equation*, Nonlinearity **22** (2009), no. 2, 485–524.

[3] S. McCalla and B. Sandstede, *Snaking of radial solutions of the multi-dimensional Swift–Hohenberg equation: A numerical study*, Phys. D **239** (2010), no. 16, 1581 – 1592.

[4] ———, *Spots in the Swift-Hohenberg equation*, Submitted, 2012.

[5] A. Scheel, *Radially symmetric patterns of reaction-diffusion systems*, Mem. Amer. Math. Soc. **165** (2003), no. 786. MR MR1997690 (2005c:35160)

[6] J. Swift and P. C. Hohenberg, *Hydrodynamic fluctuations at the convective instability*, Phys. Rev. A **15** (1977), no. 1, 319–328.

Pulses in singularly perturbed reaction-diffusion equations

Frits Veerman

(joint work with Arjen Doelman)

In the context of a general, singularly perturbed two-component system of reaction-diffusion equations

$$\begin{cases} U_t = \quad U_{xx} + F(U,V) \\ V_t = \varepsilon^2 V_{xx} + G(U,V) \end{cases}$$

with $x \in \mathbb{R}$, $t > 0$, $U, V \in \mathbb{R}$ and $0 < \varepsilon \ll 1$ asymptotically small, it is possible to construct singular stationary pulse solutions using geometric singular perturbation theory; only mild regularity assumptions on the model functions F and G are needed. The pulse is constructed to be asymptotic to the (stable) homogeneous background state $(\bar{U}, \bar{V})$ for which $F(\bar{U}, \bar{V}) = G(\bar{U}, \bar{V}) = 0$. Due to the singularly perturbed nature of the system – the diffusivity of the V-component is asymptotically small compared to that of the U-component – the existence problem exhibits a slow-fast structure, which allows for the use of geometric singular perturbation theory to prove the existence of a homoclinic pulse; see [1, 2] and the references therein.

The pulse stability can be investigated using Evans function techniques; in that way, a nonlocal eigenvalue problem (NLEP) is obtained. The Evans function can be decomposed in a fast and slow part, allowing the use of Sturm-Liouville theory for the slow and fast eigenvalue problems seperately. An explicit leading order expression for the (slow part of the) Evans function is obtained, reducing the stability analysis to finding the (complex) zeroes of that function. Here, the influence of the possible nonlinear slow dynamics (see [2]) becomes clear; new (in)stability results are obtained by studying certain parameter limits of the explicit part of the

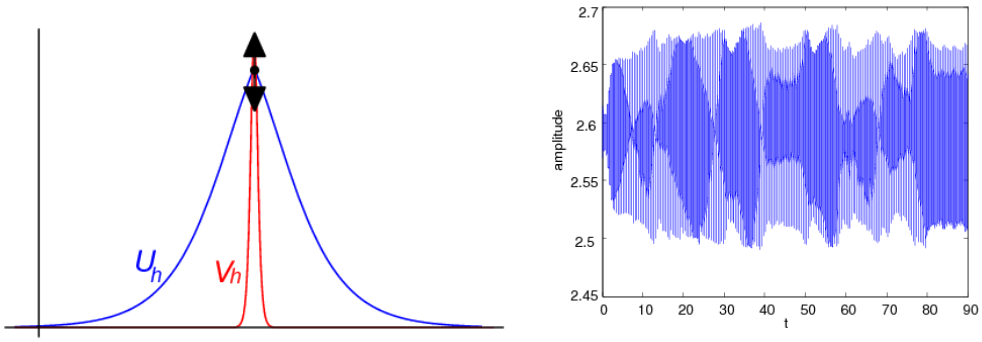

FIGURE 1. Direct numerical simulations of the stationary pulse solution to (1) near a Hopf bifurcation. The pulse oscillates with a quasiperiodically/chaotically modulated amplitude.

Evans function. In the context of the explicit slowly nonlinear Gierer-Meinhardt system studied in [2],

$$(1) \qquad \begin{cases} U_t &= U_{xx} - \left(\mu U - \nu_1 U^d\right) + \frac{\nu_2}{\varepsilon} V^2 \\ V_t &= \varepsilon^2 V_{xx} - V + \frac{V^2}{U} \end{cases}$$

it is possible to go beyond the instability results obtained for the general system and prove pulse stability for certain parameter regions.

Direct numerical simulation of the stationary pulse corraborates the analytical results; moreover, as yet unexplained quasiperiodic/chaotic behaviour is observed near Hopf bifurcations, see Figure 1.

Current research focuses on understanding this behaviour, using center manifold reduction near the Hopf bifurcation and analysing the resulting normal form, by calculating the corresponding Lyapunov coefficients to leading order. The analytical grip on these pulse solutions opens the door to future research: using the same techniques, multipulses and wavetrains can be constructed and analyzed; moreover, the dynamic interaction of these pulse solutions is yet to be understood.

REFERENCES

[1] A. Doelman, F. Veerman, *An explicit theory for pulses in two component, singularly perturbed, reaction-diffusion equations*, submitted to J. Dyn. Diff. Eq. (2012).

[2] F. Veerman, A. Doelman, *Pulses in a Gierer-Meinhardt equation with a slow nonlinearity*, to appear in Siam. J. Dyn. Sys. (1990).

Spatial decay of rotating waves in parabolic systems

DENNY OTTEN

Consider a reaction diffusion system

$$(1) \qquad \begin{aligned} u_t(x,t) &= A\triangle u(x,t) + f(u(x,t)),\ t > 0,\ x \in \mathbb{R}^d,\ d \geqslant 2, \\ u(x,0) &= u_0(x) \qquad\qquad\qquad\qquad ,\ t = 0,\ x \in \mathbb{R}^d. \end{aligned}$$

with diffusion matrix $A \in \mathbb{R}^{N,N}$, nonlinearity $f \in C^2(\mathbb{R}^N, \mathbb{R}^N)$, initial data $u_0 : \mathbb{R}^d \to \mathbb{R}^N$ and solution $u : \mathbb{R}^d \times [0, \infty[\to \mathbb{R}^N$.
A rotating wave of (1) is a special solution $u_\star : \mathbb{R}^d \times [0, \infty[\to \mathbb{R}^N$ of the form

$$u_\star(x,t) = v_\star(e^{-tS}x),$$

where $v_\star : \mathbb{R}^d \to \mathbb{R}^N$ is the profile (pattern) and $0 \neq S \in \mathbb{R}^{d,d}$ is a skew-symmetric matrix. Examples of rotating waves are spiral waves, scroll waves, spinning solitons, etc.
If u solves (1) then the function $v(x,t) = u(e^{tS}x, t)$, transformed into a rotating frame, solves

$$\begin{aligned} v_t(x,t) &= A\triangle v(x,t) + \langle Sx, \nabla v(x,t)\rangle + f(v(x,t)),\ t > 0,\ x \in \mathbb{R}^d,\ d \geqslant 2, \\ v(x,0) &= u_0(x) \qquad\qquad\qquad\qquad\qquad\qquad\quad ,\ t = 0,\ x \in \mathbb{R}^d. \end{aligned} \tag{2}$$

The linear operator is of Ornstein-Uhlenbeck type with an unbounded drift term containing angular derivatives

$$\langle Sx, \nabla v(x)\rangle := \sum_{i=1}^{d}\sum_{j=1}^{d} S_{ij}x_j\frac{\partial}{\partial x_i}v(x) = \sum_{i=1}^{d-1}\sum_{j=i+1}^{d} S_{ij}\left(x_j\frac{\partial}{\partial x_i} - x_i\frac{\partial}{\partial x_j}\right)v(x).$$

Observe that $v_\star$ is a stationary solution of (2), meaning that $v_\star$ solves

$$A\triangle v(x) + \langle Sx, \nabla v(x)\rangle + f(v(x)) = 0,\ x \in \mathbb{R}^d,\ d \geqslant 2. \tag{3}$$

Investigating steady state problems of this type is motivated by the stability theory of rotating patterns in several space dimensions, [1]. Equation (3) determines the shape and the angular speed of a rotating wave.
In this talk, we prove under certain conditions that every classical solution of (3) which falls below a certain threshold at infinity, must decay exponentially in space, meaning that the pattern is exponentially localized. This guarantees an exponentially small cut-off error if we restrict (3) to a bounded domain and justifies the numerical computation of rotating waves from boundary value problems on bounded domains.
We require $f(v_\infty) = 0$ and $\operatorname{Re}\sigma\,(Df(v_\infty)) < 0$ for some $v_\infty \in \mathbb{R}^N$. In addition to $\operatorname{Re}\sigma(A) > 0$ we impose the cone-condition

$$|\operatorname{Im}\lambda|\,|p-2| \leqslant 2\sqrt{p-1}\operatorname{Re}\lambda \quad \forall\,\lambda \in \sigma(A) \text{ for some } 1 < p < \infty$$

and assume that A, $Df(v_\infty) \in \mathbb{R}^{N,N}$ are simultaneously diagonalizable over $\mathbb{C}$. Further, we choose constants a_0, b_0, $a_{\max} > 0$ such that

$$a_0 \leqslant \operatorname{Re}\lambda,\ |\lambda| \leqslant a_{\max}\ \forall\,\lambda \in \sigma(A), \quad \operatorname{Re}\mu \leqslant -b_0 < 0\ \forall\,\mu \in \sigma(Df(v_\infty)).$$

Following [6], we call a positive function $\theta \in C(\mathbb{R}^d, \mathbb{R})$ a weight function of exponential growth rate $\eta \geqslant 0$ provided that

$$\exists\, C_\theta > 0 :\ \theta(x+y) \leqslant C_\theta\theta(x)e^{\eta|y|} \quad \forall\, x, y \in \mathbb{R}^d.$$

Finally, the exponentially weighted Sobolev spaces for $1 \leqslant p \leqslant \infty$, $k \in \mathbb{N}_0$ are defined by

$$L^p_\theta(\mathbb{R}^d, \mathbb{R}^N) := \left\{ v \in L^1_{\mathrm{loc}}(\mathbb{R}^d, \mathbb{R}^N) \mid \|\theta v\|_{L^p} < \infty \right\},$$
$$W^{k,p}_\theta(\mathbb{R}^d, \mathbb{R}^N) := \left\{ v \in L^p_\theta(\mathbb{R}^d, \mathbb{R}^N) \mid D^\beta u \in L^p_\theta(\mathbb{R}^d, \mathbb{R}^N) \; \forall\, |\beta| \leqslant k \right\}.$$

Under these assumptions the following statement holds:

Theorem 1. *For every $1 < p < \infty$, $0 < \vartheta < 1$ and for every radially nondecreasing weight function $\theta \in C(\mathbb{R}^d, \mathbb{R})$ of exponential growth rate $\eta \geqslant 0$ with*

$$0 \leqslant \eta^2 \leqslant \vartheta \frac{2}{3} \frac{a_0 b_0}{a^2_{\max} p^2}$$

there exists $K_1 = K_1(A, f, v_\infty, d, p, \theta, \vartheta) > 0$ with the following property:
Every classical solution $v_\star$ of equation (3) such that $v_\star - v_\infty \in L^p(\mathbb{R}^d, \mathbb{R}^N)$ and

$$\sup_{|x| \geqslant R_0} |v_\star(x) - v_\infty| \leqslant K_1 \text{ for some } R_0 > 0$$

satisfies

$$v_\star - v_\infty \in W^{1,p}_\theta(\mathbb{R}^d, \mathbb{R}^N).$$

In this talk we present the main idea of the proof based upon a linearization at infinity, also known as far-field linearization. Our investigations of the associated Ornstein-Uhlenbeck operator generalizes the results of [3], [4]. We determine the maximal domain of the operator in $L^p(\mathbb{R}^d, \mathbb{C}^N)$, analyze its constant and variable coefficient perturbations and derive resolvent estimates.
We apply the theory to the cubic-quintic complex Ginzburg-Landau equation

$$u_t = \alpha \triangle u + u\left(\mu + \beta |u|^2 + \gamma |u|^4\right), \quad u = u(x,t) \in \mathbb{C},$$

where $u : \mathbb{R}^d \times [0, \infty[\to \mathbb{C}$, $d \in \{2, 3\}$. For the parameters

$$\alpha = \frac{1}{2} + \frac{1}{2}i,\ \beta = \frac{5}{2} + i,\ \gamma = -1 - \frac{1}{10}i,\ \mu = -\frac{1}{2}$$

this equation exhibits so called spinning soliton solutions, [2], see Figure 1. The

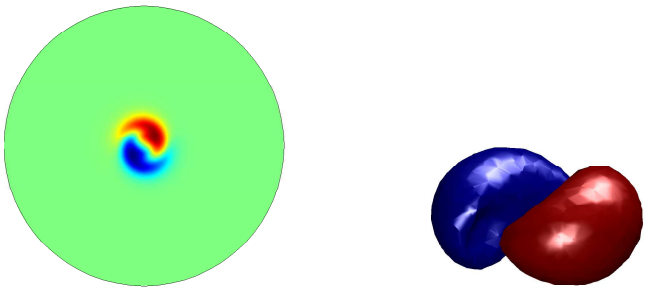

(a) $d = 2$ (b) $d = 3$

FIGURE 1. Spinning solitons of the Ginzburg-Landau equation

solitons are localized in the sense of Theorem 1 with the bound

$$0 \leqslant \eta^2 \leqslant \vartheta \frac{1}{3p^2} < \frac{1}{3p^2} \quad \text{for} \quad 2 \leqslant p \leqslant 6.$$

Details of the results may be found in the preprint [5] which forms the core of the authors' PhD thesis.

References

[1] W.-J. Beyn, J. Lorenz, *Nonlinear stability of rotating patterns*, Dyn. Partial Differ. Equ. **5**(4) (2008), 349–400.

[2] L.-C. Crasovan, B.A. Malomed, D. Mihalache, *Spinning solitons in cubic-quintic nonlinear media*, Pramana-journal of Physics **57** (2001), 1041–1059.

[3] G. Metafune, D. Pallara, V. Vespri, *L^p-estimates for a class of elliptic operators with unbounded coefficients in $\mathbf{R}^N$*, Houston J. Math. **31**(2) (2005), 605–620 (electronic).

[4] G. Metafune, *L^p-spectrum of Ornstein-Uhlenbeck operators*, Ann. Scuola Norm. Sup. Pisa Cl. Sci. (4) **30**(1) (2001), 97–124.

[5] D. Otten, *Spatial decay of rotating waves in parabolic systems*, Preprint 12139, CRC 701: Spectral Structures and Topological Methods in Mathematics, Bielefeld University, (2012), 1–91, http://www.math.uni-bielefeld.de/sfb701/files/preprints/sfb12139.pdf.

[6] S. Zelik, A. Mielke, *Multi-pulse evolution and space-time chaos in dissipative systems*, Mem. Amer. Math. Soc. **198** (2009), vi+97.

Reduction of delays in networks

Leonhard Lücken

(joint work with Jan Philipp Pade, Kolja Knauer and Serhiy Yanchuk)

Delayed interactions are a common property of coupled natural systems. For instance, signals in neural or laser networks propagate at finite speed giving rise to delayed connections. Such systems are often modeled by equations of the form

$$\frac{dx_j(t)}{dt} = f_j(x_j(t), x_1(t-\tau_{j,1}), ..., x_N(t-\tau_{j,N})), \quad j = 1, ..., N. \tag{1}$$

By a componentwise timeshift transformation (CTT)

$$y_j(t) := x_j(t+\eta_j), \ \eta_j \geq 0, \tag{2}$$

it is often possible to reduce the number of different delays considerably. The transformed solutions fulfill

$$\frac{dy_j(t)}{dt} = f_j(y_j(t), y_1(t-\tilde{\tau}_{j,1}), ..., y_N(t-\tilde{\tau}_{j,N})), \quad j = 1, ..., N. \tag{3}$$

with altered delays $\tilde{\tau}_{j,k} = \tau_{j,k} - \eta_j + \eta_k$. For example, a unidirectional ring

$$\frac{dx_j(t)}{dt} = f_j(x_j(t), x_{j+1}(t-\tau_{j+1})),$$

can always be reduced to a system with only one delay (either the same delay on all connections or zero delays on all but one connection) by choosing adequate timeshifts η_j [1, 2]. Thereby, the CTT may simplify the analysis of the system.

We show that a similar reduction is possible for arbitrary networks [3]. More precisely, there exists always a spanning tree S (a set of $N-1$ links which contains no cycles) and timeshifts $\eta_j \geq 0$ such that the transformed system has instantaneous connections on all links within S, i.e., $\tilde{\tau}(\ell) = 0$ for all $\ell \in S$.

The CTT has evoked interest as well because it serves as a strikingly simple mechanism for pattern generation [1, 2] – see fig. 1. However, previous studies

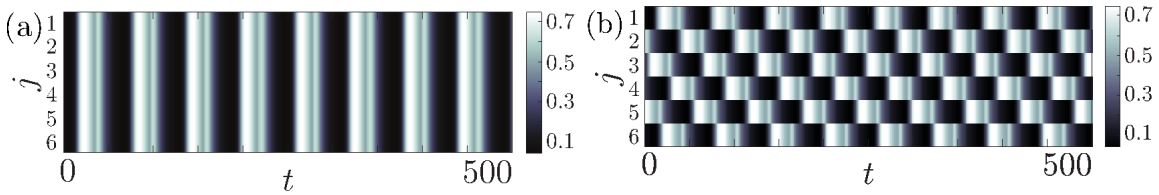

FIGURE 1. Pattern generation by componentwise timeshifts. Panel (a) shows a synchronous solution in a unidirectionally coupled ring of six identical Mackey-Glass Oscillators with homogeneous interaction delays and panel (b) shows the transformed solution in the system where the delay is concentrated on a single connection. The states of the different components are color coded in the different horizontal bands

didn't note a subtle difference between the semidynamical systems (1) and (3), which should be mentioned. They are not dynamically equivalent in the classical sense of topological conjugacy nor orbitally equivalent. This is due to the fact, that (2) is not invertible, since the possible inverse,

$$x_j(t) = y_j(t - \eta_j), \tag{4}$$

is not defined if the solution $y(t)$ of (3) is not defined for all $t < 0$. However, there exist inverse timeshifts $\tilde{\eta}_j = \bar{\eta} - \eta_j \geq 0$, $\bar{\eta} = \max_j\{\eta_j\}$, which transform (3) into (1). To state this more clearly, consider semiflows

$$\Phi : \mathbb{R} \times X \to X \text{ of (1), and } \Psi : \mathbb{R} \times \tilde{X} \to \tilde{X} \text{ of (3)},$$

where X and $\tilde{X}$ are product spaces of continuous history functions. Then, (1) and (3) are equivalent in the sense that there exist mappings

$$T : X \to \tilde{X} \text{ and } \tilde{T} : \tilde{X} \to X,$$

which fulfill

$$T \circ \Phi = \Psi \circ T, \text{ and } \tilde{T} \circ \Psi = \Phi \circ \tilde{T},$$

and

$$T \circ \tilde{T} = \Psi_{\bar{\eta}}, \text{ and } \tilde{T} \circ T = \Phi_{\bar{\eta}}.$$

This type of equivalence implies that there exists a natural one-to-one correspondence between invariant and strongly invariant sets of (1) and (3) and, given the Lipschitz-continuity of T and $\tilde{T}$, corresponding sets have the same type of stability.

References

[1] S. Yanchuk, P. Perlikowski, O. Popovych, P. Tass, *Variability of spatio-temporal patterns in non-homogeneous rings of spiking neurons*, Chaos **21**, 047511 (2011)

[2] O. Popovych, S. Yanchuk and P. Tass, *Delay- and coupling-induced firing patterns in oscillatory neural loops*, Phys. Rev. Lett. 107, 228102 (2011)

[3] L. Lücken, J. P. Pade, K. Knauer, S. Yanchuk, *Reduction of interaction delays in networks*, arXiv:1206.1170

Stabilization of symmetrically coupled oscillators by time-delayed feedback control

Isabelle Schneider

Consider a ring of identical oscillators in Hopf normal form with symmetric nearest-neighbour coupling. The system possesses a $D_n \times S^1$ - symmetry. The aim is to stabilize the inherently unstable periodic orbits with discrete rotating wave symmetry. These orbits emerge from a symmetric Hopf-bifurcation. Time-delayed feedback control (Pyragas control, [1]) is introduced.

Going beyond previous results by Fiedler et al. [2, 3], the spatio-temporal symmetry of the system is used to establish a noninvasive control method. The control term can also include multiple symmetry elements with distinct time-delays.

Due to a suitable control term the symmetric Hopf bifurcation splits into simple Hopf bifurcations with a two dimensional central manifold. As a consequence standard exchange of stability in two dimensions is now applicable.

As a result, it is for the first time possible to state explicit analytic conditions for the stabilization of the unstable periodic orbit with discrete rotating wave symmetry. These conditions are necessary and sufficient. It has to be distinguished between the sub- and supercritical cases and within the subcritical case between hard and soft springs.

The focus has mainly been on the case of three oscillators [4] as the simplest example admitting nontrivial symmetry, but the work has recently been extended to systems with n oscillators.

References

[1] K. Pyragas, *Continous control of chaos by self-controlling feedback*, Phys. Lett. A **170** (1992), 421–428.

[2] B. Fiedler, V. Flunkert, M. Georgi, P. Hövel, E. Schöll, *Refuting the odd number limitation of time-delayed feedback control*, Phys. Rev. Lett. **98** (2007), 114101.

[3] B. Fiedler, V. Flunkert, P. Hövel, E. Schöll, *Delay stabilization of periodic orbits in coupled oscillator systems*, Phil. Trans. Roy. Soc. A **368** (2010), 319–341.

[4] I. Schneider, *Stabilisierung von drei symmetrisch gekoppelten Oszillatoren durch zeitverzögerte Rückkopplungskontrolle*, Bachelor Thesis, Free University of Berlin (2011).

Non-compact Global Attractors for Slowly Non-dissipative Reaction-Diffusion Equations

Nitsan Ben-Gal
(joint work with Kristen S. Moore, Juliette Hell)

We study the asymptotic shape profiles and global attractor structure of a class of asymptotically asymmetric scalar reaction-diffusion equations

$$u_t = u_{xx} + \underbrace{b^+u^+ - b^-u^- + g(u)}_{f(u)}, \quad x \in [0,\pi], \quad u(0) = u(\pi) = 0 \tag{1}$$
$$u^+ = \max\{u, 0\}, \quad u^- = \max\{-u, 0\},$$

where $g(u)$ is uniformly bounded and $f(u) \in C^2$. For $b^+ \geq 1$ and/or $b^- \geq 1$, such equations are slowly non-dissipative, i.e. some solutions undergo infinite-time blow-up but none undergo finite-time blow-up. Reaction-diffusion equations with jumping nonlinearities, as in Equation (1), arise in the study of suspension bridge dynamics. For the special case where $b^+ = b^-$, one can obtain explicit decompositions of the non-compact global attractor structure [1]. The focus of this work is to extend these results to the asymmetric case, where $b^+ \neq b^-$.

Theorem 1. *The non-compact global attractor for Equation (1) is the union of its classical equilibria, their connecting heteroclinics, its equilibria at infinity, trans-finite heteroclinics connecting classical equilibria to equilibria at infinity, and the intra-infinite heteroclinics which connect equilibria at infinity to each other. For the near-symmetric form of Equation (1), the entire non-compact attractor can be decomposed explicitly. For stronger asymmetry and a given equilibrium v of (1) (either classical or at infinity), all classical equilibria and a subset of equilibria at infinity to which v possesses heteroclinic connections are determined.*

We refer to the set of classical equilibria and bounded heteroclinics as the bounded attractor, and the set of equilibria at infinity and intra-infinite heteroclinics as the attractor at infinity. Thus, Theorem 1 states that we are able to decompose the bounded attractor explicitly, as well as a subset of the attractor at infinity. We use time map analysis to determine that for generic choices of b^+, b^-, and $g(u)$ fulfilling our restrictions, we have a finite discrete set of classical equilibria contained within a bounded region in the Hilbert space. These equilibria lie on bifurcation surfaces in the three-dimensional bifurcation diagram, which we generate using a shooting method with Newton update and pseudoarclength continuation. The bifurcation surfaces are perturbations of the extensions of the classical Fučik spectrum curves into 3D, determined by $g(u)$.

As in both the dissipative case and the symmetric slowly non-dissipative case, we are able to use time map analysis, phase plane analysis, and nodal property methods to determine the set of classical equilibria and their zero numbers and Morse indices. We extend the y-map to the case of asymptotically asymmetric grow-up equations such as (1), which in conjunction with Matano's Principle [3] allows us to determine all possible asymptotic nodal behaviors of solutions to

(1). We apply this together with a quartet of blocking lemmas based on the zero numbers, Morse indices, and relative locations of stationary solutions in the bifurcation diagram, allowing us to obtain the complete set of bounded heteroclinic connections between classical equilibria.

Using a Poincaré compactification and the Conley index at infinity [2], we are able to determine that projections of the Fučik eigenfunctions to infinite norm compose a subset of the equilibria at infinity. We are able to uniquely determine a subset of both the transfinite heteroclinics and intra-infinite heteroclinics, specifically those connecting classical equilibria to the Fučik eigenfunctions at infinity, and the latter to each other. For $\delta << 1$ and $b^+ = b^- \pm \delta$, we are further able to use these techniques, the results from the symmetric case [1], and genericity arguments to show that the Fučik eigenfunctions are the only equilibria at infinity, and obtain the complete set of equilibria at infinity, transfinite heteroclinics, and intra-infinite heteroclinics.

The major open question for this problem is the ability to obtain the entirety of the attractor at infinity when δ is not small, i.e. in the far-from-symmetric case. The symmetry breaking removes numerous advantages which allowed us to obtain these results in [1], most notably the fact that the operator at infinity was linear (it is only half-linear for Equation (1)) and its eigenfunctions formed an orthonormal basis for the Hilbert space. Yet, our ability to obtain the complete non-compact global attractor decomposition in the near-symmetric case provides encouragement that these difficulties may be circumvented.

References

[1] N. Ben-Gal, *Non-compact global attractors for slowly non-dissipative PDEs II: the connecting orbit structure*, Accepted JDDE (2013).
[2] J. Hell, *Conley index at infinity*, arXiv preprint arXiv:1103.5335 (2011).
[3] H. Matano, *Nonincrease of the lap-number of a solution for a one-dimensional semilinear parabolic equation*, Journal of the Faculty of Science: University of Tokyo: Section IA **29** (1982), 401–441.

Control of delay-coupled network dynamics

Eckehard Schöll

Time delays arise naturally in many complex systems, for instance in neural networks or coupled lasers, as delayed coupling or delayed feedback due to finite signal transmission and processing times. Such time delays can either induce instabilities, multistability, and complex bifurcations, or suppress instabilities and stabilize unstable states. Thus, they can be used to control the dynamics [1]. Time delayed feedback [2] has been applied as a versatile and simple control method in many variants including spatio-temporal patterns [3, 4] and distributed feedback [5, 6]. Here we study synchronization in delay-coupled oscillator networks [7], using a master stability function approach, and show that for large coupling delays synchronizability relates in a simple way to the spectral properties of the network topology, allowing for a universal classification [8, 9]. As illustrative examples we consider

synchronization and desynchronization transitions in neural networks, in particular small-world networks with excitatory and inhibitory couplings [10, 11], and group synchronization in coupled chaotic lasers [12]. Within a model of Stuart-Landau oscillators, which represents a generic expansion of any system near a Hopf bifurcation into a normal form, we demonstrate that by tuning the coupling parameters one can easily control the stability of different synchronous periodic states, i.e., zero-lag, cluster, or splay states [13]. We show that adaptive algorithms of time-delayed feedback control can be used to find appropriate value of these parameters [14, 15, 16], and one can even self-adaptively adjust the network topology to realize a desired cluster state. Our results are robust even for slightly nonidentical elements of the network. Chimera states, where a network of identical oscillators splits into distinct coexisting domains of coherent (phase-locked) and incoherent (desynchronized) behaviour, have also gained much attention recently [17, 18, 19].

In summary, the master stability function of delay-coupled networks has a simple universal structure in the limit of large delay: it is rotationally symmetric around the origin and either positive and constant (if it is positive at the origin), or monotonically increasing and becomes positive at a minimum radius r_0. As a result, network structures can be classified into three types depending on the magnitude of the maximum transversal eigenvalue of the coupling matrix in relation to the magnitude of the row sum, resulting in distinct synchronization properties [8]. The rotational symmetry of the master stability function in delay-coupled networks of FitzHugh-Nagumo excitable systems has been established numerically and analytically even if the delay time τ is not large [10]. So the symmetry properties of the master stability function seem to be valid in even more general cases.

Furthermore, the master stability function approach can be extended to more general patterns of synchrony, i.e., cluster synchronization, and these can be stabilized by tuning the coupling parameters such as the coupling phase, coupling strength, and delay time [13, 12]. Adaptive control of these various synchronous states can be achieved by the speed gradient method. Choosing an appropriate goal function, a desired state of generalized synchrony can be selected by the self-adaptive automatic adjustment of a control parameter, i.e., the coupling phase. This goal function, which is based on a generalization of the Kuramoto order parameter, vanishes for the desired state, e.g., in-phase, splay, or cluster states, irrespectively of the ordering of the nodes [15]. The speed gradient method can also be applied to simultaneously tune the coupling phase, strength, and the time delay. In this way control of cluster and splay synchronization is possible without any a priori knowledge of the coupling parameters. Given the paradigmatic nature of the Stuart-Landau oscillator as a generic model, one may expect broad applicability, for instance to synchronization of networks in medicine, chemistry or mechanical engineering.

Acknowledgments
This work was supported by DFG in the framework of Sfb 910. I am indebted to

stimulating collaboration and discussion with K. Blyuss, C.-U. Choe, T. Dahms, B. Fiedler, I. Fischer, V. Flunkert, A. Fradkov, P. Hövel, W. Just, I. Kanter, A. Keane, W. Kinzel, Y. Kyrychko, J. Lehnert, K. Lüdge, Y. Maistrenko, I. Omelchenko, R. Roy, A. Selivanov, S. Yanchuk, A. Zakharova.

References

[1] E. Schöll and H. G. Schuster (Eds.): *Handbook of Chaos Control* (Wiley-VCH, Weinheim, 2008).

[2] K. Pyragas: *Continuous control of chaos by self-controlling feedback*, Phys. Lett. A **170**, 421 (1992).

[3] M. Kehrt, P. Hövel, V. Flunkert, M. A. Dahlem, P. Rodin, and E. Schöll: *Stabilization of complex spatio-temporal dynamics near a subcritical Hopf bifurcation by time-delayed feedback*, Eur. Phys. J. B **68**, 557 (2009).

[4] Y. N. Kyrychko, K. B. Blyuss, S. J. Hogan, and E. Schöll: *Control of spatio-temporal patterns in the Gray-Scott model*, Chaos **19**, 043126 (2009).

[5] Y. N. Kyrychko, K. B. Blyuss, and E. Schöll: *Amplitude death in systems of coupled oscillators with distributed-delay coupling*, Eur. Phys. J. B **84**, 307 (2011).

[6] Y. N. Kyrychko, K. B. Blyuss, and E. Schöll: *Amplitude and phase dynamics in oscillators with distributed-delay coupling*, Phil. Trans. R. Soc. A, to be published (2013).

[7] E. Schöll: *Synchronization in delay-coupled complex networks*, in *Advances in Analysis and Control of Time-Delayed Dynamical Systems* (World Scientific, Singapore, 2013), Ed. by J.-Q. Sun, Q. Ding, to be published.

[8] V. Flunkert, S. Yanchuk, T. Dahms, and E. Schöll: *Synchronizing distant nodes: a universal classification of networks*, Phys. Rev. Lett. **105**, 254101 (2010)

[9] V. Flunkert and E. Schöll: *Chaos synchronization in networks of delay-coupled lasers: Role of the coupling phases*, New. J. Phys. **14**, 033039 (2012).

[10] J. Lehnert, T. Dahms, P. Hövel, and E. Schöll: *Loss of synchronization in complex neural networks with delay*, Europhys. Lett. **96**, 60013 (2011).

[11] A. Keane, T. Dahms, J. Lehnert, S. A. Suryanarayana, P. Hövel, and E. Schöll: *Synchronisation in networks of delay-coupled type-I excitable systems*, Eur. Phys. J. B , 016202 (2012).

[12] T. Dahms, J. Lehnert, and E. Schöll: *Cluster and group synchronization in delay-coupled networks*, Phys. Rev. E **86**, 016202 (2012).

[13] C. U. Choe, T. Dahms, P. Hövel, and E. Schöll, Phys. Rev. E **81**, 025205(R) (2010).

[14] J. Lehnert, P. Hövel, V. Flunkert, P. Y. Guzenko, A. L. Fradkov, and E. Schöll: *Adaptive tuning of feedback gain in time-delayed feedback control*, Chaos **21**, 043111 (2011).

[15] A. A. Selivanov, J. Lehnert, T. Dahms, P. Hövel, A. L. Fradkov, and E. Schöll: *Adaptive synchronization in delay-coupled networks of Stuart-Landau oscillators*, Phys. Rev. E **85**, 016201 (2012).

[16] E. Schöll, A. A. Selivanov, J. Lehnert, T. Dahms, P. Hövel, and A. L. Fradkov: *Control of synchronization in delay-coupled networks*, Int. J. Mod. Phys. B **26**, 1246007 (2012).

[17] I. Omelchenko, Y. Maistrenko, P. Hövel, and E. Schöll: *Loss of coherence in dynamical networks: spatial chaos and chimera states*, Phys. Rev. Lett. **106**, 234102 (2011).

[18] I. Omelchenko, B. Riemenschneider, P. Hövel, Y. L. Maistrenko, and E. Schöll: *Transition from spatial coherence to incoherence in coupled chaotic systems*, Phys. Rev. E **85**, 026212 (2012).

[19] A. Hagerstrom, T. E. Murphy, R. Roy, P. Hövel, I. Omelchenko, and E. Schöll: *Experimental observation of chimeras in coupled-map lattices*, Nature Physics **8**, 658 (2012).

Patterns of synchrony in networks of coupled oscillators

Fatihcan M. Atay
(joint work with Özge Erdem)

The behavior of coupled oscillators are perhaps best known from synchronization studies; however, several other unique phenomena arise when one takes into account the signal transmission delays in the network. One of these is the complete cessation of oscillations, leading to the so-called oscillator death [1, 2]. Another example is the co-existence of multiple in-phase and anti-phase synchronous oscillations of different frequencies on bipartite graphs of simple phase oscillators [3]. In fact, the spatial arrangement of such solutions can be quite complicated, as manifested by *chimera states*, where the oscillators form regions of phase-locked solutions that are in anti-phase relation with the neighboring regions and separated from them by regions of incoherence [4].

The existence of such solutions leads to the question whether one can combine them in a graph in interesting ways. We are particularly interested in the case when the effect of a pair of oscillators in anti-phase cancel each other locally so as to produce an equilibrium at an intermediate node, schematically shown as

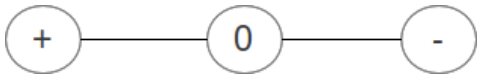

General network configurations would then consist of nodes displaying one of the patterns from the set $\{+,-,0\}$, whereby all nodes with symbol "+" oscillate in perfect synchrony with each other, but with a phase difference of π radians with the other group of synchronized nodes having symbol "−", and the nodes with symbol "0" have their oscillations quenched to an equilibrium.

The question is studied here in the setting of phase-amplitude oscillators and conditions for the stability of such patterns are derived. The combinatorial part of the problem consists of finding graphs allowing $\{+,-,0\}$ configurations in the above sense, subject to appropriate constraints (for example a "0" node should have the same number of "+" and "−" neighbors to ensure cancellation). Checking the stability of these patterns forms the dynamical part of the problem. As an example, we prove that the star graphs and some other graph types allow stable $\{+,-,0\}$ configurations:

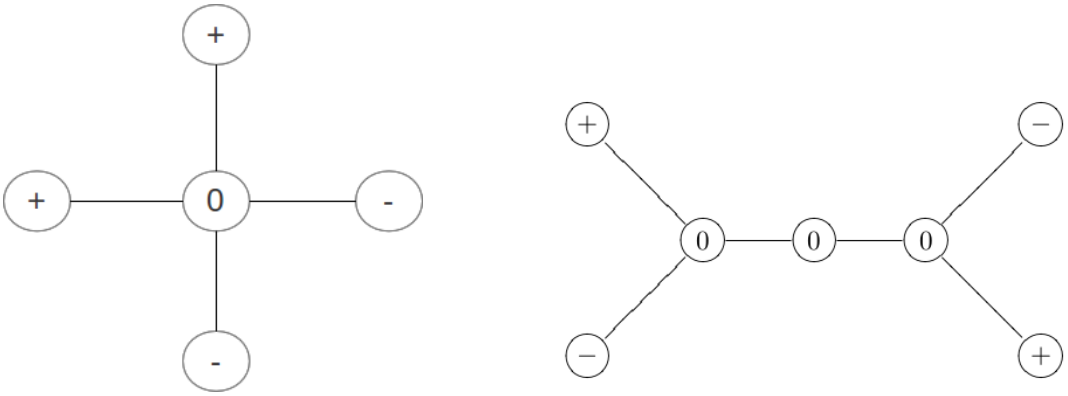

Thus, in general the questions of interest are: (1) Which graphs support stable $\{+,-,0\}$ patterns? (2) Can a graph support several such patterns (which are not related by trivial symmetries)?

References

[1] F. M. Atay, *Total and partial amplitude death in networks of diffusively coupled oscillators* Physica D **183** (2003) 1–18.

[2] F. M. Atay, *Oscillator death in coupled functional differential equations near Hopf bifurcation*, J. Differential Equations, **221** (2006) 190–209.

[3] N. Punetha, R. Ramaswamy, and F. M. Atay, *Synchronization in bipartite networks of oscillators with coupling delays*, MPI-MIS Preprint Series 4/2013.

[4] G. C. Sethia, A. Sen, and F. M. Atay, *Clustered chimera states in delay-coupled oscillator systems* Phys. Rev. Lett. **100** (2008) 144102.

Multidimensional stability of traveling waves in lattice differential equations

Aaron Hoffman

(joint work with Hermen Jan Hupkes, Erik Van Vleck)

Consider a system of lattice differential equations with nearest-neighbor coupling on the lattice $\mathbb{Z}^2$:

$$\dot{u}_{ij} = f(u_{i+1,j}, u_{i-1,j}, u_{i,j+1}, u_{i,j-1}, u_{ij}); \quad (i,j) \in \mathbb{Z}^2; \quad u_{ij}(t) \in \mathbb{R}^d$$

Assume that the system admits a smooth traveling wave which travels in a rational direction and connects two stable equilibria $u^{\pm} \in \mathbb{R}^d$:

$$u_{ij}(t) = \Phi(i\sigma_1 + j\sigma_2 + ct); \quad \Phi \in C^3(\mathbb{R}, \mathbb{R}^d); \quad (\sigma_1, \sigma_2) \in \mathbb{Z}^2; \quad \Phi(\pm\infty) = u^{\pm}.$$

Moreover impose strong spectral assumptions which guarantee that this wave is stable to perturbations that are constant in the transverse direction:

$$u_{ij}(0) = \Phi(i\sigma_1 + j\sigma_2) + v_{i\sigma_1 + j\sigma_2}.$$

We show that under additional mild spectral assumptions, the wave is stable to perturbations which are ℓ^1 in the transverse direction and ℓ^∞ in the wave direction:

$$u_{ij}(0) = \Phi(i\sigma_1 + j\sigma_2) + v_{ij}; \qquad \sup_{i\sigma_1 + j\sigma_2 = n} \sum_{j\sigma_1 - i\sigma_2 = l} |v_{ij}| < \epsilon.$$

Moreover, we establish algebraic rates of decay for the perturbation. Note however, that the wave itself does not exhibit any spatial decay in the transverse direction while we require ℓ^1 decay for the perturbation. In light of recent work in the PDE case [7], we expect that fronts would not be asymptotically stable (with or without asymptotic phase) to perturbations which are ℓ^∞-small in the transverse direction.

In spirit, our theorem says that so long as the linearization about the traveling wave is as nice as possible given that we are studying planar fronts in $\mathbb{Z}^2$, then the wave is nonlinearly stable. As such it may be regarded as a two-dimensional

version of [3, Theorem A] and also as a lattice version of [6]. Candidates for our result include the discrete Nagumo equation

$$\dot{u}_{ij} = u_{i+1,j} + u_{i-1,j} + u_{i,j+1} + u_{i,j-1} - 4u_{ij} + f(u_{ij})$$

the discrete Fitzhugh-Nagumo equation

$$\begin{cases} \dot{u}_{ij} = \alpha(u_{i+1,j} + u_{i-1,j} + u_{i,j+1} + u_{i,j-1} - 4u_{ij}) + g(u_{ij}) - w_{ij} \\ \dot{w}_{ij} = \epsilon(u_{ij} - \gamma w_{ij}) \end{cases}$$

and the Vaintchein-VanVleck equation

$$\begin{cases} \dot{x}_{ij} = d_e(y_{i+1,j} + y_{i-1,j} + y_{i,j+1} + y_{i,j-1} - 4x_{ij}) + g_e(x_{ij}) \\ \dot{y}_{ij} = d_o(x_{i+1,j} + x_{i-1,j} + x_{i,j+1} + x_{i,j-1} - 4x_{ij}) + g_o(y_{ij}) \end{cases}$$

as the one-dimensional versions of these problems all have sufficiently tame spectra [3, 4, 5]. However, line-solitons in planar Hamiltonian lattices and multidimensional systems of semi-discrete conservation laws are not candidates for our theorem, despite being stable in one space dimension [1, 8] because the spectrum for the one-dimensional problem is too complicated for our extension to the two-dimensional setting.

The strategy of proof is to separate the slowly decaying long-wave modulations of the interface from the rapidly decaying part of the perturbation via the ansatz

$$u_{ij}(t) = \Phi(n + ct + \theta_l(t)) + v_{nl}(t); \quad n = i\sigma_1 + j\sigma_2,\ l = j\sigma_1 - i\sigma_2$$

At the linear level, the coefficients are constant in l and thus can be reduced via Fourier Transform from an evolution equation in two space dimensions to a family of decoupled evolution equations in one space dimension, each of which can be analyzed using the tools of spatial dynamics, in particular as developed in [1, 2]. One now Fourier synthesizes the linear estimates obtained in the frequency domain and writes the nonlinear evolution as a fixed point equation in duhamel form. The most troublesome term arises, as expected, from the slow decay of the long-wave modulations of the interface. It can be captured in a toy model by the discrete Burgers equation:

$$\dot{\theta}_l = \theta_{l+1} + \theta_{l-1} - 2\theta_l + \theta_l(\theta_{l+1} - \theta_l)$$

The linear part is a discrete heat equation, hence generates a semigroup that decays like $t^{-1/4}$ when regarded as acting from ℓ^1 initial data to ℓ^2. As is typical the quadratic nonlinearity can be measured in ℓ^1 in terms of the ℓ^2 norms of the factors via Cauchy-Schwartz, but under the bootstrapping assumptions these factors decay like $t^{-1/4}$ and $t^{-3/4}$ respectively. The extra half-power in the second term arises because a spatial difference of a heat kernel decays faster than the heat kernel itself. This equation is critical because of the logarithmic factor in the integral estimate

$$\int_0^t (t - t_0 + 1)^{-1/4}(t_0 + 1)^{-1} dt_0 \sim (t + 1)^{-1/4} \log(t + 1)$$

which prevents the fixed point equation from closing.

However, upon using the identity

$$\theta_{l+1} - \theta_l = \frac{1}{2}\left((\theta_{l+1}^2 - \theta_l^2) + (\theta_{l+1} - \theta_l)^2\right)$$

which can be regarded as a discrete form of $uu_x = \left(\frac{1}{2}u^2\right)_x$ and summing by parts in the first term, we can improve our estimate to

$$\int_0^t (t - t_0 + 1)^{-3/4}(t_0 + 1)^{-1/2} dt_0 \sim (t+1)^{-1/4}$$

which closes. We remark that this critical term vanishes (or rather is pushed to higher order) in the special case that the wave direction is chosen to align with the lattice direction $\sigma = (1, 0)$. A significant open question regards the role of planar fronts and anisotropic effects of the lattice in the evolution of general initial data far from a planar front.

References

[1] M. Beck, H.J. Hupkes, B. Sandstede and K. Zumbrun, *Nonlinear Stability of Semidiscrete Shocks for Two-Sided Schemes* SIAM J. Math. Anal. **42** (2010) 857–903

[2] S. Benzoni-Gavage, P. Huot and F. Rousset *Nonlinear Stability of Semidiscrete Shock Waves* SIAM J. Math Anal **35** (2003) 639–707

[3] S.N. Chow, J. Mallet-Paret and W. Shen *Traveling Waves in Lattice Dynamical Systems* J. Diff. Eq. **149** (1998) 248–291

[4] H.J. Hupkes and B. Sandstede *Stability of Pulse Solutions for the Discrete Fitzhugh-Nagumo System* Trans. AMS, to appear

[5] H.J. Hupkes and E. Van Vleck *Negative Diffusion and Travelling Waves in High Dimensional Lattice Systems* preprint

[6] T. Kapitula *Multidimensional Stability of Planar Travelling Waves* Trans. AMS **349** (1997) 257–269

[7] H. Matano, M. Nara and M. Taniguchi *Stability of planar waves in the Allen-Cahn equation* Comm. PDE **34**(7-9) (2009) 976–1002

[8] G. Friesecke and R.L. Pego *Solitary Waves on Fermi-Pasta-Ulam Lattices. IV. Proof of Stability at Low Energy* Nonlinearity **17**(1) (2004) 229–251

Finding eigenvalues of holomorphic Fredholm operator pencils using boundary value problems and contour integrals

Yuri Latushkin

(joint work with W.-J. Beyn and J. Rottmann-Matthes)

Investigating the stability of nonlinear waves often leads to linear or nonlinear eigenvalue problems for differential operators on unbounded domains.

We propose to detect and approximate the point spectra of such operators (and the associated eigenfunctions) via contour integrals of solutions to resolvent equations. The approach is based on Keldysh' theorem [4] and extends a recent method [1] for matrices depending analytically on the eigenvalue parameter. We show that errors are well-controlled under very general assumptions when the resolvent equations are solved via boundary value problems on finite domains further developing

[2]. Two applications are presented: an analytical study of Schrödinger operators on the real line as well as on bounded intervals and a numerical study of the FitzHugh-Nagumo system.

We also relate the contour method to the well-known Evans function and show that our approach provides an alternative to evaluating and computing its zeroes.

A detailed exposition of the results can be found in [3].

References

[1] W.-J. Beyn, *An integral method for solving nonlinear eigenvalue problems,* Linear Algebra and Its Applications 436 (2012), 3839–3863.

[2] W.-J. Beyn and J. Rottmann-Matthes, *Resolvent estimates for boundry value problems on large intervals via the theory of discrete approximations*, Numer. Funct. Anal. Opt. **28** (2007), 603–629.

[3] W.-J. Beyn, Y. Latushkin and J. Rottmann-Matthes, *Finding eigenvalues of holomorphic Fredholm operators pencils using boundary value problems and contour integrals,* (preprint arXiv:1210.3952).

[4] R. Mennicken and M. Möller, *Non-self-adjoint Boundary Eigenvalue Problems,* North-Holland Publ., Amsterdam, 2003.

Rapid convergence to quasi-stationary states of the 2D Navier-Stokes equation

Margaret Beck

(joint work with C. Eugene Wayne)

It has been observed, numerically and experimentally, that solutions to the nearly-inviscid two-dimensional incompressible Navier-Stokes equation on the torus will rapidly approach certain long-lived quasi-stationary states. Evidence also suggests that these quasi-stationary, or metastable, states are connected with stationary solutions of the inviscid Euler equations. In [6], it is argued that certain maximum entropy solutions, determined using numerical and analytical techniques, of the inviscid Euler equation are the most probable quasi-stationary states that one would observe. They refer to these as dipole and bar states and confirm their predictions by numerically analyzing the Navier-Stokes equation and demonstrating that most solutions do indeed converge rapidly to one of these two classes of states. Furthermore, in [2], the authors consider a stochastically forced Navier-Stokes equation, and observe both the dipole and the bar states as statistical equilibria.

In this work, we provide analytical results indicating that there is a class of initial data for which solutions to the linearized equation rapidly converge to the bar states. More precisely, for small viscosity $0 < \nu \ll 1$, we prove that for a natural approximation to the linearized operator, there exists an invariant subspace in which solutions converge to the bar states at a rate that is $\mathcal{O}(e^{-\sqrt{\nu}t})$, which is much faster than the decay of the bar states themselves, which is $\mathcal{O}(e^{-\nu t})$.

Consider the 2D incompressible Navier-Stokes equation on the torus,

$$\partial_t \mathbf{u} = \nu \Delta \mathbf{u} - \mathbf{u} \cdot \nabla \mathbf{u} + \nabla p, \qquad \nabla \cdot \mathbf{u} = 0,$$

where $-\pi < x < \pi$, $-\pi < y < \pi$, $\mathbf{u} : \mathbb{T}^2 \to \mathbb{R}^2$ with periodic boundary conditions. The pressure $p(x, y, t)$ is a scalar valued function that also satisfies the periodic boundary conditions, and the viscosity ν is assumed to be small: $0 < \nu \ll 1$. The fluid vorticity ω is defined to be $\omega = \nabla \times \mathbf{u} = \partial_x \mathbf{u}_2 - \partial_y \mathbf{u}_1$. Taking the curl of the above equation, we find the two-dimensional vorticity equation

$$\partial_t \omega = \nu \Delta \omega - \mathbf{u} \cdot \nabla \omega, \tag{1}$$

where the scalar-valued function ω also satisfies periodic boundary conditions. The periodic boundary conditions for $\mathbf{u}$ imply that ω has zero mean, $\int_{\mathbb{T}^2} \omega = 0$. In this case, one can determine the velocity from the vorticity using the Biot-Savart law

$$\mathbf{u} = (-\partial_y \Delta^{-1} w, \partial_x \Delta^{-1} w).$$

The bar states and dipoles are given explicitly by

$$\omega^{\text{bar}}(x, y, t) = e^{-\nu t} \cos(x), \qquad \omega^{\text{dipole}}(x, y, t) = e^{-\nu t}(\cos(x) + \cos(y)),$$

and they are party of an infinite family of slowly-varying states given by

$$\omega^{\text{slow}}(x, y, t) = e^{-\nu m^2 t}(a_1 \cos(mx) + a_2 \sin(mx) + a_3 \cos(my) + a_1 \sin(my)).$$

We will focus on the bar states. Due to incompressibility and periodic boundary conditions, for any solution of (1) we have

$$\frac{d}{dt} \frac{1}{2} \int_{\mathbb{T}^2} \omega^2(x, y) \mathrm{d}x\mathrm{d}y = -\nu \int_{\mathbb{T}^2} |\nabla \omega(x, y)|^2 \mathrm{d}x\mathrm{d}y \leq -C\nu \int_{\mathbb{T}^2} \omega^2(x, y) \mathrm{d}x\mathrm{d}y,$$

where we have used Poincaré's inequality to obtain the final inequality. Thus, the slow decay rate of the bar states occurs on what is arguably the natural timescale for the system, determined by the viscosity ν.

Using the Ansatz $\omega = \omega^{\text{bar}} + v$, we see a perturbation of the bar state satisfies

$$\partial_t w = \mathcal{L}(t) w - \mathbf{u} \cdot \nabla w \tag{2}$$

$$\mathcal{L}(t) w = \nu \Delta w - e^{-\nu t} [\sin x \partial_y (1 + \Delta^{-1})] w, \tag{3}$$

where $\mathbf{u}$ is the velocity corresponding to w via the Biot-Savart law. Asymptotic analysis in [4] of the eigenvalues of the approximate operator $\nu\Delta - \sin x \partial_y$ suggests that solutions to the above equation should decay at the rapid rate $\mathcal{O}(e^{-\sqrt{\nu} t})$.

In order to provide some rigorous justification for this, we will focus on the linear evolution and use the theory of hypocoercive operators developed by Villani [5]. This is motivated by a similar application of that theory in [3]. However, we must first overcome two main difficulties. First, the presence of the above-mentioned infinite family of slowly decaying solutions means that we cannot expect all perturbations to decay rapidly. Therefore, we construct two invariant subspaces of solutions, effectively a center and a stable subspace, and then focus on the behavior within the stable subspace. Second, the above linear operator does not have the structure required in the abstract set-up of Villani. More precisely, it is not of the form $A^* A + B$, where $B^* = -B$. To overcome this, we employ a suitable change of variables.

To exploit the fact that the bar state is independent of y, we expand the perturbation in a Fourier series in that variable only: $v(x,y) = \sum_l \hat{v}_l(x)e^{ily}$. The above linear equation then becomes

$$\partial_t \hat{v}_l = \nu\Delta_l \hat{v}_l - \mathrm{i}le^{-\nu t}\sin x(1+\Delta_l^{-1})\hat{v}_l, \qquad \Delta_l = \partial_x^2 - l^2.$$

Within the invariant stable-like subspace, whose details can be found in [1], the change of variables $u = \sqrt{(1+\Delta_l^{-1})}\hat{v}_l$ is well-defined, and u satisfies

$$\partial_t u = \nu\Delta_l u - \mathrm{i}le^{-\nu t}\sqrt{(1+\Delta_l^{-1})}\sin x\sqrt{(1+\Delta_l^{-1})}u$$

In order to apply Villani's framework to the above linear operator, it would be natural to define $A = \partial_x$, $B = -\mathrm{i}le^{-\nu t}\sqrt{(1+\Delta_l^{-1})}\sin x\sqrt{(1+\Delta_l^{-1})}$, and $C := [A,B]$. The problem with this is that $[B,C] \neq 0$. In principle, this is not a problem, as one can consider higher order commutators: $[C,B]$, $[[C,B],B]$, ... However, to close the argument one typically needs to eventually have good control over the higher order terms, which we have not been able to obtain in our setting.

Therefore, we consider the approximate linearized equation

$$\partial_t u = \nu\Delta_l u - \mathrm{i}le^{-\nu t}\sin xu, \tag{4}$$

where we have neglected the nonlocal and typically higher-order term Δ^{-1}. For this operator, we set $A = \partial_x$, $B = -\mathrm{i}le^{-\nu t}\sin x$, $C = [A,B] = -\mathrm{i}le^{-\nu t}\cos x$, and note that $[B,C] = 0$. We can now use the functional, suggested in [5],

$$\Phi[u](t) = (u,u) + \alpha(Au,Au) - 2\beta\mathrm{Re}(Au,Cu) + \gamma(Cu,Cu)$$

for suitably chosen $\alpha,\beta,\gamma > 0$, to carry out energy estimates and obtain the following result. Define the Banach space

$$X = \Big\{ w \in L^2(\mathbb{T}^2) : \hat{w}_0 = 0, \sum_{l\neq 0}\left[\|\hat{w}_l\|^2 + \sqrt{\frac{\nu}{|l|}}\|\partial_x\hat{w}_l\|^2 + \frac{1}{\sqrt{\nu}|l|^{3/2}}\|C\hat{w}_l\|^2\right] =: \|w\|_X^2 < \infty \Big\}.$$

Theorem [1] *Given any constant τ and $T \in [0,\tau/\nu]$, there exist constants K and M that are $\mathcal{O}(1)$ with respect to ν such that the following holds. If ν is sufficiently small, then solutions to (4) with initial data $u_0 \in X$ satisfy*

$$\|u(t)\|_X^2 \leq Ke^{-M\sqrt{\nu}t}\|u_0\|_X^2, \qquad \forall t \in [0,T].$$

The result is only valid on the long, but finite, interval $[0,\tau/\nu]$. This is due to the time-dependence of the operator. In particular, if the "B" term is producing the rapid decay, we can only expect that decay to exist when B is $\mathcal{O}(1)$. This is sufficient to imply that perturbations decay rapidly to the bar states. When $t = 1/\nu$, the bar states are $\mathcal{O}(e^{-1})$, while the perturbations are $\mathcal{O}(e^{-M/\sqrt{\nu}}) \ll \mathcal{O}(e^{-1})$.

Directions for future research include obtaining a similar result for the full linear operator (3) and the nonlinear equation (2), as well as for the related equation obtained by linearization about a dipole. A long-term goal is to understand the transitions between bars and dipoles observed under stochastic forcing in [2].

References

[1] M. Beck and C. E. Wayne, *Metastability and rapid convergence to quasi-stationary bar states for the 2D Navier-Stokes equaiton*, to appear in Proc. Roy. Soc. Edinburgh. Currently available at http://arxiv.org/abs/1108.3416.

[2] F. Bouchet and E. Simonnet, *Random changes of flow topology in two-dimensional and geophysical turbulence*, Phys. Rev. Lett. **102**, no. 094504 (2009).

[3] I. Gallagher, Th. Gallay, and F. Nier, *Special asymptotics for large skew-symmetric perturbations of the harmonic oscillator*, Int. Math. Res. Not. IMRN **12** (2009) 2147–2199.

[4] J. Vanneste and J. G. Byatt-Smith, *Fast scalar decay in shear flow: modes and pseudomodes*, J. Fluid Mech. **572** (2007), 219-229.

[5] C. Villani, *Hypocoercivity*, Mem. Amer. Math. Soc. **202** (2009), 1-141.

[6] Z. Yin, D. C. Montgomery, and H. J. H. Clercx, *Alternative statistical-mechanical descriptions of decaying two-dimensional turbulence in terms of "patches" and "points"*, Phys. Fluids **15** (2003), 1937–1953.

Multiscale gradient systems and their amplitude equations

Alexander Mielke

1. Introduction. We propose a new method for deriving amplitude equations in the case that the original model is a gradient system $(X, \mathcal{F}_\varepsilon, \mathcal{R}_\varepsilon)$, i.e. the evolution is defined by the abstract balance between the viscous force and the potential restoring force:

$$0 = \mathrm{D}_{\dot u}\mathcal{R}_\varepsilon(u, \dot u) + \mathrm{D}\mathcal{F}_\varepsilon(u) \ \in X^*.$$

The state space X is a Hilbert space, and $\mathcal{F}_\varepsilon : X \to \mathbb{R}_\infty := \mathbb{R}\cup\{\infty\}$ denotes the energy functional. In general, the dissipation potential is such that $\mathcal{R}_\varepsilon(u, \cdot) : X \to [0, \infty]$ is a lower semicontinuous convex function satisfying $\mathcal{R}_\varepsilon(u, 0) = 0$. Here, we will restrict to the simplified setting that $\mathcal{R}_\varepsilon$ is independent of u and quadratic in $\dot u$, viz. $\mathcal{R}_\varepsilon(u, \dot u) = \frac{1}{2}\langle \mathbb{V}_\varepsilon \dot u, \dot u\rangle$.

The small parameter ε characterizes the ratio between the microscopic and the macroscopic length scale. The main question in evolutionary Γ-convergence is to identify conditions for the convergence of the pair $(\mathcal{F}_\varepsilon, \mathcal{R}_\varepsilon)$ to a limit $(\mathcal{F}_0, \mathcal{R}_0)$ such that the solutions $u_\varepsilon : [0, T] \to X$ for $(\mathcal{F}_\varepsilon, \mathcal{R}_\varepsilon)$ converge to the solutions $u_0 : [0, T] \to X$ of $(X, \mathcal{F}, \mathcal{R})$. We will use ideas of the recently derived sufficient conditions for evolutionary Γ-convergence for gradient systems [SaS04, Ste08, Ser10, MRS13, Mie13] and for rate-independent systems [MRS08, MiS11].

As an application we consider the Swift-Hohenberg equation (SHe)

$$v_\tau = -(1+\Delta)^2 v + \mu v + \gamma v^2 - v^3 \quad \text{with } |\gamma| < \gamma_*. \tag{1}$$

We will consider the one-dimensional case under the assumption that we are in the weakly unstable regime, i.e. $\mu = \varepsilon^2$. It was shown formally in [Eck65] that the typical solutions can be approximated by a modulated role pattern in the form $u(\tau, y) = \mathrm{Re}\,\big(A(\varepsilon^2\tau, \varepsilon y)\mathrm{e}^{\mathrm{i}y}\big)$ and that the amplitude function $A(t, x) \in \mathbb{C}$ satisfies the Ginzburg-Landau equation (GLe)

$$A_t = 4A_{xx} + A - \rho|A|^2 A, \quad \text{where } \rho = \tfrac{3}{8}(1 - \tfrac{\gamma^2}{\gamma_*^2}) > 0. \tag{2}$$

While τ and y denote the microscopic time and space scale, the variables $t = \varepsilon^2\tau$ and $x = \varepsilon y$ denote the macroscopic time and space scale.

First mathematical justification of this approximation was given in [vHa91, Sch94]. We refer to [Mie02] for a survey and to [KSM92] for a 4-page proof of the result in the case of cubic nonlinearities, i.e. $\gamma = 0$. We also will see that the case $\gamma \neq 0$ is substantially different. The comparison of the global attractors and the inertial manifolds of (1) and (2) are done in [MiS96] and [MSZ00], respectively.

2. Gradient systems and Γ-convergence. We highlight two different results on evolutionary Γ-convergence that are relevant for the Swift-Hohenberg equation. In both cases we consider the gradient system $(X, \mathcal{F}_\varepsilon, \mathcal{R}_\varepsilon)$, where X is a Hilbert space and $\mathcal{R}_\varepsilon(v) = \frac{1}{2}\langle v, \mathbb{V}_\varepsilon v\rangle$. We always assume that $\mathcal{R}_\varepsilon$ is bounded uniformly by the norm in X, namely

$$\exists\, C \geq 1\ \forall\, \varepsilon \in [0,1]\ \forall\, v \in X: \quad \tfrac{1}{C}\|v\|^2 \leq \mathcal{R}_\varepsilon(v) \leq C\|v\|^2. \tag{3}$$

Second we assume that the functionals $\mathcal{F}_\varepsilon$ have uniformly compact sublevels:

$$\forall\, E \in \mathbb{R}\ \exists\, K \subset X \text{ compact } \forall\, \varepsilon \in [0,1]\ \forall u \in X: \quad \mathcal{F}_\varepsilon(u) \leq E \ \Rightarrow\ u \in K. \tag{4}$$

The following result is a special case of the much more general upper semicontinuity result of the solution sets for nonsmooth generalized gradient systems in [MRS13, Thm. 4.4].

Theorem 1. *Given suitable natural conditions on $(X, \mathcal{F}_\varepsilon, \mathcal{R}_\varepsilon)$ including (3) and (4) assume the Mosco convergences $\mathcal{F}_\varepsilon \overset{\mathrm{M}}{\to} \mathcal{F}_0$ and $\mathcal{R}_\varepsilon \overset{\mathrm{M}}{\to} \mathcal{R}_0$. Then, the solutions $u_\varepsilon : [0,T] \to X$ of $(X, \mathcal{F}_\varepsilon, \mathcal{R}_\varepsilon)$ satisfy*

$$\begin{aligned} &u_\varepsilon(0) \rightharpoonup u_0(0) \text{ in } X \text{ and } \mathcal{F}_\varepsilon(u_\varepsilon(0)) \to \mathcal{F}_0(u_0(0)) \\ \Longrightarrow\quad &\forall\, t \in [0,T]:\ u_\varepsilon(t) \rightharpoonup u_0(t) \text{ in } X \text{ and } \mathcal{F}_\varepsilon(u_\varepsilon(t)) \to \mathcal{F}_0(u_0(t)). \end{aligned}$$

A second result is based on the concept of *evolutionary variational inequalities* (EVI), which was introduced in [AGS05] for gradient systems with geodesically λ-convex functionals. In our simplified setting, the family $(X, \mathcal{F}_\varepsilon, \mathcal{R}_\varepsilon)_{\varepsilon\in[0,1]}$ is called uniformly geodesically λ-cconvex, if

$$\forall\, \varepsilon \in [0,1]: \quad u \mapsto \mathcal{F}_\varepsilon(u) - \lambda\mathcal{R}_\varepsilon(u) \text{ is convex.} \tag{5}$$

Then, $u_\varepsilon : [0,T] \to X$ is a solution of $0 = \mathrm{D}\mathcal{R}_\varepsilon(\dot u) + \mathrm{D}\mathcal{F}_\varepsilon(u)$ if and only if

$$\begin{aligned} \forall\, w \in X: \quad &\frac{\mathrm{d}^+}{\mathrm{d}t}\mathcal{R}_\varepsilon(u_\varepsilon(t)-w) + \lambda\mathcal{R}_\varepsilon(u_\varepsilon(t)-w) \\ &\qquad \leq \mathcal{F}_\varepsilon(w) - \mathcal{F}_\varepsilon(u(t)) \text{ for a.a. } t \in [0,T]. \end{aligned} \tag{EVI_λ}$$

As a special case of the results in [Sav11] we obtain the following:

Theorem 2. *Given suitable natural conditions on $(X, \mathcal{F}_\varepsilon, \mathcal{R}_\varepsilon)$ including (3), (4), and (5) assume the Γ-convergence $\mathcal{F}_\varepsilon \overset{\Gamma}{\to} \mathcal{F}_0$ and the continuous convergence $\mathcal{R}(w_\varepsilon) \to \mathcal{R}_0(w_0)$ whenever $w_\varepsilon \rightharpoonup w_0$ and $\sup_{\varepsilon\in[0,1]} \mathcal{F}_\varepsilon(w_\varepsilon) < \infty$. Then, the solutions $u_\varepsilon : [0,T] \to X$ of $(X, \mathcal{F}_\varepsilon, \mathcal{R}_\varepsilon)$ satisfy*

$$u_\varepsilon(0) \rightharpoonup u_0(0) \text{ and } \sup_{\varepsilon\in]0,1[} \mathcal{F}_\varepsilon(u_\varepsilon(0)) < \infty \quad\Longrightarrow\quad \forall\, t \in [0,T]:\ u_\varepsilon(t) \to u_0(t).$$

3. The Ginzburg-Landau equation as evolutionary Γ-limit. By $\mathbb{S}_\ell$ we denote the macroscopic interval $[0,\ell]_{\rm per} = \mathbb{R}_{/(\ell\mathbb{Z})}$ with periodic boundary conditions and use $X := \mathrm{L}^2(\mathbb{S}_\ell)$ as the underlying the Hilbert space. The rescaled Swift-Hohenberg equation (1) is a gradient system $(X, \mathcal{F}_\varepsilon^{\rm SH}, \mathcal{R}^{\rm SH})$ with

$$\mathcal{F}_\varepsilon^{\rm SH}(u) := \int_0^\ell \frac{1}{2\varepsilon^2}\big(u(x)+\varepsilon^2 u''(x)\big)^2 + \frac{\mu}{2}u(x)^2 + \frac{\gamma}{3\varepsilon}u(x)^3 + \frac{1}{4}u(x)^4\,\mathrm{d}x$$

and $\mathcal{R}^{\rm SH}(v) = \frac{1}{2}\|v\|^2$. Since the solutions behave like $u(t,x) = \mathrm{Re}(A(t,x)\mathbf{E}_\varepsilon(x)$ with $\mathbf{E}_\varepsilon(x) := \mathrm{e}^{\mathrm{i}x/\varepsilon}$, we choose $\varepsilon = \ell/(2\pi N)$ for $N \in \mathbb{N}$ and let $N \to \infty$. Moreover, we consider the transformed (but still equivalent) gradient system $(X, \mathcal{F}_\varepsilon, \mathcal{R}_\varepsilon)$ for A given by $\mathcal{F}_\varepsilon(A) := \mathcal{F}^\varepsilon(\mathrm{Re}(A\mathbf{E}_\varepsilon))$ if $A \in X_N$ and $\mathcal{F}_\varepsilon(A) = \infty$ else. Also $\mathcal{R}_\varepsilon$ can be defined such that $\mathcal{R}_\varepsilon(\dot A) = \mathcal{R}(\mathrm{Re}(\dot A\mathbf{E}_\varepsilon))$. For $\gamma^2 < \gamma_*^2$ it can be shown that $\mathcal{F}_\varepsilon \overset{\rm M}{\to} \mathcal{F}_0 = \mathcal{F}_{\rm GL}$ and $\mathcal{R}_\varepsilon \overset{\rm M}{\to} \mathcal{R}_0 = \mathcal{R}_{\rm GL}$ with

$$\mathcal{F}_{\rm GL}(A) = \int_0^\ell 2|A'|^2 - \frac{1}{2}|A|^2 + \frac{\rho}{4}|A|^4\,\mathrm{d}x \text{ and } \mathcal{R}_{\rm GL}(V) = \|V\|_2^2 \quad \text{with } \rho = \tfrac{3}{8}\big(1-\tfrac{\gamma^2}{\gamma_*^2}\big)$$

We obtain evolutionary convergence via Theorem 1 for all γ with $\gamma^2 < \gamma_*^2$. Theorem 2 is only applicable in the case $\gamma = 0$, since uniform geodesic λ-convexity fails for $\gamma \neq 0$. These convergence results greatly weakens the necessary convergence of the initial data (the so-called well-preparedness). Moreover, the results can be generalized to localized perturbations as well, see [Mie13].

Acknowledgment: Research partially supported by DFG under SFB 910 Subproject A5.

References

[AGS05] L. Ambrosio, N. Gigli, and G. Savaré. *Gradient flows in metric spaces and in the space of probability measures*. Lectures in Mathematics ETH Zürich. Birkhäuser Verlag, Basel, 2005.

[Eck65] W. Eckhaus. *Studies in non-linear stability theory*. Springer-Verlag New York, New York, Inc., 1965.

[KSM92] P. Kirrmann, G. Schneider, and A. Mielke. The validity of modulation equations for extended systems with cubic nonlinearities. *Proc. Roy. Soc. Edinburgh Sect. A*, 122, 85–91, 1992.

[Mie02] A. Mielke. The Ginzburg–Landau equation in its role as a modulation equation. In B. Fiedler, editor, *Handbook of Dynamical Systems II*, pages 759–834. Elsevier, 2002.

[Mie13] A. Mielke. Deriving amplitude equations via evolutionary Γ-convergence. *In preparation*, 2013. In preparation.

[MiS96] A. Mielke and G. Schneider. Derivation and justification of the complex Ginzburg-Landau equation as a modulation equation. In P. Deift, C. Levermore, and C. Wayne, editors, *Dynamical systems and probabilistic methods in partial differential equations (Berkeley, CA, 1994)*, pages 191–216. Amer. Math. Soc., Providence, RI, 1996.

[MiS11] A. Mielke and U. Stefanelli. Linearized plasticity is the evolutionary Γ-limit of finite plasticity. *J. Europ. Math. Soc.*, 2011. To appear. WIAS preprint 1617.

[MRS08] A. Mielke, T. Roubíček, and U. Stefanelli. Γ-limits and relaxations for rate-independent evolutionary problems. *Calc. Var. Part. Diff. Eqns.*, 31, 387–416, 2008.

[MRS13] A. Mielke, R. Rossi, and G. Savaré. Nonsmooth analysis of doubly nonlinear evolution equations. *Calc. Var. Part. Diff. Eqns.*, 46(1-2), 253–310, 2013.

[MSZ00] A. Mielke, G. Schneider, and A. Ziegra. Comparison of inertial manifolds and application to modulated systems. *Math. Nachr.*, 214, 53–69, 2000.

[SaS04] E. Sandier and S. Serfaty. Gamma-convergence of gradient flows with applications to Ginzburg-Landau. *Comm. Pure Appl. Math.*, LVII, 1627–1672, 2004.

[Sav11] G. Savaré. Gradient flows and diffusion semigroups in metric spaces under lower curvature bounds. In preparation, 2011.

[Sch94] G. Schneider. Error estimates for the Ginzburg-Landau approximation. *Z. angew. Math. Phys.*, 45(3), 433–457, 1994.

[Ser10] S. Serfaty. Gamma-convergence of gradient flows on Hilbert spaces and metric spaces and applications. *Preprint Jussieu*, 2010.

[Ste08] U. Stefanelli. The Brezis-Ekeland principle for doubly nonlinear equations. *SIAM J. Control Optim.*, 47(3), 1615–1642, 2008.

[vHa91] A. van Harten. On the validity of the Ginzburg-Landau equation. *J. Nonlinear Sci.*, 1(4), 397–422, 1991.

About the validity of Whitham's equation

Guido Schneider

(joint work with Kourosh, Sanei Kashani)

Whitham's approximation is a multiple scaling ansatz which allows to describe slow modulations in time and space of periodic wave trains in general dispersive wave systems. We prove the validity of Whitham's equations for a Boussinesq equation coupled with a Klein-Gordan equation. The proof is based on an infinite series of normal form transforms and an energy estimate. We expect that the steps persuaded will be a part of a general approximation theory for Whitham's equations. In detail, we consider the system of partial differential equations

$$\partial_t^2 v = \partial_x^2 v - v + u^2 + 2uv + v^2, \tag{1}$$

$$\partial_t^2 u = \partial_x^2 u + \partial_t^2 \partial_x^2 u + \partial_x^2 (u^2 + 2uv + v^2), \tag{2}$$

with $u = u(x,t)$, $v = v(x,t)$, x, $t \in \mathbb{R}$. Then we make the ansatz

$$\psi_u^{\text{Whitham}}(x,t) = U(\varepsilon x, \varepsilon t) \quad \text{and} \quad \psi_v^{\text{Whitham}} = V(\varepsilon x, \varepsilon t), \tag{3}$$

with $0 < \varepsilon \ll 1$ a small perturbation parameter, and find

$$\begin{aligned} \text{Res}_u &= -\partial_t^2 u + \partial_x^2 u + \partial_x^2 \partial_t^2 u + \partial_x^2 (u^2 + 2uv + v^2) \\ &= \varepsilon^2 (-\partial_T^2 U + \partial_X^2 U + \partial_X^2 (U^2 + 2UV + V^2)) + \varepsilon^4 \partial_T^2 \partial_X^2 U, \\ \text{Res}_v &= -\partial_t^2 v + \partial_x^2 v - v + v^2 + 2uv + v^2 \\ &= -V + U^2 + 2UV + V^2 + \varepsilon^2 (-\partial_T^2 V + \partial_X^2 V). \end{aligned}$$

Hence equating the coefficient in front of ε^0 in Res_v to zero yields

$$-V + U^2 + 2UV + V^2 = 0$$

and so $V = H(U) = U^2 + \mathcal{O}(U^3)$ due to the implicit function theorem for U and V of order $\mathcal{O}(1)$, but sufficiently small. Equating the coefficient in front of ε^2 in Res_u to zero gives

$$-\partial_T^2 U + \partial_X^2 U + \partial_X^2 (U^2 + 2UV + V^2) = 0. \tag{4}$$

By substituting $V = H(U)$ into (4) we find

$$-\partial_T^2 U + \partial_X^2 U + \partial_X^2 (U^2 + 2UH(U) + H(U)^2) = 0. \tag{5}$$

We prove the following approximation result.

Theorem. *There exists a $C_1 > 0$ such that the following is true. Let $U \in C([0,T_0], H^6(\mathbb{R},\mathbb{R}))$ be a solution of (5) with $\sup_{T\in[0,T_0]} \|U(\cdot,T)\|_{H^6} \leq C_1$ and let $V = H(U)$. Then there exist $\varepsilon_0 > 0$ and $C_2 > 0$ such that for all $\varepsilon \in (0,\varepsilon_0)$ we have solutions (u,v) of (1)-(2) such that*

$$\sup_{t\in[0,T_0/\varepsilon]} \sup_{x\in\mathbb{R}} |(u,v)(x,t) - (U,V)(\varepsilon x, \varepsilon t)| \leq C_2 \varepsilon^{3/2}.$$

The scaling used in the ansatz (3) is the same scaling as it is used for the derivation of Whitham's equations. They are derived from the Lagrangian of the underlying problem leading to a system of conservation laws. Our system (5) can be rewritten in conservation law form as

$$\begin{aligned} \partial_T U &= \partial_X W, \\ \partial_T W &= \partial_X (U + U^2 + 2UH(U) + H(U)^2). \end{aligned}$$

The resonance structure of our system is the same as it occurs for the situation one is really interested in, namely the description of slow modulations in time and space of a periodic traveling wave in a dispersive wave system by Whitham's equations, cf. [3, 1].

Whitham's equations belongs to a set of famous amplitude equations containing the Ginzburg-Landau equation, the KdV equation, the NLS equation, Burgers equation, and so called phase diffusion equations. They play an important rôle in the description of spatially extended dissipative or conservative physical systems. For all other amplitude equations there exists a satisfying mathematical theory showing that the original system behaves as predicted by the associated amplitude equation. For Whitham's equations, so far only one approximation result has been established, namely the validity of Whitham's equations for the NLS equation as original system which however has a much simpler resonance structure [2].

The proof is based on the following ideas. System (1)-(2) can be written as first order system

$$\partial_t W = \Lambda W + B(W,W),$$

with Λ a linear skew symmetric operator and B a bilinear symmetric mapping. The error function R defined through $W = \psi + \varepsilon^\beta R$ fulfils

$$\partial_t R = \Lambda R + 2B(\psi, R) + \varepsilon^\beta B(R,R) + \varepsilon^{-\beta} \mathrm{Res}(W).$$

We have to prove an $\mathcal{O}(1)$-bound for R on an $\mathcal{O}(\varepsilon^{-1})$-time scale. In order to do so we have to control the terms on the right hand side on this long time scale. The first

term is skew-symmetric and will lead to oscillations, but to no growth rates. The last two term can be $\mathcal{O}(\varepsilon)$-bounded on the required time scale easily. However, the second term $2B(\psi, R)$ is only $\mathcal{O}(1)$-bounded. One approach to control this term is its elimination by a near-identity change of variables $R = \tilde{R} + M(\psi, \tilde{R})$ with M a suitable chosen bilinear mapping. It turns out that only parts of this term can be eliminated and so the terms splits into a resonant and a non-resonant part, i.e.,

$$B(\psi, R) = B_r(\psi, R) + B_{nr}(\psi, R).$$

After the transform the relevant part of the equation for the new error function $\tilde{R}$ is of the form

$$\partial_t \tilde{R} = \Lambda \tilde{R} + B_r(\psi, \tilde{R}) + B_r(\psi, M(\psi, \tilde{R}) + \mathcal{O}(\varepsilon).$$

Hence with the transform new terms of order $\mathcal{O}(1)$, namely $B_r(\psi, M(\psi, \tilde{R})$, are created. They can be split again into resonant and non-resonant terms. Another normal form transform is necessary to eliminate these resonant terms, but again terms of order $\mathcal{O}(1)$ are created. However, they are cubic w.r.t. ψ. This goes ad infinum and so the convergence of the composition of these infinitely many transformations has to be proven. Since the n-th transformation is of order $\mathcal{O}(\|\psi\|^n)$ the convergence finally can be established for $\|\psi\| = \mathcal{O}(1)$, but sufficiently small. After all these transformations the equations for the error are of the form

$$\partial_t R = \Lambda R + F(\psi, R) + \mathcal{O}(\varepsilon)$$

where F is a function which is linear w.r.t. R and which contains infinitely many resonant terms. Since all these terms have a long wave character w.r.t t a suitable chosen energy $E(R)$ satisfies

$$\partial_t E(R) = \mathcal{O}(\varepsilon),$$

and so an $\mathcal{O}(1)$-bound for the error R can be established on the $\mathcal{O}(\varepsilon^{-1})$-time scale.

References

[1] C. Cercignani and D.H. Sattinger, *Scaling limits and models in physical processes*, DMV Seminar, 28. Birkhäuser Verlag, Basel, 1998 vi+191 pp.

[2] Wolf-Patrick Düll, Guido Schneider, *Validity of Whitham's equations for the modulation of wave-trains in the NLS equation*, J. Nonlinear Science **19(5)**: 453-466, 2009.

[3] G.B. Whitham, *Linear and nonlinear waves*, Reprint of the 1974 original. Pure and Applied Mathematics, John Wiley & Sons, Inc., New York, 1999.

Exotic behavior of hexagonal Faraday waves

Laurette S. Tuckerman
(joint work with Nicolas Périnet, Damir Juric)

The Faraday instability [1] describes the generation of surface waves between two superposed fluid layers subjected to periodic vertical vibration. Although these waves usually form crystalline patterns, i.e. stripes, squares, or hexagons, they can form more complicated structures such as quasicrystals or superlattices [2, 3]. The first detailed spatio-temporal experimental measurements of the interface height $z = \zeta(x, y, t)$ were undertaken by [4]. We have recently carried out the first three-dimensional nonlinear simulations of the Faraday instability [5] using the same experimental parameters, but in the minimal domain that can accomodate a hexagonal pattern.

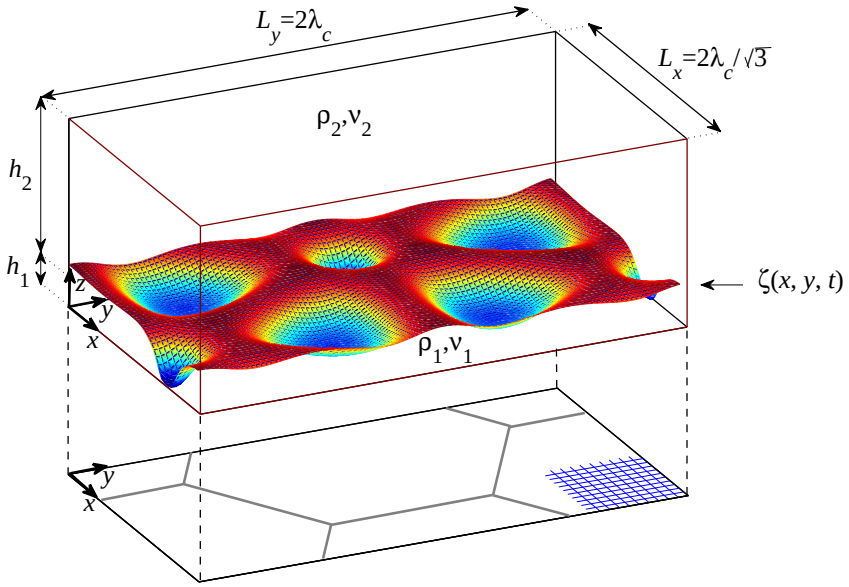

Figure 1. Instantaneous realization of hexagaonal Faraday waves in computational domain with periodic horizontal dimensions $2\lambda_c/\sqrt{3} \times 2\lambda_c$, where $\lambda_c = 13.2$ mm is the critical wavelength determined by Floquet analysis [6], Physical parameters, taken from [4], are $\rho_1 = 1346\,\mathrm{kg\,m^{-3}}$, $\nu_1 = 5.35 \times 10^{-6}\,\mathrm{m^2\,s^{-1}}$, $h_1 = 1.6$ mm and $\rho_2 = 949\,\mathrm{kg\,m^{-3}}$, $\nu_2 = 2.11 \times 10^{-5}\,\mathrm{m^2\,s^{-1}}$, $h_2 = 8.4$ mm for the density, kinematic viscosity, and height of the lower and upper fluids, respectively, surface tension $\sigma = 35\,\mathrm{mN\,m^{-1}}$, and imposed vibrational frequency and amplitude $f = 12$ Hz and $a = 38.0\,\mathrm{m\,s^{-2}}$.

Starting from an initial random perturbation, our simulations produced a subharmonically oscillating hexagonal pattern. The subsequent evolution is shown in figure 2 via the instantaneous maximum height and its envelope, surrounded by sets of instantaneous visualizations of the interface over one subharmonic period

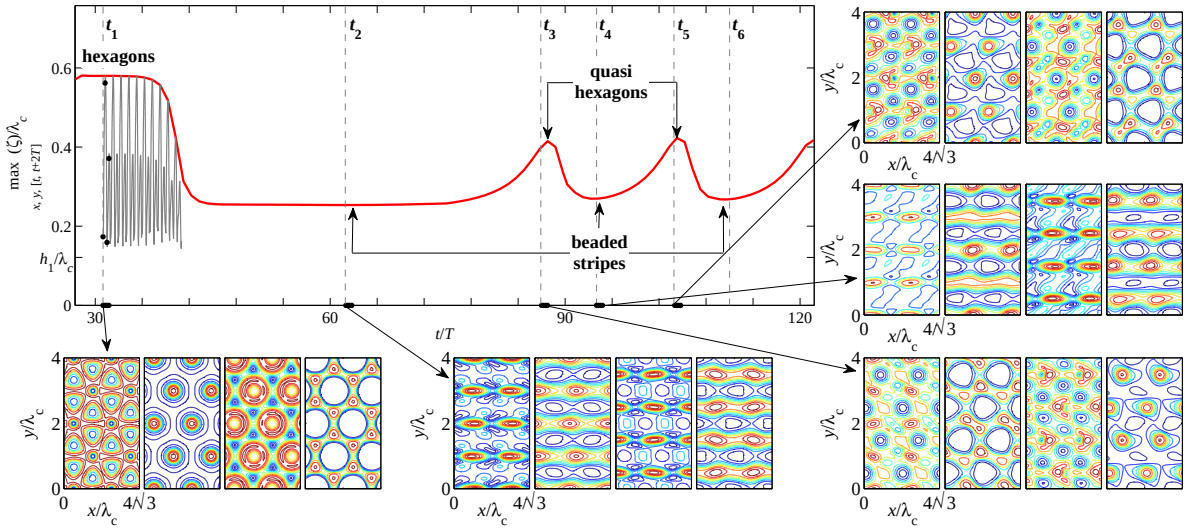

FIGURE 2. Maximum interface heights $\max_{x,y} \zeta(x,y,t)$ (rapidly oscillating curve) and $\max_{x,y,[t,t+T]} \zeta(x,y,t)$ (smooth envelope). Surrounding visualizations show instantaneous contour plots of $\zeta(x,y,t)$ at times $t_i + jT/4$, $j = 0,1,2,3$, indicated by black dots. Visualizations show hexagons at t_1, symmetric and nonsymmetric beaded stripes at t_2 and t_4 and quasi-hexagons at t_3 and t_5.

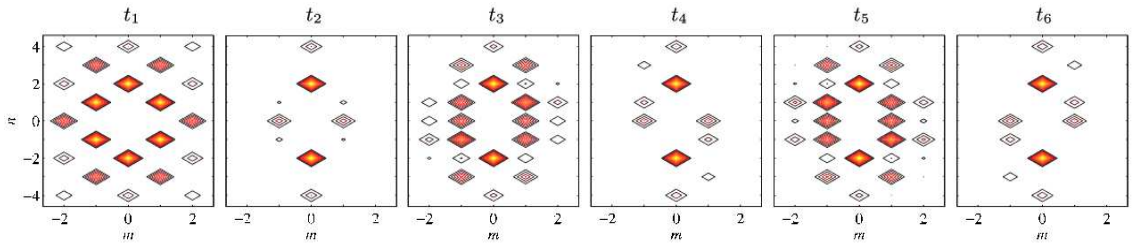

FIGURE 3. Time-filtered spatial Fourier spectra $\zeta_{mn}(t_i)$: hexagons at t_1, beaded stripes at t_2, quasi-hexagons at t_3 and t_5, nonsymmetric beaded stripes at t_4 and t_6.

T. At times $t_1 + jT/4$ the pattern has hexagonal symmetry. These are succeded by the patterns at $t_2 + jT/4$, which we call beaded stripes. They satisfy:

$$\zeta(x, n\lambda_c - y) = \zeta(x,y) = \zeta(m\lambda_c/\sqrt{3} + \tilde{x}_0 - x, y + n\lambda_c) \tag{1}$$

which describe the crystallographic group isomorphic to $Z_2 \times Z_2$ called pmg or p2mg [7]. The patterns which occur later are less symmetric; we call those which appear at t_3 and t_5 quasi-hexagons, and those which appear at t_4 and t_6 nonsymmetric beaded stripes. These each appear in two forms, which are related by the spatio-temporal symmetry:

$$\zeta(m\lambda_c/\sqrt{3} + x_0 - x, y + y_0, t_{3,4} + T/2) = \zeta(x,y,t_{5,6}) \tag{2}$$

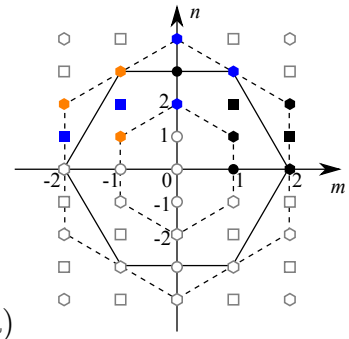

a)

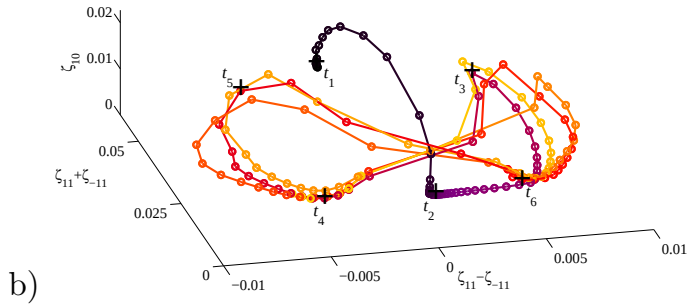

FIGURE 4. a) Spatial Fourier grid of the domain. b) Phase portrait of temporal evolution of modes from an extended simulation.

To quantify this behavior, we define the time-filtered spatial Fourier transform:

$$\frac{\zeta(\mathbf{x},t)}{\lambda_c} = \sum_{m,n} e^{i\mathbf{k}_{mn}\cdot\mathbf{x}}\hat{\zeta}_{mn}(t)\ , \qquad \zeta_{mn}(t) \equiv \max_{[t,t+T]} |\hat{\zeta}_{mn}(t)| \tag{3}$$

for the wavenumbers $\mathbf{k}_{mn} \equiv \left(\sqrt{3}m\mathbf{e}_x + n\mathbf{e}_y\right) k_c/2$ allowed by our domain. Fig. 3 shows that the spectrum for the hexagonal pattern at time t_1 consists primarily of $(m,n) = (\pm1,\pm1)$ and $(0,\pm2)$, with $k/k_c = 1$, but also higher-order hexagonal modes. The spectrum at t_2 is dominated by modes $(0,\pm2)$ and $(\pm1,0)$, which combine to form the beaded striped patterns – with one bead over L_x and two stripes over L_y – seen in Fig. 2 at t_2. The spatio-temporal symmetry (2) is manifested by $\zeta_{-m,n}(t_{3,4}) = \zeta_{mn}(t_{5,6})$. Note that the amplitudes of modes $\pm(1,1)$ exceed those at $\pm(1,-1)$ at t_3, t_6 and vice versa for t_4, t_5.

Figure 4b projects the dynamics onto the coordinates $\zeta_{11}+\zeta_{-1,1}$, $\zeta_{11}-\zeta_{-1,1}$ and ζ_{10}. The concentration of points indicate that the hexagonal pattern at time t_1 and the beaded striped pattern at t_2 are saddles. Afterwards, the trajectory consists of two crossed loops connecting t_3, t_4, t_5 and t_6. Several dynamical-systems scenarios lead to limit cycles which visit symmetrically related sets, e.g. Hopf bifurcations [8] or heteroclinic cycles [9].

REFERENCES

[1] M. Faraday, Phil. Trans. R. Soc. Lond. **121**, 299 (1831).
[2] W. S. Edwards and S. Fauve, Phys. Rev. E **47**, R788 (1993).
[3] A. M. Rucklidge, M. Silber, and A. C. Skeldon, Phys. Rev. Lett. **108**, 074504 (2012).
[4] A. V. Kityk, J. Embs, V. V. Mekhonoshin, and C. Wagner, Phys. Rev. E **72**, 036209 (2005).
[5] N. Périnet, D. Juric, and L. S. Tuckerman, J. Fluid Mech. **635**, 1 (2009).
[6] K. Kumar and L. S. Tuckerman, J. Fluid Mech. **279**, 49 (1994).
[7] C. Wagner, H. W. Müller, and K. Knorr, Phys. Rev. E **62**, R33 (2000).
[8] T. Clune and E. Knobloch, Physica D **74**, 151 (1994).
[9] P.-L. Buono, M. Golubitsky, and A. Palacios, Physica D **143**, 74 (2000).

Three-Wave Interactions, Quasipatterns and Spatiotemporal Chaos

Alastair Rucklidge
(joint work with Gérard Iooss, Anne Skeldon, Mary Silber)

Three-wave interactions play a key role in 2D pattern formation problems where there are quadratic nonlinearities, such as the Faraday wave experiment. These experiments have produced exotic patterns such as quasipatterns and spatiotemporal chaos. We consider first the question of existence of quasipattens as solutions of a pattern-forming PDE, and point out the difficulties caused by small divisors. We then turn to the stability of quasipatterns, and show how three-wave interactions between two circles of wavevectors could stabilise quasipatterns. However, this only occurs when the ratio of wavenumber is $2\cos 75^\circ = \frac{1}{2}(\sqrt{6}-\sqrt{2})$. For other values of the wavenumber ratio, complex patterns are expected, and indeed are found in simlations of model PDEs.

Quasipatterns (two-dimensional patterns that are quasiperiodic in any spatial direction) remain one of the outstanding problems of pattern formation. As with many problems involving nonlinearity and quasiperiodicity, there is a small divisor problem. We consider 8-fold, 10-fold, 12-fold, and higher order quasipattern solutions of the Swift–Hohenberg equation, and prove that a formal solution, given by a divergent series, may be used to build a smooth quasiperiodic function which is an approximate solution of the pattern-forming PDE up to an exponentially small error [2].

Quasipatterns can be stabilised by the interaction of two linearly unstable (or weakly stable) length scales with a wavenumber ratio of q, with $\frac{1}{2} < q < 1$ [3]. In two dimensions, with two critical circles having a radius ratio within a factor of two, nonlinear interactions can occur between two waves on the outer circle and one on the inner (figure 1a), or between two waves on the inner circle and one on the outer (figure 1b). For the special wavelength ratio of $2\cos 75^\circ = \frac{1}{2}(\sqrt{6}-\sqrt{2}) = 0.5176$, the angle between two waves on the inner circle is 30° and the angle between two waves on the outer circle is 150°. This combination allows 12 waves on each circle to interact with each other through three-wave resonances, and form a 12-fold quasipattern, without having to invoke additional waves (figure 1c). Any other ratio between the two circles leads potentially to an infinite number of interacting waves (figure 1d). This distinguishes 12-fold quasipatterns from all others [4], and may be the reason that 12-fold quasipatterns are the most commonly observed, in the Faraday wave experiments and indeed in soft-matter quasicrystals.

As well as wavelength ratios, it is important to consider the nature of the nonlinear three-wave interaction in the regime where both are excited. There are two main possibilities: either the waves mutually reinforce each other, leading to steady patterns with waves from both circles, or the waves compete with each other, leading to one circle or the other dominating, or the interesting possibility of spatio-temporal chaos (STC). The two cases are distinguished by the signs of the quadratic coefficients in the dynamical equations that describe the three-wave interaction. We have recently [4] shown that changes in sign of these coefficients,

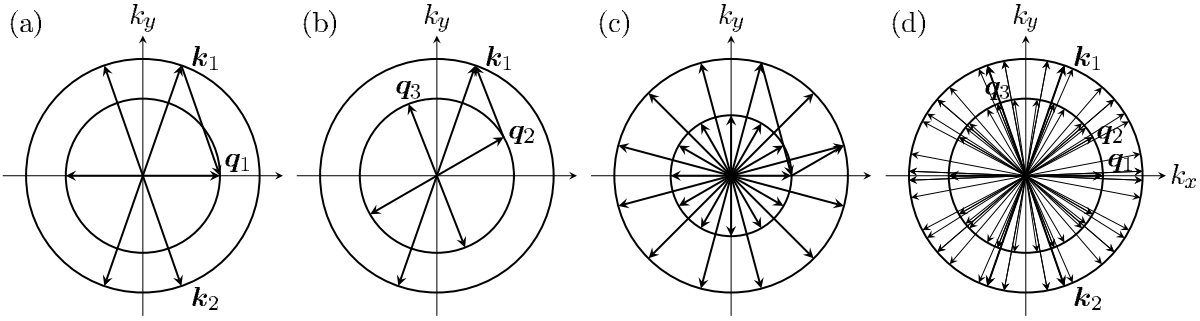

FIGURE 1. Three-wave interactions between two wavenumbers [4]. (a) With $\boldsymbol{k}_1 + \boldsymbol{k}_2 = \boldsymbol{q}_1$, two long wavevectors can interact with a short one; (b) similarly, with $\boldsymbol{q}_2 + \boldsymbol{q}_3 = \boldsymbol{k}_1$, two short can interact with a long one. (c) With a wavenumber ratio $q = \frac{1}{2}(\sqrt{6}-\sqrt{2}) = 0.5176$, twelve short waves interact with twelve long ones, resulting in 12-fold QPs. (d) For any other value of q, the set of waves generated by three-wave interactions does not close, resulting in complex patterns.

computed from the Navier–Stokes equations for the Faraday wave experiment, line up very well with experimentally observed changes from quasipatterns to STC, giving confidence that quantitative connections can be made between theory and experiment.

In order to explore the role of three-wave reinforcement or competition, we have been working with a Swift–Hohenberg-like PDE [4]:

$$\frac{\partial U}{\partial t} = \mathcal{L}(\mu,\nu)U + Q_1 U^2 + Q_2 U\nabla^2 U + Q_3\,|\nabla U|^2 - U^3, \tag{1}$$

where Q_1, Q_2 and Q_3 are parameters that control the three-wave interactions, and

$$\mathcal{L}(0,0)U = \frac{\sigma_0}{q^4}(1+\nabla^2)^2(q^2+\nabla^2)^2 U, \tag{2}$$

with μ and ν parameters that control the growth rates of modes with $k = 1$ and $k = q$ respectively, and σ_0 controls the depth of the minimum between $k = q$ and $k = 1$. This PDE readily produces quasipatterns (for the wavenumber ratio $q = \frac{1}{2}(\sqrt{6} - \sqrt{2}) = 0.5176$) and STC (figure 2).

REFERENCES

[1] G. BATTAGLIA & A.J. RYAN, *Effect of amphiphile size on the transformation from a lyotropic gel to a vesicular dispersion*, Macromolecules, 39 (2006), 798–805.

[2] G. IOOSS & A.M. RUCKLIDGE, *On the Existence of Quasipattern Solutions of the Swift–Hohenberg Equation*, J. Nonlinear Sci., 20 (2010), 361–394.

[3] A.M. RUCKLIDGE & M. SILBER, *Design of parametrically forced patterns and quasipatterns*, SIAM J. Appl. Dynam. Syst., 8 (2009), 298–347.

[4] A.M. RUCKLIDGE, M. SILBER & A.C. SKELDON, *Three-wave interactions and spatiotemporal chaos*, Phys. Rev. Lett., 108 (2012), 074504.

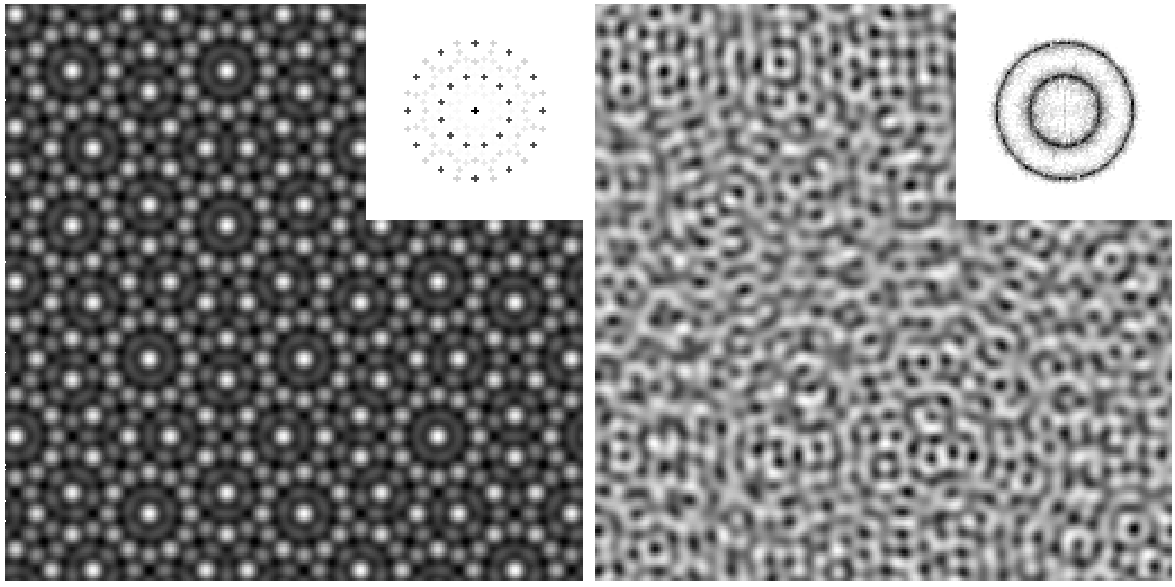

FIGURE 2. Quasipattern (left) and spatio-temporal chaos (right) in (1); see [4] for details. Fourier transforms are inset.

Coagulation dynamics for random fronts and branching processes

ROBERT L. PEGO

(joint work with G. Menon, B. Niethammer, G. Iyer, N. Leger)

Smoluchowski's coagulation equations are oversimplified rate equations (a kind of kinetic equation) for the evolution of the size distribution of objects that cluster. They are related in remarkable ways to models of random shock clustering, the merging of ancestral trees, and the fundamental limit theorems in probability related to Levy-stable laws and infinite divisibility. We reviewed results obtained over the last several years that concern dynamic scaling limits and self-similar behavior:

(1) in 'solvable' cases for which the classical Smoluchowski equation may be solved by transformation into simple PDEs.
(2) for a 'min-driven' coagulation model that roughly describes the merging of domains in the Allen-Cahn equation, and
(3) of size distributions of 'clans' of related individuals in critical continuous-state branching processes (CSBPs).

1. The classical Smoluchowski coaguation equation governs the evolution of a size-distribution measure $\nu_t(dx)$ on $E = (0, \infty)$, and takes the weak form

$$\frac{d}{dt}\int_E f(x)\nu_t(dx) = \frac{1}{2}\int_E\int_E (f(x+y) - f(x) - f(y))K(x,y)\nu_t(dx)\nu_t(dy)$$

where f is an arbitrary test function on E. With rate kernel $K(x,y) = 2$, $x+y$ or xy, the Laplace transform makes the equation equivalent to simple nonlinear PDE. Following earlier work that characterized all self-similar solutions and their domains of attraction for these kernels, [4] studies the *scaling attractor* and the

dynamics on it. For definiteness consider the additive kernel $K = x + y$. Then the scaling attractor is the set of cluster points of arbitrarily rescaled mass distributions $F_t(dx) = x\nu_t(dx)$ for solutions:

Definition. A probability measure $\hat{F}(dx)$ on $[0, \infty]$ is a point in the scaling attractor A if there exist a sequence of positive numbers $b_n \to \infty$ and a sequence of solutions all defined for $t \in (0, \infty)$ such that the corresponding mass distribution functions satisfy $F^{(n)}_{t_n}(b_n dx) \to \hat{F}(dx)$ weakly as $n \to \infty$.

Points in the scaling attractor are the values at $t = 0$ of eternal solutions defined for all $t \in (-\infty, \infty)$. In turn (due to a result of Bertoin) eternal solutions are parametrized in terms of a family of "Lévy-Khintchine" measures G_* that arise *in the backward-time limit* $t \to -\infty$ from the rescaled measures $G_t(dx) = xe^{-t}F_t(e^t dx)$. The LK-measures G_* are characterized by the property that $(1 \wedge x^{-1})G_*(dx)$ is a finite measure on on $[0, \infty]$. Every such measure corresponds to a unique enternal solution in this way.

Remarkably, the nonlinear dynamics on the scaling attractor becomes purely dilational in terms of the representing LK-measure: the time-t map $\hat{F}_0 \mapsto \hat{F}_t$ on the scaling attractor corresponds to the map

$$G_*(dx) \mapsto e^{2t}G_*(e^{-t}dx)$$

on LK-measures. By consequence, the time dynamics is conjugate to continous-time shift dynamics, and we can exhibit a number of signatures of chaotic dynamics (sensitivity to the initial tails of the size distribution): a dense set of scaling-periodic solutions; a single solution trajectory with scaling limits dense in the scaling attractor; and an asymptotic shadowing result for solutions with similar initial tails. Many of these results and their proofs are strongly analogous to classical limit theorems concerning infinitely divisibility in probability theory.

2. On a large scale, a cartoon that models the very slow dynamics in the 1D Allen-Cahn PDE is a "1D bubble bath." Points on the line separate "bubbles" (domains) whose pattern evolves by two simple rules: (i) the smallest bubble "pops" and joins with its two neighbors; (ii) repeat. Simulations show that the bubble size distribution approaches a common self-similar form for a variety of initial distributions.

A kind of coagulation equation arises as a continuous-time model for the evolution of the size distribution of bubbles. A remarkable solution procedure for this equation was found by Gallay and Mielke [1], and used to establish a number of strong results involving rates of convergence to self-similar form. In [3] we revisited this model using methods developed for solvable Smoluchowski equations. We (i) extended well-posedness theory to handle size distributions that are arbitrary measures with support bounded away from 0; (ii) established necessary and sufficient conditions on initial data for solutions to have a single proper scaling limit as $t \to \infty$; and (iii) provided a Lévy-Khintchine representation formula for the eternal solutions in this model. The criterion for a scaling limit is that the first-moment distribution function is regularly varying (i.e., power law up to a factor that is slowly varying at infinity). The proofs involve simple scaling rigidity arguments

as one finds in Feller's book, combined with the delicate exponential Tauberian theorem of de Haan. One curious point involves multiple collisions: k clusters can coalesce with probability p_k. When $\Sigma p_k k \log k = \infty$, the scaling symmetry of the model is broken, up to a slowly varying factor, which can nevertheless be dealt with.

3. A family of coagulation models with multiple collisions appear in a very natural way in *critical continuous-state branching processes* (CSBPs), as pointed out a few years ago by Bertoin and Le Gall. These equations have the weak form

$$\partial_t \int_E f(x)\,\nu_t(dx) = \sum_{k=2}^{\infty} R_k(t)\, I_k(f,\nu_t), \tag{1}$$

$$I_k(f,\nu_t) = \int_{E^k} \Big(f(x_1+\cdots+x_k) - \sum_{j=1}^{k} f(x_j) \Big) \prod_{j=1}^{k} \frac{\nu_t(dx_j)}{\langle 1,\nu_t\rangle}.$$

where $\nu_t(dx)$ is a measure on $E=(0,\infty)$ that as a continuum limit of size distribution of "clans" of individuals descended from a common ancestor in time t. Here I_k describes the effect of k clans conjoining on the generalized moment $\langle f,\nu_t\rangle$, and the rates have a special form given by

$$R_k = \int_0^\infty \frac{e^{-y}y^k}{k!}\pi\left(\frac{dy}{\langle 1,\nu_t\rangle}\right) = \frac{(-1)^k\Psi^{(k)}(\langle 1,\nu_t\rangle)}{k!},$$

in terms of the *branching measure* $\pi(dy)$ and the *branching mechanism* Ψ:

$$\Psi(u) = \int_{(0,\infty)} \big(e^{-ux} - 1 + ux\big)\,\pi(dx).$$

With $f = 1-e^{-qx}$ the dynamics for $\varphi(t,q) = \langle 1-e^{-qx},\nu_t\rangle$ become equivalent to

$$\partial_t\varphi(t,q) = -\Psi(\varphi(t,q)).$$

We assume $\int_1^\infty \Psi(u)\,du < \infty$, which means the branching process becomes extinct almost surely. Then the coagulation equation has a *fundamental solution* $\mu_t(dx)$, whose Laplace exponent $\Phi(t,q) = \langle 1-e^{-qx},\mu_t\rangle$ satisfies

$$\partial_t\Phi = -\Psi(\Phi), \qquad \Phi(0,q) = q.$$

The critical CSBP is determined by the measure μ_t, and we have the following result [2] that characterizes when the long-time limit is self-similar:

Theorem The following are equivalent:

(i) there exist a probability measure $\tilde{\mu}_t$ and $\lambda(s)>0$ such that for some $t>0$,

$$\mu_t^{(s)}(dx) := \frac{\mu_{st}(\lambda(s)dx)}{\langle 1,\mu_s\rangle} \quad \xrightarrow{s\to\infty} \tilde{\mu}_t(dx).$$

(ii) Ψ is regularly varying at 0 with index $1<\gamma\le 2$, and $\tilde{\mu}_t$ is self-similar, with generalized Mittag-Leffler profile

$$\int_0^x \tilde{\mu}_1(dy) = F_{r,s}(\beta x) = \sum_{k=1}^{\infty} \frac{1}{kB(k,r)}\cdot\frac{(-1)^{k+1}(\beta x)^{sk}}{\Gamma(1+sk)},$$

where $r = (\gamma - 1)^{-1}$, $s = \gamma - 1$, $\beta = \langle x, \tilde{\mu}_1 \rangle^{-1}$. Furthermore, $\lambda(s) \sim \beta \langle 1, \tilde{\mu}_s \rangle^{-1}$.

References

[1] T. Gallay and A. Mielke, *Convergence results for a coarsening model using global linearization*, J. Nonlinear Sci., **13** (2003), pp. 311–346.

[2] G. Iyer, N. Leger and R. L. Pego, *Limit theorems for Smoluchowski dynamics associated with critical continuous-state branching processes*, submitted.

[3] G. Menon, B. Niethammer, and R. L. Pego, *Dynamics and self-similarity in min-driven clustering*, Transactions Amer. Math. Soc. **362** (2010), 6591–6618.

[4] G. Menon and R. L. Pego, *The scaling attractor and ultimate dynamics for Smoluchowski's coagulation equations*, J. Nonlinear Sci., **18** (2008), 143–190.

Exponential integrators for parabolic problems with time dependent coefficients

David A. Hipp, Marlis Hochbruck, Alexander Ostermann

1. Introduction

In this note, we outline the numerical solution of linear parabolic problems with time dependent coefficients. We focus on exponential integrators, which constitute a class of efficient methods for stiff problems [5]. In the time invariant case, exponential integrators represent quadrature rules with operator-valued weights, and their implementation requires the evaluation of the action of certain matrix functions. A natural extension to nonautonomous problems are Magnus integrators [1]. They are particulary efficient in the hyperbolic case (e.g., Schrödinger equations with time dependent potential), where high oscillations are present [4]. In the parabolic case, however, they often suffer from a strong order reduction [7]. Therefore, we consider a new class of high-order exponential integrators for such situations. We restrict our attention here to the description of a third-order method for the homogeneous problem. The full error analysis and the extension to inhomogeneous problems will be reported elsewhere. Our construction of the integrator is strongly motivated by the construction of the corresponding evolution system (see, e.g., [6]), which we recall below. As an application, we solve a 2d heat equation on an evolving domain and compare our result with those obtained by other methods.

2. Nonautonomous parabolic problems

We consider the time discretization of an abstract nonautonomous parabolic initial value problem

$$\frac{\mathrm{d}}{\mathrm{d}t} u(t) + A(t)u(t) = 0, \quad u(0) = u_0, \quad 0 \le t \le T, \tag{1}$$

stated in a Banach space $\mathcal{X}$. We study this problem in the framework of [6, Section 5.6] with Lipschitz continuous $t \mapsto A(t)A(\sigma)^{-1}$. The construction of our

numerical method for solving (1) is strongly motivated by the corresponding construction of the evolution system in [6, Section 5.6]. We start from the ansatz

$$u(t) = \mathrm{e}^{-tA_0}u_0 + \int_0^t \mathrm{e}^{-(t-s)A(s)}R(s,0)u_0\,\mathrm{d}s, \tag{2}$$

where $A_0 = A(0)$, and $R(t,0)$ is the solution of the integral equation

$$R(t,0) = \big(A_0 - A(t)\big)\mathrm{e}^{-tA_0} + \int_0^t R_1(t,s)R(s,0)\,\mathrm{d}s$$

with kernel $R_1(t,s) = \big(A(s) - A(t)\big)\mathrm{e}^{-(t-s)A(s)}$. Under appropriate smoothness assumptions, it can be shown that

$$\widetilde{u}(\tau) = \mathrm{e}^{-\tau A_0}u_0 + \int_0^\tau \mathrm{e}^{-(\tau-s)A_1}R_1(s,0)u_0\,\mathrm{d}s \tag{3}$$

is a fourth-order approximation to $u(\tau)$ for τ sufficiently small.

3. A third-order exponential integrator

In order to obtain a practical scheme from the approximation (3), we write down the general step starting from an approximation $u_n \approx u(t_n)$ and replace the integrand $R_1(t_n + s, t_n)$ by its quadratic interpolation polynomial, interpolating $R_1(t_n + \theta\tau, t_n)$ at the nodes $\theta = 0$, $\frac{1}{2}$, and 1. Carrying out the integration gives us the numerical scheme

$$u_{n+1} = T_n u_n, \tag{4a}$$

which is a recurrence relation with the discrete evolution operator

$$\begin{aligned} T_n = \mathrm{e}^{-\tau A_n} &+ 4\tau\Big(\varphi_2(-\tau A_{n+1}) - 2\varphi_3(-\tau A_{n+1})\Big)\big(A_n - A_{n+\frac{1}{2}}\big)\mathrm{e}^{-\frac{\tau}{2}A_n} \\ &+ \tau\Big(4\varphi_3(-\tau A_{n+1}) - \varphi_2(-\tau A_{n+1})\Big)\big(A_n - A_{n+1}\big)\mathrm{e}^{-\tau A_n}, \end{aligned} \tag{4b}$$

where $A_k = A(k\tau)$. The entire functions $\varphi_k(z)$ are defined by the recursion

$$\varphi_{k+1}(z) = \frac{\varphi_k(z) - 1/k!}{z}, \quad \varphi_0(z) = \mathrm{e}^z, \qquad k \geq 0.$$

Under appropriate smoothness assumptions, the exponential integrator (4) is a third-order method. Details of the proof and an extension to inhomogeneous problems will be reported elsewhere.

4. Application: Parabolic problems on evolving domains

As an application, we model a diffusion problem on a temporally evolving domain. The derivation of the equation and the choice of the finite element method is motivated by [2, 3]. Let $\Omega_0 \subset \mathbb{R}^2$ be an open, bounded set and let X_t be a diffeomorphism between Ω_0 and its image Ω_t for all $t \in [0,T]$. Let $\mathcal{N}_T$ be the union of all sets $\{t\} \times \Omega_t$, $t \in [0,T]$. We denote the material time derivative of a function $v : \mathcal{N}_T \to \mathbb{R}$ by $\dot{v}$ and define the function space

$$V = \big\{v : \mathcal{N}_T \to \mathbb{R}\ ;\ v(t,\cdot) \in H^1(\Omega_t),\ \dot{v}(t,\cdot) \in L^2(\Omega_t) \text{ for all } t \in [0,T]\big\}.$$

The weak formulation of a diffusion equation on the evolving domain Ω_t can be stated as follows: Find $u \in V$ such that for all $t \in (0,T]$ and all $v \in V$ it holds

$$\frac{\mathrm{d}}{\mathrm{d}t}\int_{\Omega_t} uv\,\mathrm{d}x + \alpha\int_{\Omega_t}\nabla u\cdot\nabla v\,\mathrm{d}x = \int_{\Omega_t} u\dot{v}\,\mathrm{d}x, \tag{5}$$

subject to the initial condition $u(0,\cdot) = u_0$ and to homogeneous Dirichlet boundary conditions $u(t,x) = 0$ for all $x \in \partial\Omega_t$. Here α denotes the diffusion constant.

For the spatial discretization of (5), we consider a triangulation of Ω_0 with nodes $a_1,\dots,a_K$ and corresponding nodal basis functions $\phi_1,\dots,\phi_K$. We then define the basis functions $\Phi_i \in V$ by $\Phi_i(t,x) = \phi_i(X_t^{-1}(x))$. They satisfy in particular $\dot{\Phi}_i = 0$. The function spaces $V_h = \operatorname{span}\{\Phi_1,\dots,\Phi_K\}$ and

$$U_h = \Big\{u \in V\ ;\ u(t,\cdot) = \textstyle\sum_{i=1}^K U_i(t)\Phi_i(t,\cdot),\ U_i \in C^1\big([0,T],\mathbb{R}\big)\Big\}$$

fulfill $V_h \subset U_h \subset V$. In general, a transformed triangulation is not again a triangulation. Thus we use a linearized transformation $X_{t,h} \approx X_t$ instead. This also simplifies the computation of the mass and stiffness matrices.

For the spatial discretization of (5) we use a Petrov–Galerkin method: find $u_h \in U_h$ such that for all $t \in (0,T]$ and all $v_h \in V_h$:

$$\frac{\mathrm{d}}{\mathrm{d}t}\int_{\Omega_t} u_h v_h\,\mathrm{d}x + \alpha\int_{\Omega_t}\nabla u_h\cdot\nabla v_h\,\mathrm{d}x = \int_{\Omega_t} u_h\dot{v}_h\,\mathrm{d}x = 0, \tag{6}$$

and $u_h(0,\cdot) = u_0 \in V$. From (6) we obtain the stiff ODE

$$\frac{\mathrm{d}}{\mathrm{d}t}\Big(M(t)U(t)\Big) = -S(t)U(t) \tag{7}$$

with mass matrix M and stiffness matrix S, which can be transformed to a standard form for $V(t) = M(t)U(t)$, if necessary.

5. Numerical tests

For a first numerical test, we choose $\Omega_0 = [0,1]\times[0,\frac{3}{2}]$ and $t \in [0,1]$. We consider a nonlinear transformation mapping the rectangle Ω_0 into a bottle-like domain Ω_t, cf. Fig. 1. Since the actual transformation is quite complicated to write down, we omit the formulas here. A Matlab file containing the details can be obtained from the authors. We consider problem (5) with initial value

$$u_0(x) = g(x_1)\chi_{[0,1/3]}(x_1) + g(1-x_1)\chi_{[2/3,1]}(x_1),\quad g(\xi) = \sin\big(6\pi\xi - \tfrac{\pi}{2}\big) + 1$$

and diffusion constant $\alpha = 0.01$. Some snapshots of the solution on a refined mesh with 1.871 nodes are presented in Fig. 1.

In Fig. 2, we plotted error versus time steps for different numerical integrators on the refined mesh. The error is computed with respect to a reference solution computed by the RadauIIA method of order 5 with step size $\tau = 0.001$. We compare the exponential integrator (4) with the exponential midpoint rule, two fourth-order Magnus integrators (one of them uses Gauss nodes [1, eq. (254)], the other one ist based on Simpson's rule [1, eq. (256)]), and the RadauIIA method of order 3. The numerically observed order of both the exponential integrator (4)

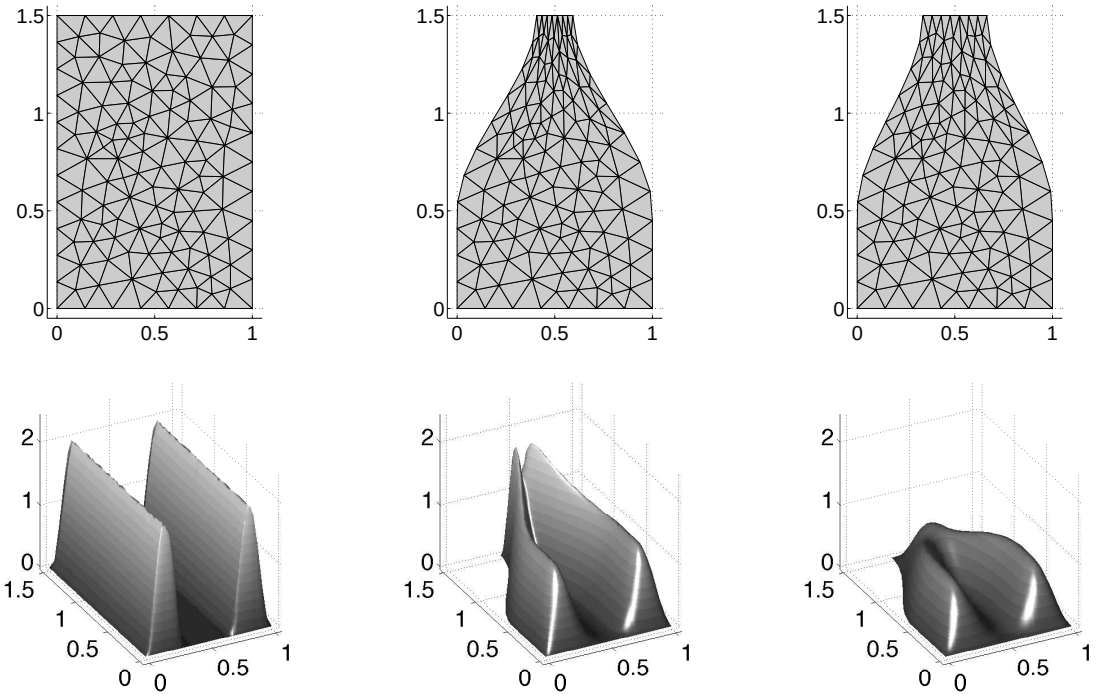

FIGURE 1. Above: the domain Ω_t for $t = 0$, $t = 0.37$, and $t = 0.74$ on a coarse mesh with 131 nodes; below: the solution for $t = 0$, $t = 0.37$, and $t = 0.74$ on a refined mesh with 1.871 nodes.

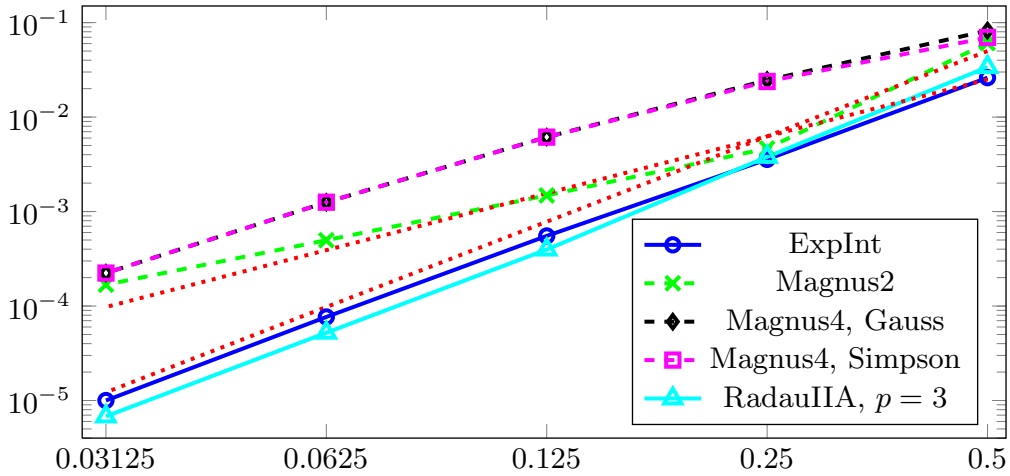

FIGURE 2. Errors of various integrators plotted over different time steps $\tau = 2^{-j}$, $j = 1, \ldots, 5$ at $t = 1$ in the maximum norm. For comparison, we added dotted lines with slopes two and three.

and the RadauIIA method is about three, while the Magnus integrators suffer from order reduction.

References

[1] S. Blanes, F. Casas, J.A. Oteo, and J. Ros. The Magnus expansion and some of its applications. *Physics Reports*, 470(5-6):151–238, 2009.

[2] G. Dziuk and C. M. Elliott. Finite elements on evolving surfaces. *IMA J. Numer. Anal.*, 27(2):262–292, 2007.

[3] G. Dziuk, Ch. Lubich, and D. Mansour. Runge–Kutta time discretization of parabolic differential equations on evolving surfaces. *IMA J. Numer. Anal.*, 32(2):394–416, 2012.

[4] M. Hochbruck and Ch. Lubich. On Magnus integrators for time-dependent Schrödinger equations. *SIAM J. Numer. Anal.*, 41(3):945–963, 2003.

[5] M. Hochbruck and A. Ostermann. Exponential integrators. *Acta Numerica*, 19:209–286, 2010.

[6] A. Pazy. *Semigroups of Linear Operators and Applications to Partial Differential Equations*. Springer, Berlin, Heidelberg, New York, corr. 2nd printing edition, 1992.

[7] M. Thalhammer. A fourth-order commutator-free exponential integrator for nonautonomous differential equations. *SIAM J. Numer. Anal.*, 44(2):851–864, 2006.

Waves in lattices with imperfections

John Mallet-Paret

(joint work with Shui-Nee Chow, Kening Lu, and Wenxian Shen)

We study wave motion in lattice differential equations, specifically, in systems of the form

$$\dot{u}_i = \alpha_i(u_{i+1} - u_i) + \beta_i(u_{i-1} - u_i) - f_i(u_i), \qquad i \in \mathbf{Z}. \tag{1}$$

This system is a spatially discrete Allen-Cahn equation with spatial variations (or imperfections). The coupling constants α_i and β_i are positive (diffusive coupling) and bounded, but need not be large; that is, the system need not be near the continuum limit. The nonlinearities f_i typically are of bistable type. For the spatially independent case

$$\dot{u}_i = \overline{\alpha}(u_{i+1} - u_i) + \overline{\beta}(u_{i-1} - u_i) - \overline{f}(u_i), \qquad i \in \mathbf{Z}, \tag{2}$$

the existence of a traveling wave front $\overline{u} : \mathbf{R} \to \ell^\infty$, where $\overline{u}_i(t) = \varphi(i - ct)$ joins the two equilibria $\varphi(-\infty) = 0$ and $\varphi(\infty) = 1$, is known [2], [3]. The wave speed c may either be nonzero, or zero (a standing wave).

In the present work, for the spatially varying system (1), we consider three cases.

(A) Small perturbations from the spatially independent system: Here $|\alpha_i - \overline{\alpha}|$ and $|\beta_i - \overline{\beta}|$ are small, with each f_i near $\overline{f}$, and where the unperturbed system (2) has a wave moving with speed $c \neq 0$. Using the moving coordinate system developed in [1], the existence of a generalized traveling wave is shown, namely, a solution $u : \mathbf{R} \to \ell^\infty$ to (1) with $\|u(t) - \overline{u}(t)\|$ small for all t. (The norm is in ℓ^∞.)

(B) Large perturbations in the coupling constants: Here we take $\alpha_i = \beta_i$ a bounded sequence, and bounded away from zero, with all $f_i = \overline{f}$ the same. For the spatially periodic case $\alpha_{i+p} = \alpha_i$ there is either a traveling wave with nonzero speed, or else a maximal ordered collection of standing waves joined by monotone connecting orbits. In any case these compose an invariant set $\Gamma \subseteq \ell^\infty$, which can be regarded as a generalized traveling wave. For the case of general (nonperiodic) α_i,

one makes approximations by periodic coefficients with spatial periods $p_n \to \infty$, and takes the limit $\Gamma_n \to \Gamma_*$ of the resulting invariant sets. The limiting set Γ_* is shown to be nondegenerate, namely it is composed of elements $u \in \ell^\infty$ for which $\lim_{i\to-\infty} u_i = 0$ and $\lim_{i\to\infty} u_i = 1$. Extensions to certain cases when $\alpha_i \neq \beta_i$ can be made.

(C) Large perturbations in the nonlinearities: Here $\alpha_i = \overline{\alpha}$ and $\beta_i = \overline{\beta}$ for all i. Further, $f_i = \overline{f}$ for $i \leq 0$, but in general $f_i \neq \overline{f}$ for $i > 0$. It is assumed that $c > 0$ for the unperturbed system (2), that is, the wave moves to the right. Then the existence of a solution $u : \mathbf{R} \to \ell^\infty$ to (1) which approaches the unperturbed wave $\overline{u}(t)$ as $t \to -\infty$ is shown using upper and lower solutions. Further, if $f_i = \overline{f}$ for all but finitely many i, then one of the following four possibilities holds as $t \to \infty$:

(a) Transmission: $\|u(t) - \overline{u}(t + \sigma(t))\| \to 0$ for some phase shift $\sigma(t)$.

(b) Blockage: $\|u(t) - v\| \to 0$ for some $v \in \ell^\infty$ with $\lim_{i\to-\infty} v_i = 0$ and $\lim_{i\to\infty} v_i = 1$.

(c) Residue: $\|u(t) - \overline{u}(t + \sigma(t)) - v\| \to 0$ where the "residue" $v \in \ell^\infty$ satisfies $\lim_{i\to\pm\infty} v_i = 0$, and thus is small as $i \to \pm\infty$.

(d) Large Residue: Here $\lim_{t\to\infty} u_i(t) = v_i$ for every i, where $\lim_{i\to-\infty} v_i = 0$ but $\lim_{i\to\infty} v_i = a$; here $a \in (0, 1)$ is the unstable zero of $\overline{f}$, so $\overline{f}(a) = 0$. The case of Large Residue is not generic (and in a sense is of codimension one), and in many cases can be ruled out (for example, when $\overline{\alpha} = \overline{\beta}$).

References

[1] S.-N. Chow, J. Mallet-Paret, and W. Shen, *Traveling waves in lattice dynamical systems*, J. Differential Equations **149** (1998), 248–291.

[2] J. Mallet-Paret, *The global structure of traveling waves in spatially discrete dynamical systems*, J. Dynam. Differential Equations **11** (1999), 49–127.

[3] B. Zinner, *Existence of traveling wavefront solutions for the discrete Nagumo equation*, J. Differential Equations **96** (1992), 1–27.

Chaos via Variable Delay

Hans-Otto Walther

Making a constant delay in a differential equation variable can change the solution behaviour considerably. We give an example where the introduction of a state-dependent delay in a hyperbolic linear equation creates a homoclinic loop [5]. Close to the homoclinic loop complicated motion is expected, similar to Shilnikov's example [3] in $\mathbb{R}^4$.

We begin with the simplest differential equation for negative feedback with a time lag, namely,

$$x'(t) = -\alpha\, x(t-1) \tag{1}$$

with a parameter $\alpha > 0$. The initial value problem given by Eq. (1) for $t > 0$ and initial data $x|[-2, 0] = \phi \in C = C([-2, 0], \mathbb{R})$ defines a strongly continuous semigroup T of solution operators on the Banach space C. For $\frac{\pi}{2} < \alpha < \frac{5\pi}{2}$ the state $0 \in C$ is hyperbolic with 2-dimensional unstable space, and without

real spectrum (of the generator of the semigroup T). For such α close to $\frac{5\pi}{2}$ we construct a continuously differentiable delay functional $d : U \to (0, 2)$, $U \subset C$ open, with $d(\phi) = 1$ close to $0 \in C$, so that the (nonlinear) equation

$$x'(t) = -\alpha\, x(t - d(x_t)) \tag{2}$$

(with $x_t = x(t + \cdot)$) has a solution $h : \mathbb{R} \to \mathbb{R}$ which is homoclinic to zero, with the minimal intersection property

$$\dim D_2F(t_+ - t_-, h_{t_-})T_{h_{t_-}} W^u \cap T_{h_{t_+}} W^s = 1$$

for t_- close to $-\infty$ and t_+ large. Here W^u and W^s are the local unstable and stable manifolds of the stationary state $\phi = 0$ of the semiflow F of Eq. (2) on the *solution manifold*

$$X = \{\phi \in U \cap C^1 : \phi'(0) = -\alpha\, \phi(-d(\phi))\}.$$

In fact, X is a continuously differentiable submanifold of codimension 1 in the Banach space $C^1 = C^1([-2, 0], \mathbb{R})$, each initial value $\phi \in X$ defines a maximal solution of Eq. (2) which has all segments x_t in X, and the curves $t \mapsto x_t$ define a continuous semiflow on X with continuously differentiable solution operators $F(t, \cdot)$, which in turn yields continuously differentiable local invariant manifolds, among others [4, 1].

The delay functional d is not of the simple form $d(\phi) = \tilde{d}(\phi(0))$, along a solution of Eq. (2) the delay is not everywhere monotonically increasing, and along the homoclinic solution the oscillation frequency (a modified count of sign changes per interval of length 2) is *increasing*. Moreover, the construction does *not* carry over to the case

$$x'(t) = \beta\, x(t - 1), \quad \beta > 0, \tag{3}$$

of positive feedback with a constant time lag because here modifications of the delay obviously do not destroy positivity, that is, positive invariance of the cone of non-negative functions. This precludes homoclinics with minmal oscillation frequency as $t \to -\infty$; complicated motion as in Shilnikov's simpler scenario [2] in $\mathbb{R}^3$ can not be achieved by making the delay in the positive feedback equation (3) variable.

A proof that close to the homoclinic loop of Eq. (2) chaotic motion does exist is in preparation (joint work with Bernhard Lani-Wayda).

References

[1] F. Hartung, T. Krisztin, H. O. Walther, and J. Wu, *Functional differential equations with state-dependent delays: Theory and applications*, in *HANDBOOK OF DIFFERENTIAL EQUATIONS, Ordinary Differential Equations*, vol. 3, A. Canada, P. Drabek, and A. Fonda eds., pp. 435-545, Elsevier Science B. V., North Holland, 2006.

[2] L. P. Shilnikov, *A case of the existence of a denumerable set of periodic motions*, Sov. Math. Dokl. **6** (1965), 163–166.

[3] L. P. Shilnikov, *The existence of a denumerable set of periodic motions in four-dimensional space in an extended neighbourhood of a saddle-focus.* Soviet Math. Dokl. **8** (1967), 54–58.

[4] H. O. Walther, *The solution manifold and C^1-smoothness of solution operators for differential equations with state dependent delay.* J. Differential Eqs. **195** (2003), 46–65.

[5] H. O. Walther, *A homoclinic loop generated by variable delay*, preprint (2012), 44 pp.

Attractor Spindles for Delay Differential Equations

Tibor Krisztin
(joint work with Gabriella Vas, Hans-Otto Walther, Jianhong Wu)

The delay differential equation

$$\dot{x}(t) = -\mu x(t) + f(x(t-1))$$

with $\mu > 0$ and smooth monotone nonlinearity $f : \mathbb{R} \to \mathbb{R}$ appears in several applications. For example, in the study of neural networks $f(\xi) = \alpha \tanh(\beta\xi)$ with $\alpha > 0$ and $\beta > 0$.

The natural phase space is $C = C([-1, 0], \mathbb{R})$ equipped with the supremum norm. For any $\varphi \in C$, there is a unique solution $x^\varphi : [-1, \infty) \to \mathbb{R}$. For each $t \geq 0$, $x_t^\varphi \in C$ is defined by $x_t^\varphi(s) = x^\varphi(t+s)$, $-1 \leq s \leq 0$. The map $F : [-1, \infty) \times C \ni (t, \varphi) \mapsto x_t^\varphi \in C$ is a continuous semiflow. Very much is known about the global dynamics of F. A discrete Lyapunov functional, as a key technical tool, combined with several other dynamical system methods makes is possible to prove a Poincaré–Bendixson type result [6], and to obtain a lot of information about the structure of the global attractor [1,2,4,7]. For some particular nonlinearities like $f(x) = \alpha \tanh(\beta x)$ or $f(x) = \alpha \tan^{-1}(\beta x)$ with $\alpha \neq 0$ and $\beta > 0$, a complete picture is available [2,3,4]. However, for most of the nonlinearities such a nice description is not known.

We assume $f(0) = 0$ and a dissipativity condition: $|f(\xi)| < \mu|\xi|$ outside a bounded neighbourhood of 0. Then $\mathbb{R} \ni \xi \mapsto -\mu\xi + f(\xi) \in \mathbb{R}$ has at least 3 zeros, one is 0; denote ξ_{-1} and ξ_1 the largest negative and the smallest positive zeros, respectively. These zeros determine equilibrium points of F, denoted also by $\xi_{-1}, 0, \xi_1$. Under these hypotheses the semiflow F has a global attractor $\mathcal{A} \subset C$.

The derivatives $D_2F(t, 0)$, $t \geq 0$, form a strongly continuous semigroup, and the spectrum of the generator of the semigroup consists of simple eigenvalues. The number of eigenvalues in the open right half plane depends on μ and $f'(0)$, and can be given explicitly. Assume that 0 is hyperbolic, and there are $2N + 1$ eigenvalues with positive real parts for some integer $N \geq 0$.

Let$W^u_{loc}(0)$ denote a local unstable manifold of the equilibrium 0. Define W_{2N+1} as the global forward extension of $W^u_{loc}(0)$ under the semiflow F. Clearly, $\overline{W_{2N+1}} \subset \mathcal{A}$. Under some additional minor concavity and symmetry conditions on f, it was shown in [2,3] that $\overline{W_{2N+1}} = \mathcal{A}$.

The geometric and topological structures of the closure $\overline{W_3}$ of W_3 and the dynamics of the restricted flow of F on $\overline{W_3}$ are fully described in [1,2]. It was shown that the set $\overline{W_3}$ consists of 3 stationary points $0, \xi_{-1}, \xi_1$ and a unique periodic orbit $\mathcal{O}$; there exists a smooth disk in $\overline{W_3}$ bordered by this periodic orbit and consists of all connecting orbits from the stationary solution 0 to the periodic orbit; this disk seperates $\overline{W_3}$ into two halves each of which belongs to the domain of attraction of ξ_{-1} and ξ_1, respectively.

There is a similar complete description of the structure of $\overline{W_{2N+1}}$ for general N. To state our results precisely we define a discrete Lyapunov functional $V : C \setminus \{0\} \to \{0, 2, 4, \ldots\} \cup \{\infty\}$. $V(\phi)$ denotes the number of sign changes of $\phi \in C$ in the interval $[-1, 0]$ if this number is even or infinity; $V(\phi)$ is the number of sign changes plus 1 if ϕ has odd number of sign changes.

Our result on the structure of $\overline{W_{2N+1}}$ is as follows:

(i) *W_{2N+1} and $\overline{W_{2N+1}}$ are invariant under F, and $\overline{W_{2N+1}}$ is compact;*
(ii) *W_{2N+1} is a $(2N+1)$-dimensional C^1-submanifold of C;*
(iii) *ξ_{-1}, ξ_1 and 0 are the only stationary points in $\overline{W_{2N+1}}$;*
(iv) *For each $k \in \{1, \ldots, N\}$ there exists a periodic solution $p^{2k} : \mathbb{R} \to \mathbb{R}$ with $V(p^{2k}_t) = 2k$ for all $t \in \mathbb{R}$ and $\mathcal{O}_{2k} = \{p^{2k}_t : t \in \mathbb{R}\} \subset \overline{W_{2N+1}}$;*
(v) *$\mathcal{O}_2, \mathcal{O}_4, \ldots, \mathcal{O}_{2N}$ are the only periodic orbits in $\overline{W_{2N+1}}$;*
(vi) *$\mathcal{O}_{2k}$ has exactly $2k-1$ Floquet multipliers outside the unit circle, $1 \le k \le N$;*
(vii) *For each $k \in \{1, 2, \ldots, N\}$ the set*

$$\{\phi \in W_{2N+1} \setminus \{0\} : V(x^\phi_t) = 2k \text{ for } t \in \mathbb{R}\} \cup \{0\} \cup \mathcal{O}_{2k}$$

is a 2-dimensional C^1-submanifold of C with boundary;
(viii) *For each $k \in \{1, \ldots, N\}$ the set*

$$\{\phi \in W_{2N+1} : \omega(\phi) = \mathcal{O}_{2k}\}$$

is a $(2N-2k+2)$-dimensional C^1-submanifold of W_{2N+1};
(ix) $\overline{W_{2N+1}} = W_{2N+1} \cup \{\xi_{-1}, \xi_1\} \cup W^u_{str}(\mathcal{O}_2) \cup W^u_{str}(\mathcal{O}_4) \ldots \cup W^u_{str}(\mathcal{O}_{2N})$.

Here, for a nontrivial periodic orbit $\mathcal{O}$, the Floquet multipliers of $\mathcal{O}$ outside the unit circle of $\mathbb{C}$ determine a local unstable manifold of $\mathcal{O}$, and the forward extension of such a local unstable manifold is called the strong unstable set $W^u_{str}(\mathcal{O})$ of $\mathcal{O}$. Remark that the hyperbolicity of the periodic orbits, stated in (iv), is not known. However, there are at most 2 Floquet multipliers with absolute value 1; one of them is trivially 1.

Now, in addition, we assume the following:
There exist ξ_2 and ξ_3 such that $\xi_{-1} < \xi_0 := 0 < \xi_1 < \xi_2 < \xi_3$ are 5 consecutive zeros of $\mathbb{R} \ni \xi \mapsto -\mu\xi + f(\xi) \in \mathbb{R}$ with $f'(\xi_j) < \mu < f'(\xi_k)$ for $j \in \{-1, 1, 3\}$ and $k \in \{0, 2\}$. We denote the corresponding equilibrium points of F also by ξ_j for $j \in \{-1, 0, 1, 2, 3\}$. Then ξ_{-1}, ξ_1, ξ_3 are stable, and ξ_0, ξ_2 are unstable. By the monotone property of f, the subsets

$$C_{j,k} = \{\phi \in C : \ \xi_j \le \phi(s) \le \xi_k, \ -1 \le s \le 0\}$$

of the phase space C with $j \in \{-1, 1\}$ and $k \in \{1, 3\}$ are positively invariant under the semiflow F. The structures of the global attractors $\mathcal{A}_{-1,1}$ and $\mathcal{A}_{1,3}$ of the restrictions $F|_{[0\infty)\times C_{-1,1}}$ and $F|_{[0\infty)\times C_{1,3}}$, respectively, are (at least partially) well understood, as described above. In particular cases, $\mathcal{A}_{-1,1}$ and $\mathcal{A}_{1,3}$ have spindle-like structures described in [1,2,3,4], $\mathcal{A}_{-1,1}$ is the closure of the unstable set of ξ_0 containing the equilibrium points ξ_{-1}, ξ_0, ξ_1, periodic orbits in $C_{-1,1}$ and heteroclinic orbits among them; and analogously for $\mathcal{A}_{1,3}$.

Let $\mathcal{B}$ denote the global attractor of the restriction $F|_{[0\infty)\times C_{-1,3}}$. It is easy to see that if $\xi_{-1}, 0, \xi_1, \xi_2, \xi_3$ are the only zeros of $-\mu\xi + f(\xi)$, then $\mathcal{B} = \mathcal{A}$. The problem, whether under these hypotheses

$$\mathcal{A} = \mathcal{A}_{-1,1} \cup \mathcal{A}_{1,3}$$

holds or not, arose in [1].

The main result of [5] is that $\mathcal{A}$ can be more complicated. We constructed examples so that there exist periodic orbits in $\mathcal{A}\backslash(\mathcal{A}_{-1,1} \cup \mathcal{A}_{1,3})$, and also decsribed the dynamics in $\mathcal{A} \setminus (\mathcal{A}_{-1,1} \cup \mathcal{A}_{1,3})$.

We remark that Fiedler, Rocha and Wolfrum [8] studied scalar semilinear parabolic equations of the form

$$u_t = u_{xx} + f(x, u, u_x)$$

defined on the interval $0 \le x \le 2\pi$ with periodic boundary conditions $u(t, 0) = u(t, 2\pi)$, $u_x(t, 0) = u_x(t, 2\pi)$. Under suitable regularity and dissipativity assumptions on the nonlinearity f they obtained a description of the global attractor. Surprisingly, the structures of the attractors obtained for the delay differential equation and for the above parabolic equation are similar. It would be interesting to describe the analogy between these two different types of equations.

References

[1] T. Krisztin, H.-O. Walther and J. Wu, *Shape, Smothness and Invariant Stratification of an Attracting Set for Delayed Monotone Positive Feedback*, Fields Institute Monographs, Vol. 11, Amer. Math. Soc., Providence, RI, 1999.

[2] T. Krisztin and H.-O. Walther, *Unique periodic orbits for delayed positive feedback and the global attractor*, J. Dynam. Differential Equations **13** (2001), 1–57.

[3] T. Krisztin, *Unstable sets of periodic orbits and the global attractor for delayed feedback*, Topics in Functional Differential and Difference Equations, Fields Institute Communications **29** (2001), 267–296.

[4] T. Krisztin, *Global dynamics of delay differential equations*, Periodica Mathematica Hungarica **56** (2008), 83–95.

[5] T. Krisztin and G. Vas, *Large-Amplitude Periodic Solutions for Differential Equations with Delayed Monotone Positive Feedback*, J. Dynam. Differential Equations **23** (2011), 727–790.

[6] J. Mallet-Paret, and G. Sell, *The Poincaré–Bendixson theorem for monotone cyclic feedback systems with delay*, J. Differential Equations **125** (1996), 441–489.

[7] C. McCord, and K. Mischaikow, *On the global dynamics of attractors for scalar delay equations*, J. Amer. Math. Soc. **9** (1996), 1095–1133.

[8] B. Fiedler, C. Rocha, M. Wolfrum, *Sturm global attractors for S^1-equivariant parabolic equations,* Networks and Heterogeneous Media **7** 2012, 617–659.

Connection Graphs for Sturm Attractors of S^1-Equivariant Parabolic Equations

Carlos Rocha

(joint work with Bernold Fiedler, Matthias Wolfrum)

We consider semilinear parabolic equations of the form

$$u_t = u_{xx} + f(u, u_x)$$

defined on the circle $x \in S^1 = \mathbb{R}/2\pi\mathbb{Z}$. For a dissipative nonlinearity f the equation generates a dissipative semiflow in the appropriate function space, and the corresponding global attractor $\mathcal{A}_f$ is called a Sturm attractor. For Neumann boundary conditions there is a purely combinatorial characterization of the Sturm attractor in terms of a permutation σ_f – the Sturm permutation. We use this permutation to obtain a characterization of Sturm attractors $\mathcal{A}_f$ in our case of periodic boundary conditions. With this characterization we obtain in [1] the connection graphs $\mathcal{G}_f$ corresponding to the heteroclinic connecting orbits of $\mathcal{A}_f$. In this talk we present these results and survey the method that supports their proofs. An example of the type of (directed acyclic) graphs $\mathcal{G}_f$ that we obtain is shown in Figure 1 in the case of permutations σ_f in $\mathcal{S}(9)$. Here the (spatially homogeneous) equilibria correspond to the edges represented by black dots, and the periodic orbits (i.e. rotating waves) correspond to the edges represented by white dots.

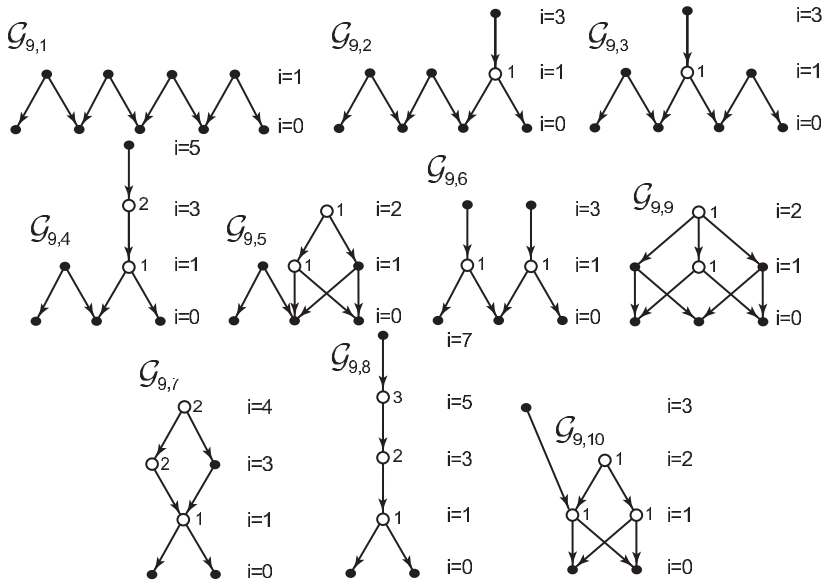

FIGURE 1. The 10 connection graphs $\mathcal{G}_f$ corresponding to the Sturm attractors $\mathcal{A}_f$ with m hyperbolic equilibria and q hyperbolic periodic orbits such that $m + 2q = 9$.

REFERENCES

[1] B. Fiedler, C. Rocha, and M. Wolfrum, *Sturm Attractors for S^1-Equivariant Parabolic Equations*, Networks and Heterogeneous Media **7** (2012), 617–659.

Combustion fronts in a gasless combustion model with heat loss

Anna Ghazaryan
(joint work with Stephen Schecter, and Peter Simon)

We consider a model for gasless combustion with heat loss,

$$\partial_t u_1 = \partial_{xx} u_1 + u_2 \rho(u_1 - \bar{u}_1) - \delta u_1,$$
$$\partial_t u_2 = \kappa \partial_{xx} u_2 - \beta u_2 \rho(u_1 - \bar{u}_1),$$

with $\beta > 0$, $\delta \geq 0$, $\kappa \geq 0$, and $\rho(u) = e^{-\frac{1}{u}}$ if $u > 0$, and 0 otherwise. Here u_1 is temperature, u_2 is reactant concentration, $u_1 = \bar{u}_1$ is the ignition temperature, ρ is the unit reaction rate, β is the exothermicity parameter, and κ describes diffusivity of the fuel. The term δu_1 represents heat loss from the system to the environment, formulated according to Newton's law of cooling. Two of the parameters, the diffusion coefficient κ for the fuel and a heat loss parameter δ, are assumed to be small.

It is known from numerical simulations [5] and topological arguments [2, 4] that the system supports two traveling fronts that lead to the unburned state. We use geometric singular perturbation theory to construct the faster one of these fronts and prove that as the heat loss parameter goes to 0, the speed of this front approaches the speed of the front in the system with zero diffusion and no heat loss. Further, we study the stability of this front in the regimes where the front does not have unstable discrete spectrum but possesses marginally unstable essential spectrum [3, 5]. For these regimes we rigorously prove that the instability of the front is convective on the nonlinear level, in other words, that the perturbations to the front lag further and further behind the interface of the front.

References

[1] A. Ghazaryan, S. Schecter, P. Simon, *Gasless combustion fronts with heat loss*, submitted.
[2] Giovangigli, V., *Nonadiabatic plane laminar flames and their singular limits*, SIAM J. Math. Anal. **21** (1990), 1305–1325.
[3] Gubernov, V. V., Sidhu, H. S., and Mercer, G. N., *The effect of ambient temperature on the propagation of nonadiabatic combustion waves*, J. Math. Chem. **37** (2005), 149–162.
[4] Roques, L., *Study of the premixed flame model with heat losses: The existence of two solutions*, European J. Appl. Math. **16** (2005), 741–765.
[5] Simon, P., Merkin, J., and Scott, S., *Bifurcations in non-adiabatic flame propagation models*, Focus on Combustion Research (2006), 315–357.

Singularities and intrinsic front dynamics of FitzHugh-Nagumo type systems

Jens D. M. Rademacher
(joint work with (in part) M. Chirilus-Bruckner, P. van Heijster, A. Doelman)

This talk concerned existence, stability and bifurcation of 'front' interface solutions to certain perturbations of the prominent Allen-Cahn model for phase separation on the line $x \in \mathbb{R}$. As in the FitzHugh-Nagumo equations, we couple the Allen-Cahn equation to linear equations. Specifically, a seemingly weak coupling is considered that on 'small' ξ and 'large' $x = \xi/\varepsilon$ spatial scales gives the systems

$$\begin{aligned} U_t &= U_{\xi\xi} + U - U^3 - \varepsilon g(V,W;\mu) & \qquad U_t &= \varepsilon^2 U_{xx} + U - U^3 - \varepsilon g(V,W;\mu) \\ \tau V_t &= V_{\xi\xi} + \varepsilon^2(U - V) & \qquad \frac{\tau}{\varepsilon^2} V_t &= V_{xx} + (U - V) \\ \theta W_t &= D^2 W_{\xi\xi} + \varepsilon^2(U - W) & \qquad \frac{\theta}{\varepsilon^2} W_t &= D^2 W_{xx} + U - W, \end{aligned}$$

which are equivalent for $\varepsilon > 0$. Here μ is a set of parameters.

The large spatial scale $x = \xi/\varepsilon$ highlights the spatial scale separation for slowly travelling waves when $0 < \varepsilon \ll 1$. The question we adress is the impact of the slowly varying components V, W on the stable stationary Allen-Cahn fronts connecting ± 1. The system falls into the category of second order semi-strong interaction models [6] and indeed it turns out that front motion with velocity of order ε^2 arises; much faster than the metastable Allen-Cahn front interaction of exponentially small order [1, 2]. We illustrate that this occurs already due to the interaction of a *single front* with the spatially slowly varying 'fields' V, W.

For the linearly coupled, and thus *minimally nonlinear* case

$$\mu = (\alpha, \beta, \gamma),\ g(V,W;\mu) = \alpha V + \beta W + \gamma \tag{1}$$

the above system is a special parameter regime of a phenomenological gas-discharge model [7] and the existence, stability as well as interaction of multi-fronts has been studied already in [3, 4, 5]. However, the detailed analysis especially of the present regime of τ, θ becomes quite involved for multi-fronts. Here we present a complete picture of the stability of single fronts and the organizing center for existence: a butterfly catastrophe, which requires coupling to both V and W. Moreover, we prove a singularity imbedding when allowing general nonlinear coupling $g(V;\mu)$ already with only one additional component V (or W).

The existence of fronts near the Allen-Cahn fronts is a singular perturbation problem, which may be summarized as follows.

Theorem 1. *For any bounded set of μ, τ, θ, D, c there is ε_0 and an open neighborhood $\mathcal{U} \subset \mathbb{R}^6$ of the singular heteroclinic solution for $\varepsilon = 0$ connecting -1 to $+1$ (or vice versa) such that for all $0 < \varepsilon < \varepsilon_0$ solutions to*

$$\Gamma := g\left(\frac{c\tau}{\sqrt{c^2\tau^2 + 4}}, \frac{c\theta}{\sqrt{c^2\theta^2 + 4D^2}}; \mu\right) = 0 \tag{2}$$

are in one-to-one correspondence to front solutions with velocity $\varepsilon^2 c$ that lie in $\mathcal{U}$ and connect the perturbed homogeneous states $U = V = W = \pm 1$. These solutions form a smooth family, which converges uniformly to the singular heteroclinic solution as $\varepsilon \searrow 0$.

In addition, for $\gamma = c = 0$ there is one smooth subfamily of odd functions of ξ.

Based on this result we prove that in the minimally nonlinear case (1), the front existence problem is organized by a butterfly catastrophe, that is $\Gamma = \mathcal{O}(c^5)$. Specifically, this occurs if and only if

$$\gamma = 0,\ 2\sqrt{2}/3 = \alpha\tau + \beta\theta/D,\ \alpha D^3\tau^3 + \beta\theta = 0. \tag{3}$$

In particular, $\alpha\beta < 0$ is required so that both V and W are involved; otherwise the organizing center is a cusp. However, the unfolding is incomplete since Γ is an odd function of c and adding further linearly coupled linear equations do not complete the unfolding. A nonlinear symmetry breaking term such as ηV^2 in g is required to provide a versal unfolding. More generally, we prove that any singularity can be imbedded into the existence problem by suitable choice of g already when W is absent.

In addition to this existence analysis, we study stability of the fronts for the minimally nonlinear case, and derive via an Evans-function approach the following result.

Theorem 2. *Consider the case* (1) *and choose a parameter curve μ_ε so that a front exists for $0 < \varepsilon < \varepsilon_0$ as in Theorem 1. Then the critical eigenvalues of the linearization in the front are of the form $\lambda = \varepsilon^2\hat{\lambda} + \mathcal{O}(\varepsilon^{5/2})$, where $\hat{\lambda}$ is a root of*

$$E(\hat{\lambda}) := -\frac{\sqrt{2}}{6}\hat{\lambda} + \alpha\left(\frac{1}{\sqrt{c^2\tau^2+4}} - \frac{1}{\sqrt{c^2\tau^2+4(\hat{\lambda}\tau+1)}}\right) + \beta\left(\frac{1}{\sqrt{c^2\theta^2+4D^2}} - \frac{1}{\sqrt{c^2\theta^2+4D^2(\hat{\lambda}\theta+1)}}\right). \tag{4}$$

Moreover, E possesses at most two complex roots in addition to $\hat{\lambda} = 0$. At a butterfly catastrophe (3)*, E has a double root at $\hat{\lambda} = 0$ and the third (real) root has negative real part if and only if $\beta D^3 > -\alpha$.*

Notably, the (slightly rewritten) existence problem $\Gamma = 0$ depends on θ/D, while the (slightly rewritten) E depends on β/D. However, the joint existence and stability problem depends on β, θ and D individually.

Based on Theorem 2, for $\beta D^3 > -\alpha$, *we further prove a center manifold reduction to a scalar ODE* whose steady states correspond to fronts connected by heteroclinic orbits. The stable equilibria correspond to stable fronts in the PDE and *the heteroclinic connections describe accelerating, decelerating or even direction reversing fronts.* Due to Theorem 1 the organization of equilibria can be

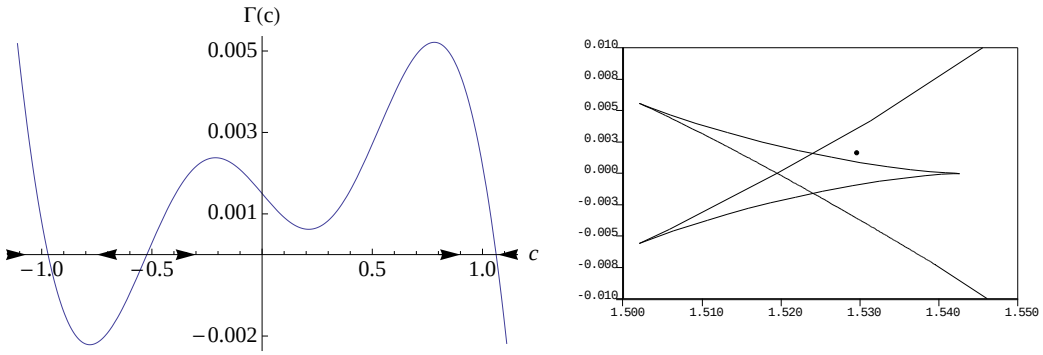

FIGURE 1. $\tau = 1$, $\theta = 2$, $\beta = -0.3$. (a) Graph of $\Gamma(c)$ for $\gamma = 0.0015$, $\alpha = 1.53$ with flow on center manifold illustrated by arrows; (b) curves of folds, bullet marks the location of (a).

directly read off the graph of Γ as a function of c. More importantly, *the nature of velocity changes can be read off the graph of* Γ *directly*: the vector field is topologically given by $\dot{z} = \Gamma(z)$. See Figure 1 for an illustration.

More generally, the two nonzero eigenvalues of a front can also cross the imaginary axis and we thus expect a Hopf bifurcation, which is numerically corroborated. However, our computation of the normal form coefficients of the center manifold reduction is so far incomplete. In fact, the unfolding of the possible triple root of the Evans function is expected to contain a Bogdanov-Takens bifurcation with symmetry, which would provide a rich set of solutions.

The manuscripts with full details are in preparation for publication.

REFERENCES

[1] J.Carr and R.Pego, *Metastable patterns in solutions of* $u_t = \varepsilon^2 u_{xx} - f(u)$, Comm. Pure Appl. Math, **42** (1989), 52–576 .

[2] G. Fusco, J.K. Hale. *Slow-Motion Manifolds, Singular Perturbations Dormant Instability, and Singular Perturbations.* J. Dyn. Diff. Eq. **1** (1989), 75–94.

[3] A. Doelman, P. van Heijster, T.J. Kaper. *Pulse dynamics in a three-component system: existence analysis.* J. Dyn. Diff. Eq. **21** (2009), 73–115.

[4] P. van Heijster, A. Doelman, T.J. Kaper. *Pulse dynamics in a three-component system: stability and bifurcations.* Physica D **237** (2008), 3335–3368.

[5] P. van Heijster, A. Doelman, T.J. Kaper, K. Promislow. *Front interactions in a three-component system.* SIAM J. Appl. Dyn. Sys. **9** (2010), 292–332.

[6] J.D.M. Rademacher. *First and second order semi-strong interaction in reaction-diffulsion systems.* SIAM J. Appl. Dyn. Sys. (to appear)

[7] C.P. Schenk, M. Or-Guil, M. Bode, H.-G. Purwins. *Interacting pulses in three-component reaction-diffusion systems on two-dimensional domains.* PRL **78**(19) (1997), 3781–3784.

Heterogeneity-induced pulse generators

Yasumasa Nishiura
(joint work with Masaki Yadome and Takashi Teramoto)

1. Introduction

Pulse wave is the main careers of information and the effect of heterogeneity in the media is of great importance for the understanding of signaling processes in biological and physiological systems. The role of heterogeneity in the media does not remain a perturbative effect, in fact it influences a lot over the concerned system and even produces a qualitatively new dynamics. It is known that heterogeneities produce various types of ordered patterns called heterogeneity-induced patterns [1, 2], which sometimes work as blockers for propagation waves. There is, however, another aspect of heterogeneity-induced dynamics, namely it creates a spontaneous generator of pulses without any triggers and external forces. We present a representative example of such a pulse generator (PG) and try to clarify the underlying mathematical mechanism from dynamical system view point. More detailed discussions are found in [3, 4]. Our model takes the following 1D three-component reaction diffusion (RD) system:

$$\left\{\begin{array}{rcl} u_t &=& d_u u_{xx} + f(u) - k_3 v - k_4 w + k_1, \\ \tau v_t &=& d_v v_{xx} + u - v, \\ \theta w_t &=& d_w w_{xx} + u - w, \end{array}\right. \tag{1}$$

where $d_u, d_v, d_w > 0$ are diffusion coefficients. We specify the nonlinearity as $f(u) = k_2 u - u^3$, which allows us to regard (1) as a generalized version of the FitzHugh-Nagumo equations by adding the second inhibitor w. Here we employ the following parameters: $k_1 = -5.7, k_2 = 2.0, k_3 = 1.0, k_4 = 8.5, (d_u, d_v, d_w) = (0.9 \times 10^{-4}, 1.0 \times 10^{-3}, 0.6 \times 10^{-2}), \tau = 52, \theta = 1$. The model (1) is a typical example of one-activator-two-inhibitor system, which was first proposed as a qualitative model of gas discharge phenomena [5]. The heterogeneity is introduced to the controllable parameter k_1 that corresponds to the applied voltage or external stimulus in neural tissues.

A precise form for the spatial heterogeneity of jump type for k_1 is given by

$$k_1 = k_{1L} + \epsilon\chi(x), \quad \chi(x) = \frac{1}{1 + e^{-\gamma x}}.$$

The height of jump ϵ is taken as the bifurcation parameter. The parameter γ controls the steepness of the slope around the jump point, but we fix it to be 100. Due to the jump from k_{1L} to $k_{1L} + \epsilon$, we lose the translation invariance and constant homogeneous state.

From this jump heterogeneity traveling pulses can be produced spontaneously without any triggers or external forces. Note that our PG is quite different from the pulse emission phenomena reported in [6, 7] in the sense that our PGs are robust, exist on intervals, and have variety of generating manners. On the other hand the pulse-emission discussed in [8] is close to ours, however its underlying structures

for the onset and generating mechanism remains completely open. Here we report on how such a PG emerges depending on the height and try to understand the generating mechanism from bifurcational view point.

The pulse generators (PGs) can be regarded as time-periodic heteroclinic orbits of (1) connecting the left homogeneous state to the wave train far right, in fact the emitted pulses eventually could form a wave train far from the jump point.

2. Results

Pulse generators (PGs) can display a variety of spatio-temporal patterns depending on the jump height ϵ ranging from time-periodic to even chaotic emission of pulses (see [3, 4]). For the onset of PGs, it is closely related to the "disappearance regime" of stable heterogeneity-induced ordered patterns, namely PGs start to emerge in the region where all the stable patterns induced by the heterogeneity, including standing pulses (SPs) and breather (SB), disappear. In fact such a regime exists in between $\epsilon = 0.2960$ and $\epsilon = 0.3025$. The SPs lose their stabilities via Hopf bifurcations and the period-doubling (PD) bifurcation occurs on the SB branch as shown in [4]. It is remarked here that we found a new type of unstable standing pulse named by SP2, which turns out to be the destination of PGs as its period goes to infinity.

We trace the PG branch as a periodic solution and find that it persists robustly for the wide range of ϵ values. As ϵ is increased or decreased, the PG branch turns back via saddle-node (SN) bifurcations. It is numerically suggested that both arms of unstable branches are eventually terminated at the homoclinic orbits of SP2 as the period $T \to \infty$. In fact each periodic orbit spends most of time around SP2 and approaches into the homoclinic orbit.

Moreover, an intensive numerical global bifurcation analysis shows that the PG behaviors emerge almost exactly at the point where the stable SP and SB cease to exist. It is worth noting that all the unstable branches of PGs terminate at homoclinic bifurcations of SP2. This implies that the onset of various types of PGs could be characterized via unfoldings of multi-homoclinic-loop structure of SP2. It is conjectured that it is a double-homoclinic point of butterfly type.

3. Discussion

We present 1D heterogeneity-induced pulse generators arising in the three-component RD system. The simplest jump heterogeneity is employed here and the resulting PGs are robust against the change of the height. The traveling pulses are produced spontaneously around the jump point and they are emitted in one direction. The pulse-sink boundary condition allows us to reduce the PGs to periodic solutions so that we can trace their global behaviors as the height of the jump varies. Exploring the parameter space, we find various types of PGs, i.e., pulse-emitting manner has a variety as shown in [4]. Nevertheless there seems to exist a hidden organizing center producing those PGs inspired by the common features shared among the global behaviors of PG branches. For instance the PG branches terminate at the same unstable stationary pattern SP2 when PG's

periods tend to infinity. These observations indicate that there exists a hierarchical structure of bifurcating branches of PGs originated in a multi-homoclinic-loop structure at SP2 of butterfly type. For this purpose we are currently investigating the orientabilities for homoclinic center manifolds and searching for singularities of higher codimension in the extended parameter space.

References

[1] Yuan, X., Teramoto, T., and Nishiura, Y., *Heterogeneity-induced defect bifurcation and pulse dynamics for a three-component reaction-diffusion system*, Phys. Rev. E. **75** (2007) 036220

[2] Teramoto, T., Yuan, X., Bär, M., and Nishiura, Y., *Onset of unidirectional pulse propagation in an excitable medium with asymmetric heterogeneity*, Phys. Rev. E. **79** (2009) 046205

[3] Nishiura, Y., Teramoto, T., and Yadome, M., *Heterogeneity-induced pulse generators*, to appear in the proceedings of ICCN2011.

[4] Yadome, M., Nishiura, Y. and Teramoto, T., *Onset of heterogeneity-induced pulse generators in a generalized FitzHugh-Nagumo system*, preprint.

[5] Schenk, C. P., Or-Guil, M., Bode, M., and Purwins, H. -G., *Interacting Pulses in Three-Component Reaction-Diffusion Systems on Two-Dimensional Domains*, Phys. Rev. Lett. **78** (1997) 3781–3784

[6] Ermentrout, G. B., and Rinzel, J., *Reflected waves in an inhomogeneous excitable medium*, SIAM J. Appl. Math. **56** (1996) 1107–1128

[7] Cytrynbaum, E. N., and Lewis, T. J., *A Global bifurcation and the appearance of a one-dimensional spiral wave in Excitable media*, SIAM J. Appl. Dyn. Syst. **8** (2009) 348–370

[8] Prat, A., Li, Y. -X., and Bressloff, P., *Inhomogeneity-induced bifurcation of stationary and oscillatory pulses*, Physica D. **202** (2005) 177–199

Existence and Homogenisation of Travelling Waves Bifurcating from Resonances of Diffusion and Reaction in Periodic media

Karsten Matthies

(joint work with Adam Boden)

The existence of travelling wave type solutions is studied for a reaction diffusion equation in $\mathbb{R}^2$ with a nonlinearity which depends periodically on the spatial variable:

$$u_t = \operatorname{div}(A\nabla u) + f\left(\frac{x}{\varepsilon}, u\right), \tag{1}$$

where A is a real symmetric positive definite matrix, $\varepsilon > 0$ and the nonlinearity $f(\xi, u)$ is periodic in ξ with periodic cell $[0, 2\pi]^2$, i.e.

$$f(\xi_1 + \xi_2, u) = f(\xi_1, u) \text{ for all } \xi_2 \in (2\pi\mathbb{Z})^2 .$$

We treat the coefficient of the linear term as a parameter, i.e.

$$f(\xi, u) = -\mu u + p(\xi)q(u), \tag{2}$$

where $\mu \in \mathbb{R}$, $p \in H^2\left(T^2\right)$ the periodic Sobolev space on $[0, 2\pi]^2$ and $q \in C^2(\mathbb{R})$ with $q(0) = 0$, $q'(0) = 0$ and $q''(0) \neq 0$.

We look for generalised travelling wave solutions of the form

$$u(x,t) = v^\varepsilon \left(x \cdot k - ct, \frac{x}{\varepsilon} \right), \tag{3}$$

where the profile function $v^\varepsilon = v^\varepsilon(\tau, \xi)$ is periodic in ξ with periodic cell $[0, 2\pi]^2$. This type of travelling wave solution has a profile which varies as it moves over the periodic cells and therefore is able to incorporate the effects of the periodic dependence in the nonlinearity into the solution.

We formulate the problem of finding solutions of type (3) as an infinite spatial dynamical system. Using a centre manifold reduction we obtain a finite dimensional dynamical system on the centre manifold with fully degenerate linear part of dimensions 1 and 2. Firstly if the parameter μ in the nonlinearity is close to zero then the problem reduces to a one dimensional centre manifold. For which we can study the dynamics directly to find conditions for the existence of generalised travelling wave solutions.

The other case we consider is when the parameter μ is close to a non-zero eigenvalue which leads to a two dimension centre manifold. in this case we use Conley index to obtain conditions on the nonlinearity for the existence of generalised travelling wave solutions.

The analysis provides an approach to the homogenisation problem for μ near 0 as the period of the periodic dependence in the nonlinearity tends to zero, then we obtain

$$v^\varepsilon(\tau, \xi) = v^0(\tau) + O(\varepsilon) \text{ as } \varepsilon \to 0$$

uniformly on $\mathbb{R}$, where the limiting profile v^0 is a heteroclinic connection between equilibria which satisfies the ordinary differential equation

$$v^0_\tau = -\frac{\delta v^0 + p_0 q(v^0)}{c},$$

which interestingly is a first order equation, while a formal homogenisation would lead to a second-order equation.

The reported work is based on the paper [2] and the PhD thesis of Boden [1].

References

[1] A. Boden, *Travelling Waves in Heterogeneous Media*, PhD thesis, University of Bath, 2012.
[2] A. Boden and K. Matthies, *Existence and Homogenisation of Travelling Waves Bifurcating from Resonances of Diffusion and Reaction in Periodic media*, submitted 2012.

Domain and wall pattern in ferromagnets

Felix Otto

Ferromagnetic materials are characterized by a non-vanishing spontaneous magnetization. On a mesoscopic level, it can be thought of as a unit-length vector field $m(x)$ defined on the sample $x \in \Omega$. Experiments show that this vector field features "domains", i. e. subregions of Ω where it is nearly constant, separated by comparatively sharp transition layer, so-called walls. There is a well-accepted

variational model: Experimentally observed magnetization configurations should be (stable) stationary points of an energy functional. This variational problem is non-convex (because of the unit-length constraint) and non-local (because of the long-range magnetostatic interaction). Moreover, it features widely separated length scales: On the one hand, a material parameter, the exchange length, which is of the order of a few nanometer and on the other hand, the length scale given by the sample Ω (e. g. thickness and width of the cross section if Ω is a thin film element). Hence the energy landscape features many local minimizers and is not well-accessible to brute-force numerical simulation.

In my talk, I focussed on a specific, but ubiquitous pattern, the so-called concertina pattern. It is a periodic domain and wall structure arising in thin-film ferromagnets with an elongated cross-section. This pattern is a local (not a global) minimizer that arises from a subcritical bifurcation and undergoes a cascade of secondary bifurcations. We developed an understanding of these bifurcation and thus the hysteresis of the sample. Actually, the secondary bifurcations are a consequence of a side band instability. Our understanding arises from a combination of the rigorous derivation of suitably reduced model, and numerical simulation and qualitative analysis of this more tractable reduced model.

The relevant experiments and a condensed description of our analysis (both theoretical and by numerical simulation) can be found in [1]. I recommend to have a glance over this paper as a motivation, especially Sections 1 A, 1 E to I, and Sections II and III, but don't get frustrated if you are not used to the applied jargon.

I now address our work in more detail. We started by identifying the appropriate parameter regime (as it turns out: one of four in a two-dimensional parameter space), by identifying the scaling law of the critical external magnetic field at which the uniform magnetization becomes unstable. This is done by deriving matching upper and lower bounds on the Rayleigh quotient of the Hessian — a linear analysis, which nonetheless is not-trivial because the Hessian is not explicitly diagonalizable. The proof can be found in [2, Theorem 1], which is a cute application of the idea of establishing upper and lower bounds on the minimal energy of a variational problem that match in terms of scaling; where upper bounds are obtained via physically motivated constructions and "Ansatz-free" lower bounds follow from suitable interpolation inequalities. The form of the unstable mode can be explicitly identified in the regime of interest; its period agrees well with the experimentally observed period of the concertina [1, I.G].

As a next step, we rigorously derived a "reduced" variational model that zooms in on the bifurcation. It is much simpler than the original one in the sense that it is dimensionally reduced and that it only has a single non-dimensional parameter (the strength of the external field) — and thus is numerically well-tractable. The derivation is a nice application of the concept of Γ-convergence; the analytically more challenging part consists in the fact that we take a weak underlying topology and that we need to establish (compensated) compactness. The proof can be found in [3, Theorem 3].

We finally analyzed the secondary bifurcations of the solutions to the reduced problem. We started be establishing a non-obvious coercivity of the reduced variational problem: It implies that the average period of the minimizer increases linearly (modulo a logarithm) as a function of the external field. You will find the proof of this in [4, Theorem 1]. It boils down to a somewhat non-standard analysis of Burgers' equation.

We then related the numerically observed secondary instabilities that lead to an increase of the period to a side band instability, see Section III in [1]. In this variational context, the side band instability is a consequence of the *concavity* of the energy per period in the length w of the period [1, III.B]. The fact that this concavity indeed leads to a long wave-length instability is a consequence of a Bloch wave analysis [1, III.C]. This instability can also be heuristically understood close to (slightly subcritical) bifurcation [1, III.D] and is confirmed on the level of domain theory (where walls are replaced by sharp discontinuities).

All the references below refer on the preprints that can be downloaded from my homepage http://www.mis.mpg.de/applan/members/felix-otto/publications/micromagnetics.html.

References

[1] Jutta Steiner, Jeff McCord, Rudolf Schäfer, Holm Wieczoreck, Felix Otto. Formation and coarsening of the concertina magnetization pattern in elongated thin-film elements. *Phys. Rev. B* **85**, 104407 (2012). See MPI MIS Preprint 40/2011

[2] Ruben Cantero-Alvarez and Felix Otto. Critical fields in ferromagnetic thin films: Identification of four regimes. *J. Nonlinear Sci.* **16(4)**, 351-383, (2006).

[3] Ruben Cantero-Alvarez, Felix Otto, and Jutta Steiner. The concertina pattern: A bifurcation in ferromagnetic thin films. *J. Nonlinear Sci.* **17(3)**, 221-281 (2007).

[4] Felix Otto and Jutta Steiner. The concertina pattern - from micromagnetics to domain theory. *Calc. VarPartial Differential Equations* **39**, 139–181, (2010).

Chimera states: patterns of coherence and incoherence in coupled oscillator systems

Matthias Wolfrum

Chimera states are particular trajectories in systems of coupled phase oscillators that display a spatio-temporal pattern consisting of regions with coherent and incoherent motion that emerge spontaneously in a system of identical units. They constitute a new paradigm of dynamical behavior that can serve as a prototype for various physical phenomena including e.g. the coexistence of synchronous and asynchronous neural activity in the brain. For their mathematical investigation, one has to employ concepts from the field of pattern formation, deterministic chaos, and statistical physics.

The simplest system, where chimera states can be observed consists of N identical phase oscillators that are arranged in a ring structure where each oscillator

is coupled to R closest neighbors on both sides:

$$\frac{d\vartheta_j}{dt} = \omega - \frac{1}{N}\sum_{k=-R}^{R} \sin(\vartheta_j - \vartheta_{j+k} + \alpha), \qquad j = 1 \dots N \tag{1}$$

Here $j = 1, \dots N$ is the number of the oscillator and all indices have to be considered modulo N. The parameter ω denotes the natural frequency an the α is a phase-lag in the coupling. The appearance of chimera states (cf. Fig 1) does not depend on the specific structure of Eq. (1). Necessary ingredients for the numerical observation of chimera states are: (i) a discrete oscillatory medium; (ii) a non-local coupling, i.e. some interaction providing an average over local subpopulations; (iii) a well tuned balance between attraction and repulsion, in Eq. (1) controlled by choosing α sightly smaller than $\pi/2$.

Scaling invariance and thermodynamic limit description: As demonstrated in Fig. 2, the numerically observed chimera states show a scaling invariance, when the coupling range is considered as a macroscopic quantity $r := R/N$. This motivates the formulation of a limit equation for $N \longrightarrow \infty$ of the form of a continuity equation

$$\frac{\partial f}{\partial t} + \frac{\partial}{\partial \vartheta}(fv) = 0 \tag{2}$$

for a probability density $f(\vartheta, x, t)$ where the flux

$$v(\vartheta, x, t) = \omega - \int_{-1}^{1} G(x-y) \int_0^{2\pi} f(\vartheta', y, t) \sin(\vartheta - \vartheta' + \alpha) \mathrm{d}\vartheta' \mathrm{d}y$$

is defined here with a general 2-periodic coupling function that has to be chosen as $G(x) = \frac{1}{2r}$ for $|x| < r$ and zero elsewhere, in order to recover an integral version of Eq. (1). Due to the purely sinusoidal interaction function, this equation can be further simplified. Indeed, it turns out that solutions of the form

$$f(\vartheta, x, t) = \frac{1 - |z|^2}{2\pi(1 - 2|z|\cos(\vartheta - \arg(z) + |z|^2)}$$

where the complex local mean field $z(\cdot, t) : \mathbb{R} \to C_{\mathrm{per}}([-1, 1], \mathbb{C})$ satisfies the equation

$$\frac{dz}{dt} = i\omega z + \frac{1}{2}e^{-i\alpha}\mathcal{G}z + \frac{1}{2}e^{i\alpha}z^2\mathcal{G}\bar{z}$$

with $|z| \leq 1$ and

$$(\mathcal{G}w)(x) := \int_{-1}^{1} G(x-y)w(y)\mathrm{d}y$$

form an invariant manifold for Eq. (2). Chimera states appear for this equation as periodic solutions of the form $z(x,t) = a(x)e^{i\Omega t}$ and the complex local mean field can be interpreted as follows: In the coherent region, we have $|z(x,t)| = 1$ and $\arg(z(x,t))$ indicates the phase of the synchronized oscillators; $|z(x,t)| = 0$ implies complete incoherence and a uniform distribution of the oscillator phases. For $0 < |z(x,t)| < 1$ we have an incoherent motion with non-uniform distribution of the oscillators, where $\arg(z(x,t))$ indicates the phase of the peak of the distribution.

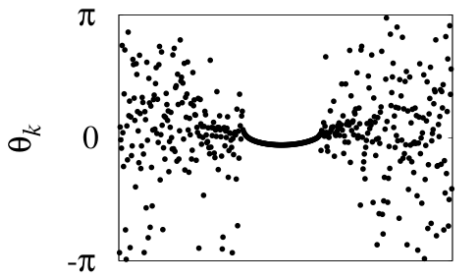

FIGURE 1. Snapshot of a chimera state, numerical solution of Eq. (1) with $N = 200$, $R = 70$, $\alpha = 1.46$, $\omega = 0$

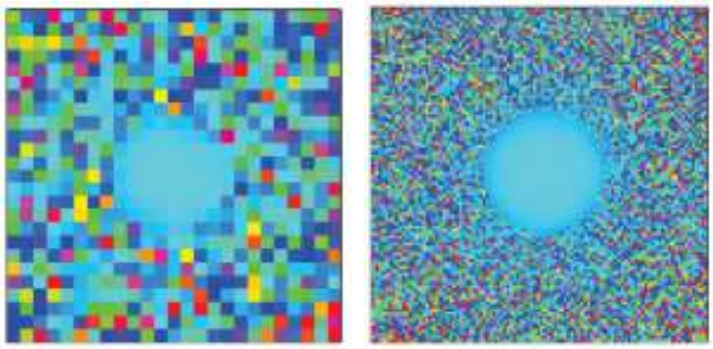

FIGURE 2. Chimera states in a two-dimensional array of $N = 25 \times 25$ and $N = 100 \times 100$, respectively. Other parameters $\alpha = 1.54$, $R/N = 0.4$

After this preparation, we are able to perform a stability and bifurcation analysis of chimera states in the limit of $N \longrightarrow \infty$. *Finite size effects:* In the original system (1) with finite N, chimera states turn out to be chaotic transients that collapse after a finite time of existence. Their average life time grows exponentially with respect to the system size N. We can relate their properties to the thermodynamic limit results in the following two points:

- *Stability boundaries:* Approaching the the parameter values of a stability boundary in the thermodynamic limit system, the average life time of a corresponding finite N chimera state decreases to zero; i.e. the finite N chimera state disappears without a bifurcation.
- *Lyapunov spectrum:* The Lyapunov spectrum of a finite N chimera state consists of a weakly chaotic part and a stable part. At the other hand, in the thermodynamic limit system we obtain continuous spectrum that lies partially on the imaginary axis. It turns out that this continuous spectrum can be obtained as the limit of the Lyapunov spectra for finite N.

Details can be found in the references below.

References

[1] O.E. Omel'chenko, M. Wolfrum, Y.L. Maistrenko, *Chimera states as chaotic spatio-temporal patterns*, Phys. Rev. E **81** (2010), 065201/1–065201/4.

[2] M. Wolfrum, O. Omel'chenko, S. Yanchuk, Y. Maistrenko, *Spectral properties of chimera states*, Chaos, **21** (2011), 0013112/1-013112/8.

[3] M. Wolfrum, O. Omel'chenko, *Chimera states are chaotic transients*, Phys. Rev. E **84** (2011), 015201/1-015201/4.

[4] O. Omel'chenko, M. Wolfrum, S. Yanchuk, Y. Maistrenko, O. Sudakov, *Stationary patterns of coherence and incoherence in two-dimensional arrays of non-locally coupled phase oscillators*, Phys. Rev. E **85** (2012), 036210/1–036210/5.

[5] O. Omel'chenko, M. Wolfrum, *Nonuniversal transitions to synchrony in the Sakaguchi–Kuramoto model*, Phys. Rev. Lett. **109** (2012), 164101/1–164101/4.

Death, life, and afterlife in shear turbulence

Dwight Barkley

This work explores the connection between the transition to turbulence in pipe flow and the dynamics of excitable media, as exemplified by nerve cells. The primary goal is to leverage years of extensive analysis of excitable media to understand the dynamics of pipe flow. There are several active areas of research in pipe flow that can be analyzed in this context [1, 2].

Figure 1 conveys the essential message and serves to motivate this work. Two very different physical systems are shown. The first is pipe flow, Fig. 1(a). In the quiescent, or unexcited state, flow through the pipe is laminar and individual fluid parcels move in straight lines parallel to the pipe axis. The second system is the axon of a nerve cell, Fig. 1(b). Here in the quiescent state, or resting state, the cell membrane is polarized with the inside of the cell at a lower voltage potential than the outside. In both systems the quiescent state is stable to small, sub-threshold perturbations and hence the systems remain in the quiescent state indefinitely unless perturbed sufficiently.

Consider now the response of these systems to large, super-threshold, perturbations. For pipe flow, a localized patch of turbulence can be created which moves down the pipe at approximately constant speed. Such a patch of turbulence is called a puff. A typical experimental measurement of a puff would be the fluid pressure near the pipe wall for example. Likewise, a resting nerve axon can be stimulated by the injection of current. The response is a pulse of depolarization, known as an action potential, which travels down the axon. The standard measurement is the membrane potential, i.e. the voltage difference between the inside and outside of the cell. As with the puff, the shape and speed of the action potential are dictated by properties of the medium and not the stimulus initiating it.

While Fig. 1 is only a cartoon, the shape of the pressure and voltage signals shown are representative of those of real systems [3, 4]. The two signals share the same features apart from the fact that they are approximately the mirror images

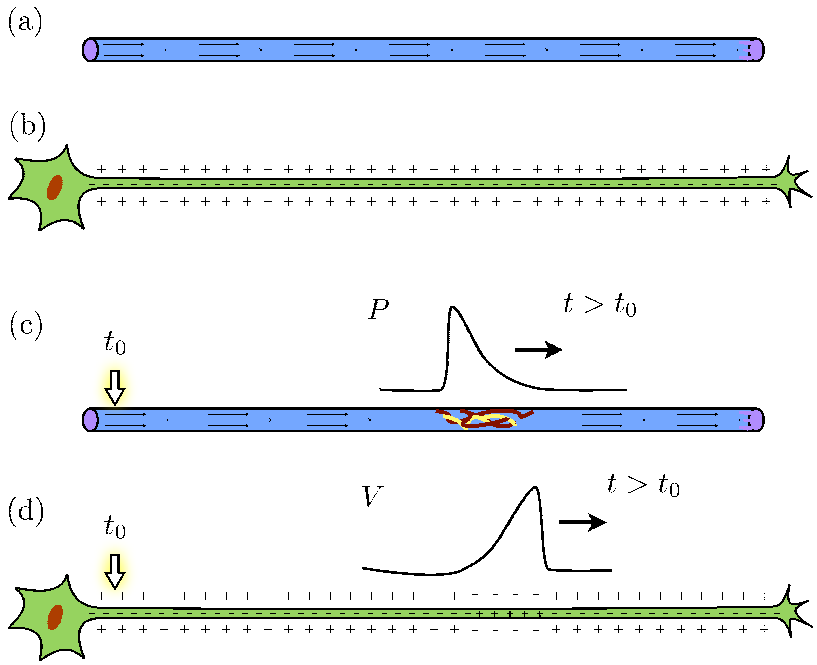

FIGURE 1. Cartoon illustrating the analogy between pipe flow and a nerve axon. In the absence of stimulation, both systems remain in the quiescent state: (a) flow through the pipe is laminar and (b) the axon is negatively polarized. Following an appropriate stimulation at some time t_0, a localized patch of turbulence moves down the pipe (c) and an action potential propagates down the axon (d).

of one another. This is not an coincidence, but rather a manifestation of the fact that pipe flow is an excitable medium, similar in many respects to a nerve axon.

Two models for pipe flow are presented. These are given in terms of two quantities, the turbulence intensity q and the axial (streamwise) velocity u, as a function of distance x on the pipe axis.

The first is the continuous model

$$q_t + Uq_x = q\left(u + r - 1 - (r+\delta)(q-1)^2\right) + q_{xx}, \tag{1}$$

$$u_t + Uu_x = \epsilon_1(1-u) - \epsilon_2 uq - u_x, \tag{2}$$

where r plays the role of Reynolds number. U accounts for downstream advection by the mean velocity. The model includes minimum derivatives, q_{xx} and u_x, needed for turbulent regions to excite adjacent laminar ones and for left-right symmetry breaking.

While the continuous model capture the basic properties of puffs and slugs, the turbulence model is too simplistic to show puff decay and puff splitting. Evidence suggests that pipe turbulence is locally a chaotic repeller [5]. Hence a more realistic model is obtained by replacing the turbulent branches in the continuous model with

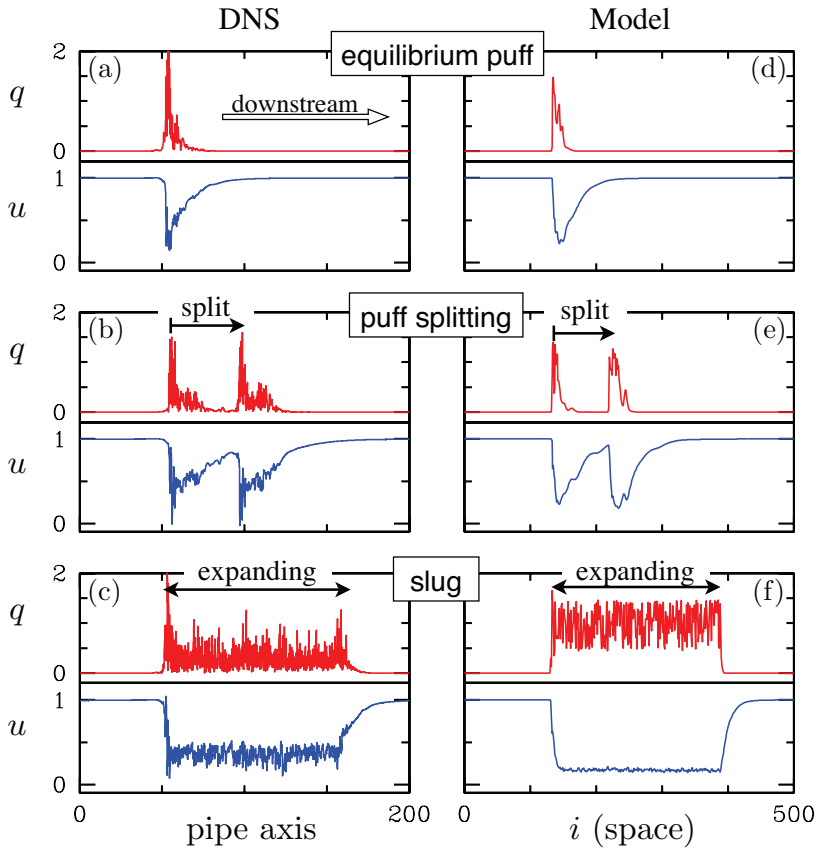

FIGURE 2. Regimes of transitional pipe flow. Left column is from full DNS. (a) Puff at $Re = 2000$ that will decay at a later time. (b) Puff splitting at $Re = 2275$. The downstream (right) puff split from the upstream one at an earlier time. (c) Expanding slug flow at $Re = 3200$. Right column shows corresponding states from the simple one-dimensional discrete model.

a wedged-shaped region of transient chaos. The discrete model is

$$q_{i+1}^{n+1} = F(q_i^n + d(q_{i-1}^n - 2q_i^n + q_{i+1}^n), u_i^n), \tag{3}$$

$$u_{i+1}^{n+1} = u_i^n + \epsilon_1(1 - u_i^n) - \epsilon_2 u_i^n q_i^n - c(u_i^n - u_{i-1}^n), \tag{4}$$

where q_i^n and u_i^n denote values at spatial location i and time n. This model is essentially a discrete version of Eqs. (1)-(2), except with chaotic q dynamics generated by the map F. Details of the tent map F are given in [1].

With these models puff decay (death), puff splitting (life) and slug formation (afterlife) can be effectively studied. Comparison with full simulation of the Navier-Stokes equations is shown in Fig. 2.

REFERENCES

[1] D. Barkley, *Simplifying the complexity of pipe flow*, Phys. Rev. E **84** (2011), 016309.
[2] D. Barkley, *Modeling the transition to turbulence in shear flows*, J. Phys: Conf. Seri. **318** (2011), 032001.

[3] K. Avila, D. Moxey, A. de Lozar, M. Avila, D. Barkley and B. Hof, *The Onset of Turbulence in Pipe Flow*, Science **333** (2011), 192–196.
[4] A.L. Hodgkin and A.F. Huxley, *A quantitative description of membrane current and its application to conduction and excitation in nerve*, J. Physiol. (London) **117** (1952), 500–544.
[5] B. Eckhardt, T. M. Schneider, B. Hof, and J. Westerweel, *Turbulence transition in pipe flow*, Annu. Rev. Fluid Mech. **39** (2007), 447–468.

Reporter: Sergey B. Tikhomirov

Participants

Prof. Dr. Fatihcan M. Atay
Max-Planck-Institut für Mathematik
in den Naturwissenschaften
Inselstr. 22 - 26
04103 Leipzig
GERMANY

Dr. Dwight Barkley
Mathematics Institute
University of Warwick
Gibbet Hill Road
Coventry CV4 7AL
UNITED KINGDOM

Prof. Dr. Thomas Bartsch
Mathematisches Institut
Justus-Liebig-Universität Gießen
Arndtstr. 2
35392 Gießen
GERMANY

Dr. Margaret Beck
Department of Mathematics
Heriot-Watt University
Riccarton
Edinburgh EH14 4AS
UNITED KINGDOM

Dr. Nitsan Ben-Gal
Institute of Mathematics and its
Applications
College of Science and Engineering
University of Minnesota
207 Church Street SE 306 Lind Hall
Minneapolis, MN 55455
UNITED STATES

Prof. Dr. Wolf-Jürgen Beyn
Fakultät für Mathematik
Universität Bielefeld
Postfach 100131
33501 Bielefeld
GERMANY

Dr. Martina Chirilus-Bruckner
Division of Applied Mathematics
Brown University
Box F
182 George Str.
Providence, RI 02912
UNITED STATES

Prof. Dr. Bernold Fiedler
Institut für Mathematik I (WE 1)
Freie Universität Berlin
Arnimallee 2-6
14195 Berlin
GERMANY

Dr. Marek Fila
Institute of Applied Mathematics
Comenius University
Mlynska dolina
84248 Bratislava
SLOVAKIA

Dr. Anna R. Ghazaryan
Department of Mathematics
Miami University
Oxford, OH 45056
UNITED STATES

Dr. Pavel Gurevich
Institut für Mathematik I (WE 1)
Freie Universität Berlin
Arnimallee 2-6
14195 Berlin
GERMANY

Prof. Dr. Marlis Hochbruck
Karlsruher Institut f. Technologie (KIT)
Inst. f. Angew. & Numerische
Mathematik
Englerstr. 2
76131 Karlsruhe
GERMANY

Dr. Aaron H. Hoffman
Olin College
Olin Way
Needham, MA 02492-1200
UNITED STATES

Prof. Dr. Hermen Jan Hupkes
Mathematisch Instituut
Universiteit Leiden
Postbus 9512
2300 RA Leiden
NETHERLANDS

Prof. Dr. Tibor Krisztin
Bolyai Institute
University of Szeged
Aradi Vertanuk Tere 1
6720 Szeged
HUNGARY

Prof. Dr. Markus Kunze
Mathematisches Institut
Universität zu Köln
Weyertal 86 - 90
50931 Köln
GERMANY

Prof. Dr. Yuri Latushkin
Department of Mathematics
University of Missouri-Columbia
202 Mathematical Science Bldg.
Columbia, MO 65211-4100
UNITED STATES

Prof. Dr. Reiner Lauterbach
Department Mathematik
Universität Hamburg
Bundesstr. 55
20146 Hamburg
GERMANY

Leonhard Luecken
Fachbereich Mathematik
Humboldt Universität Berlin
Unter den Linden 6
10099 Berlin
GERMANY

Prof. Dr. John Mallet-Paret
Division of Applied Mathematics
Brown University
Box F
182 George Str.
Providence, RI 02912
UNITED STATES

Prof. Dr. Hiroshi Matano
Graduate School of
Mathematical Sciences
University of Tokyo
3-8-1 Komaba, Meguro-ku
Tokyo 153-8914
JAPAN

Dr. Karsten Matthies
Department of Mathematical Sciences
University of Bath
Claverton Down
Bath BA2 7AY
UNITED KINGDOM

Dr. Scott McCalla
Department of Mathematics
UCLA
Math Sciences Building 6363
520 Portola Plaza
Los Angeles, CA 90095-1555
UNITED STATES

Prof. Dr. Alexander Mielke
Weierstraß-Institut für
Angewandte Analysis und Stochastik
Mohrenstr. 39
10117 Berlin
GERMANY

Prof. Dr. Yasumasa Nishiura
WPI Advanced Institute for Material Research
Tohoku University
2-1-1 Katahira, Aoba
Sendai 980-8577
JAPAN

Prof. Dr. Sergio Oliva
Instituto de Matematica e Estatistica
Universidade de Sao Paulo (IME-USP)
Rua do Matao 1010
Sao Paulo 05508-090 - SP
BRAZIL

Denny Otten
Fakultät für Mathematik
Universität Bielefeld
Universitätsstr. 25
33615 Bielefeld
GERMANY

Prof. Dr. Felix Otto
Max-Planck-Institut für Mathematik in den Naturwissenschaften
Inselstr. 22 - 26
04103 Leipzig
GERMANY

Prof. Dr. Robert L. Pego
Department of Mathematical Sciences
Carnegie Mellon University
Pittsburgh, PA 15213-3890
UNITED STATES

Dr. Jens Rademacher
CWI
Centrum Wiskunde & Informatica
Science Park 123
1098 XG Amsterdam
NETHERLANDS

Prof. Dr. Alan Rendall
MPI für Gravitationsphysik
Albert-Einstein-Institut
Am Mühlenberg 1
14476 Golm
GERMANY

Prof. Dr. Carlos Rocha
Departamento de Matematica
Instituto Superior Tecnico
Avenida Rovisco Pais, 1
Lisboa 1049-001
PORTUGAL

Dr. Jens Rottmann-Matthes
Fakultät für Mathematik
Universität Bielefeld
Universitätsstr. 25
33615 Bielefeld
GERMANY

Prof. Dr. Alastair Rucklidge
School of Mathematics
University of Leeds
Leeds LS2 9JT
UNITED KINGDOM

Prof. Dr. Björn Sandstede
Division of Applied Mathematics
Brown University
Box F
182 George Str.
Providence, RI 02912
UNITED STATES

Prof. Dr. Arnd Scheel
School of Mathematics
University of Minnesota
127 Vincent Hall
206 Church Street S. E.
Minneapolis MN 55455-0436
UNITED STATES

Prof. Dr. Guido Schneider
Institut für Analysis, Dynamik und
Modellierung, Fak. für Math. & Physik
Universität Stuttgart
Pfaffenwaldring 57
70569 Stuttgart
GERMANY

Isabelle Schneider
Fachbereich Mathematik & Informatik
Freie Universität Berlin
Arnimallee 6
14195 Berlin
GERMANY

Prof. Dr. Eckehard Schöll
Institut für Theoretische Physik
Technische Universität Berlin
Hardenbergstr. 36
10623 Berlin
GERMANY

Hannes Stuke
Fachbereich Mathematik & Informatik
Freie Universität Berlin
Arnimallee 6
14195 Berlin
GERMANY

Dr. Sergey B. Tikhomirov
Institut für Mathematik
Freie Universität Berlin
14195 Berlin
GERMANY

Prof. Dr. Laurette Tuckerman
PMMH-ESPCI
10, rue Vauquelin
75231 Paris Cedex 5
FRANCE

Prof. Dr. Hannes Uecker
Institut fuer Mathematik
Carl v. Ossietzky-Universität Oldenburg
Fakultät V: Mathematik &
Naturwissensch.
26111 Oldenburg
GERMANY

Prof. Dr. Erik Van Vleck
Department of Mathematics
University of Kansas
405 Snow Hall
Lawrence, KS 66045-7567
UNITED STATES

Frits Veerman
Universiteit Leiden
Mathematisch Instituut
Niels Bohrweg 1
5238 CA Leiden
NETHERLANDS

Prof. Dr. Sjoerd Verduyn Lunel
Mathematisch Instituut
Universiteit Leiden
Postbus 9512
2300 RA Leiden
NETHERLANDS

Prof. Dr. Hans-Otto Walther
Mathematisches Institut
Justus-Liebig-Universität Gießen
Arndtstr. 2
35392 Gießen
GERMANY

Dr. Matthias Wolfrum
Weierstraß-Institut für
Angewandte Analysis und Stochastik
Mohrenstr. 39
10117 Berlin
GERMANY

Prof. Dr. J. Douglas Wright
Department of Mathematics
Drexel University
Korman Center 269
3141 Chestnut St.
Philadelphia, PA 19104
UNITED STATES

Prof. Dr. Serhiy Yanchuk
Fachbereich Mathematik
Humboldt Universität Berlin
Unter den Linden 6
10099 Berlin
GERMANY